Changes in Stormwater Thermal Loads Due to Bioretention Cells

William D. Paraszczuk

Thesis submitted to the faculty of the Virginia Polytechnic Institute and State University
in partial fulfillment of the requirements for the degree of

Master of Science
In
Biological Systems Engineering

Theresa M. Thompson
Erich T. Hester
David J. Sample

May 28th, 2021
Blacksburg, VA

Keywords: Bioretention, Stormwater, Urbanization, Mitigation, Thermal, Pollution

Changes in Stormwater Thermal Loads Due to Bioretention Cells

William D. Paraszczuk

Scholarly Abstract

Trout are an important game species that provide a substantial economic impact in Virginia. Along with other cold-water fish species, trout are extremely susceptible to changes in stream temperatures. Urban development and the increase in impervious surfaces alter the hydrologic cycle in urban watersheds, limiting infiltration and increasing surface runoff. Impervious surfaces absorb and store solar radiation, resulting in higher surfaces temperatures, and then transfer this thermal energy to runoff during a rainfall event, resulting in higher runoff temperatures. Bioretention cells are a common stormwater control practice identified as a possible thermal mitigation practice in urban watersheds harboring cold-water fish species. However, design specifications vary by locality and few studies have explored how design characteristics impact the temperature reduction potential. The goal of this study was to investigate changes in stormwater thermal load due to bioretention cells.

In this study two bioretention cells with differing design approaches were monitored to quantify the thermal reduction impact that the bioretention cells have on stormwater from impervious surfaces. Both cells significantly reduced stormwater outflow volume, event mean temperatures and heat loads; however, outflow temperatures repeatedly exceeded the 21°C temperature threshold for cold-water fish species. This finding indicates this practice alone may not be sufficient to reduce runoff temperatures below biological stress thresholds. In addition, previous literature suggested that deeper cells may provide more cooling benefits as deeper soil layers are cooler and have more stable temperatures. In this study, the deeper cell was not as effective in reducing runoff temperatures, likely due to surface overflow and a shorter residence time in the bioretention cell. This finding indicates there is a limit to the effectiveness of cell depth

in runoff thermal reduction and that other cell characteristics, such as subsurface drainage system length, may play an important role in runoff temperature reduction.

Changes in Stormwater Thermal Loads Due to Bioretention Cells

William D. Paraszczuk

General Abstract

Cold-water fish species such as trout are a game species of large economic value that are very susceptible to changes in water temperature. Due to warmer runoff temperatures from urban watersheds stream temperatures are increasing, posing a potential impact on the cold-water fish found in these watersheds. Bioretention cells are a common method for treating and reducing pollutants from stormwater in urban areas. Recently, research has focused on the potential of bioretention cells to reduce runoff temperatures in urban watersheds. However, research is limited and does not fully address the bioretention design characteristics that may be beneficial for reducing runoff temperatures.

In this study two bioretention with differing design approaches were monitored during summer months to quantify and assess the potential for runoff temperature reduction. Both cells reduced runoff volume, temperature, and overall heat energy leaving the cell. However, outflow temperatures were typically above the stress temperature threshold for many cold-water fish species, indicating that this practice may reduce runoff temperatures to a level that will not stress these fish species. Previous research has suggested that deeper cells may provide more cooling benefits as deeper soil layers are experience cooler and more stable temperatures. In this study, the deeper cell was not as effective in reducing runoff temperatures as the shallow cell with a greater overall volume. This finding suggests that there is a limit to the effectiveness of deeper cells and that other cell characteristics, such as cell volume, play an important role in runoff temperature reduction.

Acknowledgements

Needless to say, the past 18 months have been a trying time. Although my graduate school experience did not go as exactly I imagined, there is a lot I am thankful for and I would like to thank those that have helped me get to this point. First, I would like to thank the Biological Systems Engineering Department here at Virginia Tech and my advisor Dr. Tess Thompson for allowing me this opportunity to further my education. I know I didn't always make it easy on you Tess, but I appreciate you always being there to guide me through this. To my committee members, Dr. David Sample and Dr. Erich Hester thank you for your guidance and support throughout this project. To my lab group, "Tess's Tots", Rex Gamble, Ben Smith, Daniel Smith, Coral Hendrix and Samuel Withers, thank you for the help and support to getting to this point. I really appreciated having you all around and being able to bounce ideas off each other. Another huge thanks to Laura Lehmann, Allen Yoder, Lauren Wind, the Town of Blacksburg Utilities and the Town of Blacksburg Fire Department for their assistance with all the research set up, field work and materials needed for this project. To all my friends both here and afar, thank you for making this year as enjoyable as possible. I know were all sick of Zoom calls, but those weekly pick-me-ups really came in clutch and helped keep me motivated. Of course, last but not least to my family. Mom and Dad, thank you for everything over the years. I know you would've always liked me to be closer to home but I can't thank you enough for the all support and enabling me to go out and explore and chase my dreams. And to Joe and Nicole, thank you for all support and sibling love. This has really been an eye opening and constructive experience and I have learned more than I could imagine over the past 2 years. I look forward to utilizing the skills I have acquired at the next level.

Dedicated to my buddy Roscoe

Table of Contents

List of Figures

List of Tables

1 Introduction

Sport fishing is a valuable industry; the Virginia Department of Game and Inland Fisheries estimates that fishing alone is responsible for over $1.3 billion dollars in economic impact annually to the state (VADWR 2021). It is estimated that one out of every seven hours spent fishing in Virginia is for trout, and nearly 100,000 anglers fish for trout stocked by VDGIF annually (VADGIF 2016). Although Virginia has nearly 2,300 miles of cold-water streams harboring wild trout populations, Virginia's warm climate and anthropogenic impacts have limited year-round trout habitat to higher elevation mountain streams. As a result, nearly 80% of Virginia trout fishing relies on the over one million catchable size trout stocked annually by the Virginia Department of Game and Inland Fisheries (VADGIF 2016). In 2014, the stocking program cost an estimated $2.4 million. This cost was only partially offset by the sale of licenses, resulting in a tax burden for the state. Therefore, properly managing wild trout populations and creating habitat conducive to year-round survival may relieve stress from this trout stocking program and provide more economic gain for the state.

Brook trout (*Salvelinus fontinalis*), Brown trout (*Salmo trutta*) and Rainbow trout (*Oncorhynchus mykiss*) are three trout species found in Virginia (VADGIF 2016). The Eastern Brook trout is the official freshwater fish of Virginia and the only trout species native to the region (Vuocolo, Hofman and Benzing 2019). Due to water temperature increases and other anthropogenic changes, Brook trout have declining populations and range, especially at lower altitudes in the southern margins of their native range (Meisner 1990; Smith and Skarlew 2013). Brook trout have been removed completely from 28% of historically occupied watersheds and greater than 50% population losses have been documented in 35% of the remaining watersheds in the eastern United States (Rummel 2018). Trout and other salmonids are among the fish species

that are most susceptible to changes in water temperature (Jones and Hunt 2009). The optimal water temperature range for trout and salmonids is 7-14°C (Wardynski et al. 2014), and in general they have been observed to avoid water temperatures of 21°C and higher (Coutant 1977). Long term exposure to water temperatures of 21°C stresses these species, affecting growth, behavior, reproduction, susceptibility to disease and lifespan (Elliot and Elliot 1995; Meisner 1990). As a result, temperature is listed as a pollutant of concern for lists of impaired streams required by Section 303(d) of the Clean Water Act in many states with trout and salmon populations. However, the regular fluctuation of natural stream temperatures has made the implementation of total maximum daily loads (TMDL) programs for temperature mitigation difficult (Jones and Hunt 2009).

Continued trends in urbanization are poised to put additional strain on already impaired stream networks. The increase of impervious surfaces associated with urbanization results in increased runoff temperatures and thermal loading, raising the temperature of water bodies above historic levels (Kieser et al. 2004). Streams have a complex thermal regime; water temperatures fluctuate both on a spatial and temporal scale and any alteration to this regime may impact the behavior and life cycle of aquatic organisms (Steel et al. 2017; Wehrly et al. 2007). Stream temperature increase has been documented in highly developed areas. In a 51-year analysis from 1960-2010, Rice and Jastram (2015) observed an increase in the instantaneous water temperatures of 0.028°C per year in the mid-Atlantic region. If these trends continue at this rate, there may be long lasting effects on ecosystem processes such as biological productivity and stream metabolism, contaminant toxicity, and eutrophication which could ultimately result in the loss of aquatic biodiversity (Kaushal et al. 2010).

Stream temperatures are highly influenced by climatic factors. Solar radiation and air temperature are identified as the two major heat sources that directly impact stream temperatures (Edinger, Duttweiler and Geyer 1968; Watson and Chang 2017). As a result, streams are most susceptible to thermal pollution during summer months because air temperature and solar radiation are highest and stream baseflow is lowest (Chen, Hodges and Dymond 2021). In addition, thermal pollution from surface runoff during summer months is of key interest because pavement temperatures are highest during the summertime. Due to a lower albedo, impervious surfaces such as asphalt capture solar radiation throughout the day and store this energy as heat. During a rainfall event, this stored heat energy is then transferred to surface runoff and transported to receiving water bodies, potentially increasing stream temperatures. Asphalt temperatures can reach summertime maximum temperatures greater than 60°C (Diefenderfer 2006), and runoff temperatures from impervious surfaces were observed in excess of 30°C (Sansalone et al. 2005; Jones and Hunt 2009). Furthermore, the increase in impervious surfaces results in less infiltration and more surface runoff. This exacerbates the issue of thermal pollution; not only is the runoff warmer, a great volume is entering stream networks as surface runoff (Jones, Hunt and Winston 2012).

Bioretention cells are a popular stormwater control measure (SCM) that is commonly used for pollutant reduction and stormwater infiltration in urban watersheds. Characterized as vegetated depressions in the landscape, bioretention cells are designed to mimic pre-development hydrology, reducing peak flows and total storm water volume reduction (Debusk and Wynn 2011; VA DEQ 2013). Bioretention cells are designed to treat highly impervious drainage areas, less than 0.01 km^2, on site (VA DEQ 2013). By collecting surface runoff bioretention cells promote sediment deposition and infiltration, through which contaminants such as phosphorus, nitrogen and heavy

metals can be significantly reduced (Roy-Poirier, Champagne and Filion 2010). Cell design is usually based on local or state design specifications and is dictated by drainage area size (VA DEQ 2013), but in general, a bioretention cell design will typically include an engineered or native soil mixture to maximize infiltration, an overflow and underdrain system to adequately drain the cell and prevent flooding, and a mulch layer to promote vegetative growth and native vegetation (VA DEQ 2013).

Recently, research has focused on the potential of bioretention cells for runoff temperature reduction, especially in watersheds harboring temperature-sensitive aquatics species such as trout and other salmonids (Jones and Hunt 2009). Through infiltration, thermally enriched surface runoff can transfer heat energy absorbed from impervious surfaces to cooler soil sub layers before exiting the cell. Storm water volume lost through exfiltration into the underlying water table and through evapotranspiration processes adds an additional benefit as reducing outflow volumes will reduce the thermal impact on the receiving water body (Jones and Hunt 2009; UNHSC 2011). Previous research has indicated that bioretention facilities can reduce maximum and median runoff temperatures from inlet to outlet (Long and Dymond 2013; Jones and Hunt 2009; UNHSC 2011). However, effluent temperatures were often greater than the 21°C temperature stress threshold for cold-water species, indicating that more research is needed to inform cell design for temperature-reduction purposes.

Although previous research has established the potential for using bioretention cells to mitigate thermal loads from urban stormwater on a local scale (Long and Dymond 2013; Jones and Hunt 2009; UNHSC 2011) few studies have discussed how the design of these bioretention cells may impact the potential for thermal mitigation. Research suggests that a deeper cell design will be more effective in reducing runoff temperature as soil temperatures are typically cooler and

more stable at greater depths (Long and Dymond 2013; Jones and Hunt 2009). However, quantitative field data are limited, therefore more field data may provide insight to improve bioretention design with respect to thermal mitigation. Furthermore, there is little consistency with reporting results in studies monitoring temperature reduction through bioretention cells and other SMCs (Wardynski et al. 2014); making it difficult to compare results from existing studies. Often, only median and maximum influent and temperatures are reported (Jones and Hunt 2009; Natarajan and Davis 2010). Although these metrics may indicate temperature reduction on an individual storm basis, they may not be representative of the entire storm as the first flush will typically generate the highest runoff temperatures (Wardynski et al. 2014). In addition, temperature medians and maximums often reported do not consider flow volume and volume reduction which will ultimately have a major impact on stream temperatures. Using metrics such as event mean temperature and heat load may provide more valuable data for monitoring thermal reduction through bioretention cells as these metrics are flow-weighted (Wardyski et al. 2014).

1.1 Research Objectives

The overall goal of this research was to investigate changes in stormwater thermal load due to bioretention cells. The objectives of this research were:

1. Quantify changes in event-mean temperature and heat load during summer months due to bioretention cells
2. Identify those design characteristics that enhance thermal load reduction, particularly for the benefit of trout species.

2 Literature Review

2.1 Stream Temperatures

Stream temperature is an important habitat constraint in aquatics environments and can directly impact the behavior and life cycle of aquatic organisms (Jones and Hunt 2009; Wehrly et al. 2007). Increases in stream temperatures can have detrimental effects on stream ecology including reduced dissolved oxygen and increased metabolic rates (Winston et al. 2011), which can increase organism susceptibility to heavy metals, parasites and disease (Jones 1976; Wahli et al. 2002). Furthermore, warming water temperatures can affect the biogeochemical balance of a stream. Duan and Kaushal (2013) observed that higher water temperatures can significantly increase stream soluble reactive phosphate concentrations (SRP), while also increasing the quantity and decreasing the quality of dissolved organic carbon. An increase in SRP results in higher eutrophication potential downstream while changes in carbon quality and quantity may impact microbial metabolism and alter food chains (Duan and Kashual 2013). However, due the complex interactions between organisms in the same thermal niche the full effect of increased temperatures is hard to determine (Huff et al. 2005).

Due to climatic changes and urbanization, stream temperatures are increasing. An analysis of historical records from 40 sites across the United States found that 20 major stream and river networks have shown an annual increase in mean water temperature by 0.009-0.077°C per year (Kaushal et al. 2010). In this study, warming rates were most rapid in urbanizing areas and long-term water temperature increases were correlated to increases in air temperature. Additionally, in a study of the Chesapeake Bay region, Rice and Jastram (2015) found an annual increase of 0.023°C in monthly mean air temperature and 0.028°C in the instantaneous stream water temperatures over a 51-year assessment. If stream temperatures continue to increase at this rate,

there may be long lasting effects on ecosystem processes such as biological productivity and stream metabolism, contaminant toxicity, and eutrophication which could ultimately result in the loss of aquatic biodiversity (Kaushal et al 2010).

The mid-Atlantic region is a highly urbanized area containing numerous cities and large expanses of growing suburban development. For context, between 1982 and 1997 the Chesapeake Bay watershed lost more than 750,000 acres of forest to urban development (Chesapeake Bay Program 2021). This equates to a rate of about 100 acres a day. In addition, a multitemporal Landsat imagery study of the Chesapeake Bay watershed found an 61% increase in developed land from 1990 to 2000 (Jantz et al. 2005). Of this increase in new development, 64% occurred on agricultural and grasslands and 33% occurred on forested lands (Jantz, Goetz and Jantz 2005).

Trout and salmon are two popular game fish listed as species most sensitive to increased water temperatures (U.S. Environmental Protection Agency 2003). In particular, cold water fish species such as Brook trout, Brown trout, and Rainbow trout (*Oncorhynchus mykiss*) are coveted by anglers; however, these species require a specific water temperature to sustain a viable population. Thermally enriched runoff from urban watersheds increases average water temperature, creates heat load spikes and leads to intermittent downstream temperatures peaks which can degrade aquatic habitat and stress these aquatic species (Elliott and Elliott 1995; Jones and Hunt 2009; Wardynski et al. 2014). As stream temperature increases the amount of dissolved oxygen water can hold decreases. Low oxygen levels cause stressful conditions for these species affecting their behavior, growth, lifespan and their ability to reproduce (Meisner 1990). The optimal temperatures for trout and other salmonids range from 7-14°C (Wardynski et al. 2014). Water temperatures exceeding 21°C have a significant impact the growth of Brook trout, while temperatures exceeding 25°C over seven days can be fatal. Temperatures at or above 30°C can be

fatal, even for a short exposure of 10 minutes or less (Elliot and Elliot 1995; Wehrly et al 2007). Due to water temperature increases and other anthropogenic changes, species such as Brook Trout have declining populations and range, especially at lower altitudes in the southern margins of their native range (Meisner 1990; Smith and Skarlew 2013). Brook trout have been removed completely from 28% of historically occupied watersheds and greater than 50% population losses have been documented in 35% of the remaining watersheds in the eastern United States (Rummel 2018). Only about 5% of the brook trout populations, all of which are in Maine, remain at or near historic numbers in the United States (Smith and Skarlew 2013).

2.2 Impacts to Stream Temperatures

Much like a flow regime, stream temperatures fluctuate spatially and temporally, creating a diverse thermal regime within a stream network (Steel et al. 2017). Stream temperatures are influenced by many factors, but meteorological factors have the greatest influence because they control the heat exchange between the water and air (Janke et al. 2009; Arrington et. al 2008). Solar radiation and seasonal cycles in air temperatures are identified as two major heat sources impacting stream temperatures (Edinger et al.1968; Watson and Chang 2017). As a result, streams are most sensitives to thermal impacts during summer months when air temperature and solar radiation are highest (Chen et al. 2021; Nelson and Palmer 2007). Stream baseflow is typically lowest during summer months, exacerbating the effects of thermal pollution (Arrington et al. 2004). Vegetative shading and landcover features influence the amount of solar radiation that reaches the surface (Booth et al.2014; Watson and Chang 2017). A lowering of maximum water temperatures, by upwards of 5°C during summer months, is attributed to providing adequate riparian vegetation when compared to unshaded sections (Broadmeadow et al. 2011). Meanwhile,

deforestation will decrease shading, lower evapotranspiration rates and increase soil temperature (Nelson and Palmer 2007).

2.3 Urbanization and Runoff Temperatures

In undeveloped watersheds, rainfall events decrease or just slightly increase water temperature in stream systems (Brown and Hannah 2007). However, urbanization and the increase in impervious surfaces are increasing storm thermal loading in urban areas. Pavements like asphalt are darker surfaces that have lower albedo, meaning the pavement will absorb more solar radiation and store this as heat (Alleman and Heitzman 2019). In addition, asphalt has a low thermal conductivity, 0.75 W/m°C, meaning that thermal energy will not be readily passed through this material to underlying soil layers (Alleman and Heitzman 2019). As a result, heat energy captured as solar radiation will be stored on the surface of asphalt pavements. Diefenderfer et al. (2006) observed summer daily maximum asphalt temperatures of 60°C. Impervious surfaces transfer heat to surface runoff (Janke et al 2009; Jones and Hunt 2009; Jones, Hunt and Winston 2012), reduce runoff travel time and infiltration, resulting in more direct runoff into streams. For example, a monitoring study in Louisiana found that highway runoff temperature exceeded 29°C (Sansalone et al. 2005). In Lenoir, North Carolina, runoff temperatures from parking lots exceeded 30°C (Jones and Hunt 2009). Furthermore, runoff temperatures from summer storms typically exhibit short term spikes near the beginning of a storm as the pavement cools (Winston et al. 2011). Although temperature spikes are greatest in the afternoon, heat stored by pavement can produce runoff temperatures substantially higher than stream temperatures throughout the night and into the morning (Lieb and Carline 200). In addition, storm characteristics play a role in heat export from paved surfaces. In a modeling study, Janke et al. (2009) found that heat export and runoff temperatures are more sensitive to rainfall intensity, rainfall duration and antecedent pavement

temperature than the physical properties of the pavement itself. So further identifying storms that may produce higher thermal loads may aid in bioretention cell design.

2.4 Bioretention Cell Overview

Bioretention cells are a stormwater control measure (SCM) that is commonly used for hydrologic and water quality mitigation in watersheds impacted by urban development (Li et al. 2009; Roy-Poirier et al.2010). In general, bioretention cells are vegetated depressions in the landscape that collect surface runoff from highly impervious surfaces such as parking lots, industrial complexes and residential communities. Typically, these cells consist of native vegetation, an engineered soil mixture, and an underdrain and overflow structure connected to a storm drain system (VA DEQ 2013). Many states have state-specific design specifications for cell construction, but often these guidelines are adopted from publications by other state agencies with little consideration for modifying the guidelines to fit local conditions (Davis et al. 2009). Construction limitations often dictate the completed bioretention cell design.

The bowl of a bioretention cell refers the surface-ponding zone which has a surface area of anywhere between 2-7 percent of the total watershed area, depending on the state design guidelines and/or design goals. The maximum depth of ponding depth is typically between 15 cm (6 in.) and 30.5 cm (12 in.) with an excess outfall drain to prevent ponding above this height. The filter media should be a minimum of 61 cm (24 in.) with a recommended maximum of 182 cm (72 in.) and is generally classified as loamy sand on the USDA Texture Triangle (Figure 1-1). These soils have an approximate composition of 85-88% sand; 8-12% soil fines; and 3-5% organic matter by volume (VA DEQ 2013). The soil media should have a minimum infiltration rate of 2.5 to 5.1 cm per hour (1-2 in. per hour), but a proper mixture as described above should have a significantly higher initial infiltration rate.

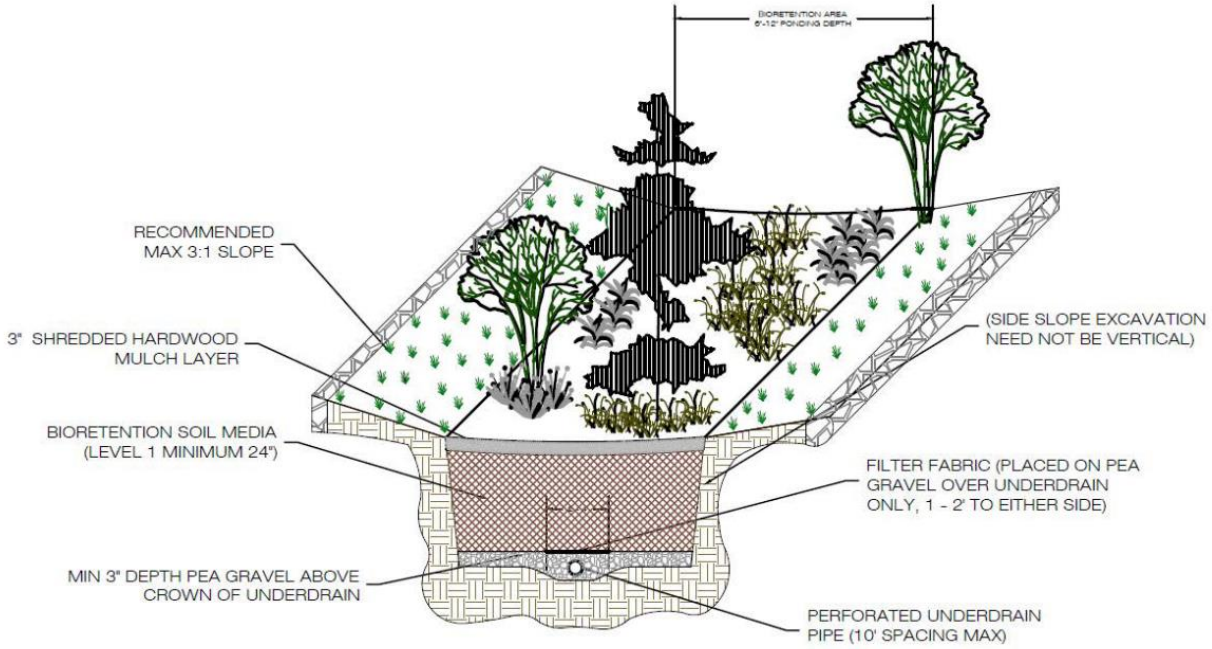

Figure 2-1. Typical bioretention cell design (VADEQ 2011).

2.5 Thermal Impact Reduction Through Bioretention

Bioretention offers a means of reducing thermal impacts to surface waters through infiltration and heat transfer. The best way to mitigate thermal pollution is to infiltrate heated runoff (Hunt et al. 2012). In a study of bioretention cells in North Carolina Jones and Hunt (2009) demonstrated that bioretention cells with deeper soil media depths were more effective at cooling surface runoff than cells with a shallower design. Effluent temperatures were generally cooler with greater soil depths during summer months, leading the researchers to suggest that optimal drain depth is between 90 and 120 cm (Jones and Hunt 2009). A deeper design will allow a larger percentage of the soil media to be dissociated from external factors, such as ambient air temperature and direct sunlight, which cause temperature fluxes in the upper levels of the soil media (Hunt, Davis and Traver 2012; Jones and Hunt 2007). Soil depths greater than 120 cm were

cooler and had stable temperatures, while depths less than 60 cm were generally warmer and experienced major daily fluctuations during summer months (Jones and Hunt 2007). The deeper soil layers with a more consistent temperature range can provide an area of greater thermal reduction potential as runoff temperatures can equilibrate with surrounding soil temperatures before leaving the cell (Jones and Hunt 2009).

Cell depth is an important consideration as deep cells can potentially increase runoff temperatures during other seasons. Deeper soil layers will typically be warmer than surface soil layers and runoff particularly during the fall which is trout spawning season (Jones and Hunt 2009). In this case these warmer soil layers become a heat source, rather than a heat sink to the infiltrating runoff. Dietz and Clausen (2005) observed a significant increase in runoff temperatures (>1.5°C) during fall and winter months at a bioretention facility in Connecticut. In addition, this study observed slight temperature increases (0.5°C) during summer months; however, these runoff temperature increases were attributed to the lower influent temperatures to the facility (Jones and Hunt 2009). Although the average inflow and outflow temperatures were below the 21° stress threshold for trout, this highlights a potential design limitation that may vary by region. The bioretention cell monitored was 60 cm deep (Dietz and Clausen 2005), which is in the lower range of the optimal depth ranged suggested for temperature reduction (Jones and Hunt 2009).

Vegetative cover will also impact soil and pore water temperatures, especially in shallower cells (Hunt, Davis and Traver 2012; Jones and Hunt 2007). Broad leaf vegetation can provide more coverage, blocking direct solar radiation from reaching the cell surface, ultimately providing more cooling effects (Hunt, Davis and Traver 2012; Jones and Hunt 2007). Mulch selection can also reduce soil temperatures as lighter colored mulch will deflect more solar radiation (Jones and Hunt 2007).

Infiltration rates may impact thermal reduction potential as well, Hunt and Lord (2007) suggest that slower rates, less than 5.08 mm per hour, may be preferable for temperature reduction. In addition, a case study by Hunt et al. (2012) suggested maximizing the hydraulic retention time (T_{hr}) in the deeper, cooler sub layers of a bioretention cell or the underlying soils as a key design component for thermal mitigation. Furthermore, differences between soil and effluent temperatures suggest that additional cooling occurs as water is collected by the underdrain system and conveyed to the outlet (Jones and Hunt 2009). Jones and Hunt (2009) also noted that in locations where the underlying soil had a high conductivity, an underdrain system may not be required as runoff will seep into underlying soils rather than be discharged. The removal of an underdrain system will increase flow reduction potential as a greater volume of runoff can infiltrate into the soil sublayers; however, this will also increase the risk of over flow during large storm events if the runoff soil media cannot drain fast enough. During a single storm event, overflow typically occurs at the tail end of the storm, so, the thermal impacts are likely minimal as runoff temperatures are typically cooler at this point. However, if a bioretention cell is not completely drained between storm events, overflow may begin earlier in the subsequent event when runoff temperatures tend to be higher (Jones and Hunt 2009).

Ultimately the amount of water exfiltrated and stored in cell soil media will have the greatest impact on the effluent volume, reducing the overall quantity of surface runoff. Bioretention offers an effective means of thermal mitigation through flow reduction (Jones and Hunt 2009). Studies have shown that the effluent volume from bioretention cells can be less than 50% of the influent volume and the greatest reductions were evident during the warm summer months (Debusk and Wynn 2011; Hunt et al. 2006; Li et al. 2009). Even when bioretention cells did not effectively lower runoff temperatures, these systems reduce thermal loads from runoff

because it is not possible for runoff volumes to increase through bioretention (Jones and Hunt 2009). Hunt and Lord (2006) suggest that internal water storage (IWS) at the bottom of cell may reduce effluent temperatures but the top of the IWS layer should be at least 0.9 m from the cell surface. IWS would also further reduce runoff volumes by promoting groundwater recharge, potentially reducing the thermal load further (Hunt and Lord 2006). Research also indicates that bioretention cells in areas with high conductivity underlying soils should not have an impermeable liner, clay or otherwise, to promote stormwater movement into shallow ground water (Jones and Hunt 2009).

Jones and Hunt (2009) also suggested that bioretention area may be a distinguishing design factor for thermal reduction potential. The researchers indicated that cells that covered smaller areas with respect to their watershed area were able to significantly reduce both the maximum and median temperatures between the inlet and outlet. Bioretention cells that covered a larger percentage of the watershed were only able to significantly reduce maximum temperatures between inlet and outlet (Jones and Hunt 2009). In this study the relatively smaller had substantially higher median and maximum higher influent runoff temperatures than the larger cell, suggesting that oversizing bioretention cells may have minimal benefits for temperature reduction. However, the larger cell generated less outflow, effectively reducing the thermal load (Jones and Hunt 2009). Li et al. (2009) indicated that cells with high media volume-to-watershed size ratios were more effective at reducing outflow. Furthermore, Jones and Hunt (2009) suggest that larger cells have relatively more soil available to absorb heat from runoff and that soil temperature changes during storm events would be limited to shallower soil depths.

Although runoff temperature reduction through bioretention cells was observed in multiple field studies, effluent temperatures were often greater than the 21°C stress threshold for cold-water

fish species (Jones and Hunt 2009; UNHSC 2011). In a field study of four bioretention cells in North Carolina, three cells produced median and maximum outflow temperatures greater than 21°C (Jones and Hunt 2009). Of these four sites, the cell with the greatest underdrain depth performed best with median and maximum effluent temperatures more than 2°C lower than the next best performing cell. However, it should be noted that median and maximum influent temperatures were significantly lower at this site (Jones and Hunt 2009). In a study comparing multiple SCMs for thermal reduction potential in New Hampshire, maximum summertime effluent temperatures through bioretention cells exceeded 22°C (UNHSC 2011). Performed by the University of New Hampshire Stormwater Center (2011), this study identified the upper optimum limit (UOL) for aquatic species as 18°C and observed that outflow from the bioretention cell exceeded this UOL 44% of the time during summer months.

2.6 Other SCMs for Thermal Mitigation

Bioretention cells are not the only SCM explored for thermal mitigation purposes. Retention ponds (Jones and Hunt 2010; UNHSC 2011), level spreaders-vegetative filter strips (Winston eta al. 2011), gravel wetlands (UNHSC 2011) and other infiltration systems, as well as underground detention systems (Natarajan and Davis 2010, UNHSC 2011), have been tested and shown to effectively reduce runoff temperatures during summer months. However, systems that promote infiltration and subsurface water storage are typically more effective at reducing runoff temperature (Hunt et al. 2012; Long and Dymond 2013; UNHSC 2011). Retention ponds and wetlands have mixed results (Jones and Hunt 2010). Provided there was adequate shading, systems that utilize surface storage can effectively reduce runoff temperatures (Kieser et al 2004). However, typically larger surface storage systems lack full shading which results in more direct solar radiation to the water surface, increasing water temperatures above the initial runoff

temperature. In addition, Jones and Hunt (2010) observed temperature stratification within the water column of these surface storage systems. Water temperatures at the bottom of the water column were consistently cooler than the water leaving the traditional outlet structures. This finding indicated that modified outlet structures that release water from the bottom of the water column should be used in regions with cold water aquatic species. Although not necessarily a SCM, subsurface drainage infrastructure in urban watersheds has shown to moderate runoff temperatures (Hathaway et al. 2016). Typically, larger urban watersheds incorporate more subsurface drainage systems and longer travel times to stream networks than smaller urban watersheds. In a statistical analysis of six watersheds in Australia and the United States, Hathaway et al. (2016) found that larger watersheds have lower maximum and minimum runoff temperatures as well as less temperature variability. This finding was attributed to the large expanses of subsurface drainage and illustrates how the location of an SCM and overall scale of the mitigation efforts may impact the effectiveness of thermal reduction efforts.

Despite being effective in reducing runoff temperatures on a local level, watershed-scale evaluations of SMCs have shown these measures alone are ineffective in reaching mitigation goals (Chen et al. 2021; Ketbachy et al. 2019). These studies modeled watershed-scale mitigation efforts using the Minnesota Urban Heat Export Tool (MINUHET) to assess the total heat load and event mean temperature leaving the watershed as well as the overall impact on stream temperatures. Ketabchy et al. (2019) explored the effects of retrofitting a 14.1 km^2 urban watershed with thermal mitigation practices (TMPs). This simulation included replacing impervious pavements and roofs with “cool” surfaces, increasing forest canopy cover and the inclusion of bioretention cells to reduce runoff temperature and heat loads in the urban watershed. In isolated scenarios with only one type of TMP, increasing forest canopy produced the greatest reduction in stream temperatures,

while cooler, less heat-absorbing surfaces reduced the total heat loads more than any other single TMP. Bioretention installations alone were the least effective mitigation method (Ketbachy et al. 2019). A comprehensive application of all TMPs resulted in the lowest total heat loads and mean temperatures, but the simulated stream temperatures still exceeded the established comprehensive mitigation plan threshold 26% of the time, indicating that mitigation goals were unattainable with this approach (Ketbachy et al. 2019). Chen et al. (2021) conducted a similar analysis in a considerably smaller urban watershed, 0.8 km^2. Using only bioretention retrofits, temperature spikes resulting from storm runoff decreased; however, this treatment method was unable to effectively reduced thermal impacts below acceptable thresholds, resulting in the conclusion that bioretention systems alone are not an effective solution for mitigating thermal degradation in streams (Chen et al. 2021).

2.7 Metrics for Monitoring Thermal Reduction

Although there are multiple studies detailing the thermal interactions within SCMs, there has been little consistency in reporting results (Wardynski et al. 2014). As a result, it can be difficult to compare thermal reduction potential among studies and SMCs. Metrics such as maximum, minimum and median inlet and outlet temperatures are often presented in SCM research can be useful for assessing temperature buffering potential for a single event. However, these measurements are limited when determining the extent of thermal reduction because they do not consider heat load (total thermal energy) exported form the SCMs (Jones and Hunt 2009; Natarajan and Davis 2010; Winston et al. 2011). Temperature is only useful when related to downstream temperature standards for a specific region and when runoff reduction is also considered (Wardynski et al. 2014).

Calculating the event mean temperature (EMT) is a representative method to compare average influent and effluent temperatures. The EMT is calculated using the Equation 1 below:

$$EMT = \frac{\int_0^T t(t)q(t)dt}{\int_0^T q(t)dt} \tag{1}$$

For this calculation, *t(t),* the instantaneous temperature and *q(t),* the instantaneous discharge, are integrated over the duration of the flow event, *T*. Since these instantaneous temperatures are weighted by discharge, this calculation offers a more representative metric and provides a better understanding of temperature reduction through a SCM (Wardynski et al. 2014). Although the EMT is a more comprehensive metric, it has limitations. Like maximum, minimum and median temperature measurements, this metric is only useful when the fraction of water removed from the SCM through exfiltration and evapotranspiration is considered (Wardynski et al. 2014). Furthermore, the EMT is a flow-weighted average so it mutes the maximum thermal exposure, therefore it mutes the full impacts of effluent stormwater on the stream and limits its usage for understanding fish stress (Wardynski et al. 2014). In addition, Wardynski et al. (2014) suggest that aggregating the influent and effluent for all storm events to calculate an "average percent removal" can be misleading. Their justification is that SMC performance will be dependent on influent temperatures and seasonal variations in runoff temperature can clutter this analysis (Strecker et al 2001).

Another metric used in SCM research is thermal load reduction (Winston et al. 2011; Wardynski et al. 2013). Thermal load considers both stormwater temperature and volume reduction through a SCM, and is defined as *H* in Equation 2 below:

$$H = Q * t * T * C * \rho \tag{2}$$

Where Q is flow rate, t is time duration, T is the temperature of the stormwater, C is the specific heat capacity of water and, ρ is the density of water. This metric is more valuable than temperature reduction alone because it accounts for volumetric loss through a SMC due to exfiltration, retention and evapotranspiration (Wardynski et al. 2014). To understand the impacts of stormwater on stream temperature, thermal load must be determined so a heat balance can be calculated for the stream. However, for any increase in stream temperature to occur, the stormwater temperature entering the stream, regardless of load, must be higher than the receiving stream water temperature (Wardynski et al. 2014). This means that heat load alone can be misleading and should analyzed in conjunction with stormwater and stream temperatures.

Lastly, neither of the metrics discussed above consider the duration of exposure of coldwater species to elevated temperatures (Ross and Hari 2007). The uniform continuous above threshold (UCAT) method, as proposed by Castelli et al. (2012), may provide the best metric for estimating the impacts of development on study reach temperatures. This method compares a study stream and a reference stream to assess a statistical probability analysis of thermal impacts on a stream (Wardynski et al. 2014). A comparison of this UCAT method provides a more holistic approach to thermal impacts than a single-value biological threshold (Wardynski et al. 2014). However, this method is data intensive and requires long term temperature data from a reference stream. In this instance, reference streams should be unaffected by development yet hydrologically and physically similar to the study stream in question, which may cause limitations in itself (Wardynski et al. 2014).

A combination of different types of metrics is necessary to understand the full thermal impacts on a stream regardless of methods and thresholds used (Wardynski et al. 2014). When assessing thermal impacts on streams, metrics should be feasible given study goals, constraints

and availability of reference data. Threshold values should reflect the goals of the study and the identified target species if biologically driven (Wardynski et al. 2014).

2.8 Summary

Urbanization and the increase of impervious surfaces can lead to higher stormwater temperatures and thermal loads to streams, increasing stream temperatures. Global trends of climate change and urbanization indicate that these impacts will only be further exacerbated as air temperatures increase and urbanization and deforestation continue to expand. The increase stream temperatures can be detrimental to aquatic life, especially cold-water fish species such as trout that can only exist within a certain temperature range. Long term exposure at 21°C is widely regarded as the temperature threshold at which trout begin to show signs of stress, affecting behavior, growth, ability to reproduce, risk for disease and ultimately death. Acute exposure to even higher water temperatures can be fatal in relatively short exposure times. Trout and other salmonids are highly sought-after game species that provide a substantial economic impact in the Commonwealth of Virginia. Due to stream temperature increase and other anthropogenic effects, these species are declining in range and populations, putting stress on the fish hatchery system to meet the demands of anglers. As a result, methods of stormwater thermal mitigation are currently being explored to reduce the impact of urbanization on cold water aquatic ecosystems.

Bioretention cells are a popular SCMs that offer a means of thermal mitigation for urban stormwater. Heat transferred to surface runoff from impervious surfaces during the summer is able to again transfer this thermal energy to a bioretention facility before reaching the stream network. In addition, bioretention enables water storage and runoff reduction through exfiltration and evapotranspiration, which effectively removes this thermally enriched runoff from reaching streams as surface flow. Studies have shown that bioretention cells are effective in reducing

thermal loads and effluent temperatures from surface runoff. Despite reducing these key factors contributing to thermal pollution, effluent temperatures from monitored bioretention cells were often above this 21°C threshold for trout during summer months, indicating bioretention alone may not reduce thermal loads to an acceptable level. However, more research is needed to explore the potential of bioretention cells to reduce thermal pollution. Design characteristics such as cell depth, shading, and ratios of cell surface area to the drainage area and storage volume to drainage area, among other factors may influence how effective these facilities can be in reducing stormwater heat loads.

3 Methodology

3.1 Methods Overview

Two bioretention cells with different design characteristics were monitored to quantify changes in EMT and thermal loads due to treatment in bioretention cells. Inflow and outflow temperature and flow rates were monitored from June 10th 2020, to September 30th 2020. For each storm that generated inflow into the cells the stormwater volume, event mean temperature (EMT) and heat load were calculated for inflow and outflow. Statistical tests were performed to test for significance between inlet and outlet EMTs and heat loads. In addition, vertical soil temperature profiles were created for each storm as well as the entirety of the monitoring period to identify summertime patterns and temperature trends during storm events. Lastly, a multiple linear regression of explanatory variables for high EMTs from the parking lot drainage areas was conducted to identify the driving forces elevating stormwater temperatures.

3.2 Site Overview

The two bioretention cells monitored in this study are located in Blacksburg, Virginia (37° 14’ N, 80° 24’ W). Blacksburg is located in the Valley and Ridge physiographic province, which

is characterized by dolomite and limestone geology resulting in the karst topography found in the area. From 1981 to 2010, the average daily and maximum summertime temperatures for Blacksburg are 21°C and, 27.2°C, respectively, and on average the area receives 301 mm of precipitation during summer months (NCDC 2021). Both cells were located in the Stroubles Creek watershed, a mostly urban watershed that includes the majority of the Town of Blacksburg and the entirety of the main Virginia Tech campus. In 1996, Stroubles Creek was listed as impaired on the Virginia 303(d) list for aquatic life and bacterial impairments, with sediment identified as the source of the benthic macroinvertebrate community impairment (Wynn et al. 2010). Since then, the Town of Blacksburg, Virginia Tech Facilities, and the Biological Systems Engineering department have worked collaboratively to implement SCMs throughout the Stroubles Creek watershed to reduce sediment and nutrient loads to Stroubles Creek.

3.3 Aquatic Center Cell Design

The first of the bioretention cells monitored for this study was located near the Blacksburg Aquatics Center (37° 14’ 36” N, 80° 24’ 42” W), draining a 1,600 m^2 asphalt parking lot (Figure 3-1). The pavement color was determined using Palette Cam, a mobile phone application that identifies the hexadecimal color numbers and RGB values in a desired section of a photo (Mathers 2016). The asphalt in the parking lot is weathered and some spots were recently patched so the color varies throughout the lot. Pavement colors were identified at three distinct locations along with an estimated percent coverage in order determine a representative color spectrum of the surface (Table 3-1)

This cell was constructed in 2007 as a design project for students in the BSE Comprehensive Design Project class (Morin and Debusk 2008). The bioretention cell has a cubic shape that is 4.6 m wide, 7.6 m long and 1.8 m deep resulting in a surface area of 34.96 m^2 and a

cell volume of 62.93 m^3 (Figure 3-2) (Willard et al. 2017). Due to site constraints, this cell had a SCM surface area to drainage area ratio of approximately 2.1% which is lower than recommend minimum ratio, 2.5%, (VADCR 1999) and the standard design ratios of 5-7% discussed by Hunt and Lord (2006) (DeBusk and Wynn 2011). In accordance with the *Virginia Stormwater Management Handbook*, the cell is designed to detain the first 13 mm of runoff from the parking lot and match the predevelopment peak flows of both a 2-year and 10-year 24-hr storm event (VADCR 1999).

Table 3-1. Aquatics Center cell parking lot color description and estimated area coverage.

Hexadecimal Number	RBG Number	Percent of Area Covered
#a59c90	R:165 G:156 B:144	20%
#444446	R:68 G:68 B:70	60%
#6a6a6c	R:106 G:106 B:108	20%

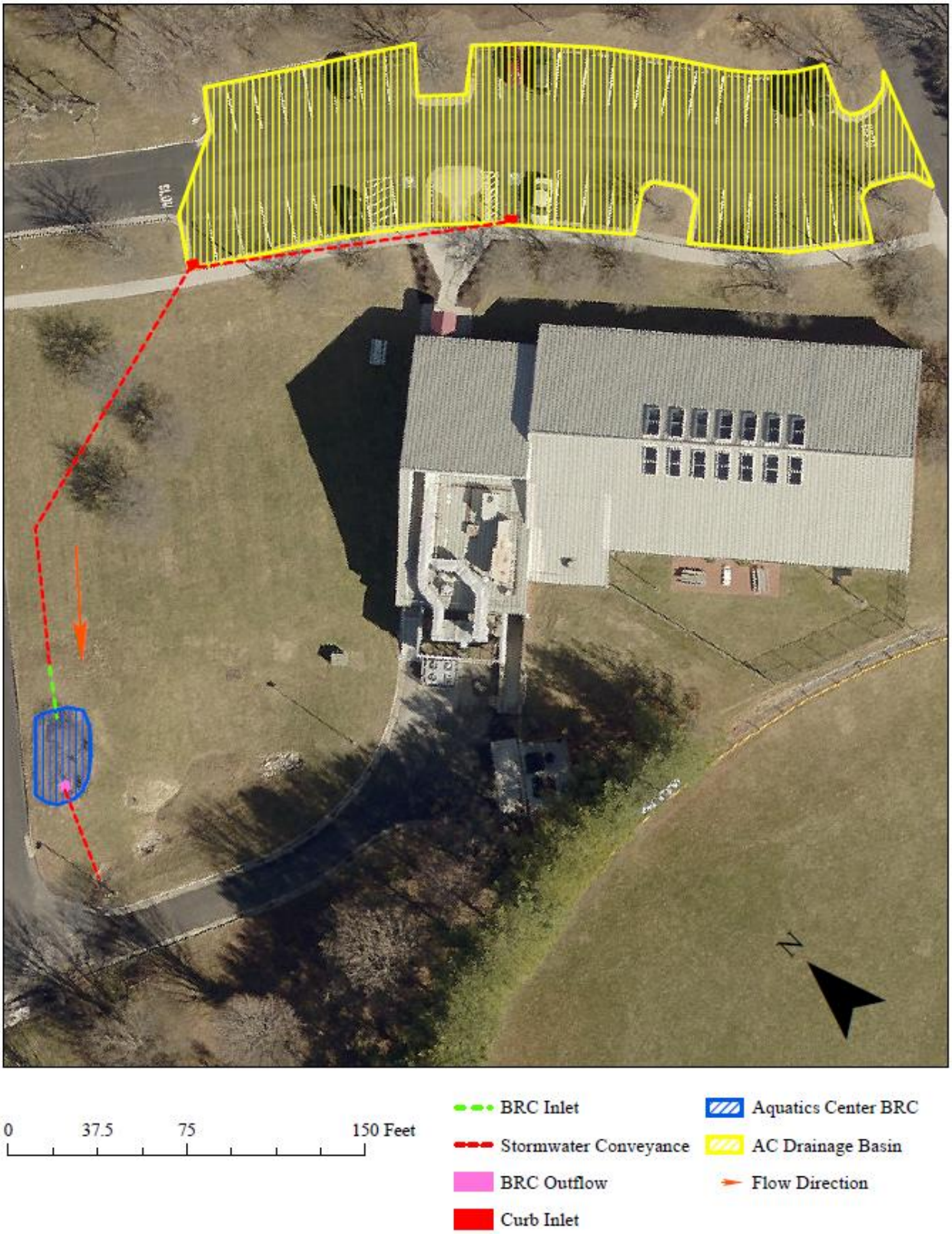

Figure 3-1. Aquatics Center cell plan view

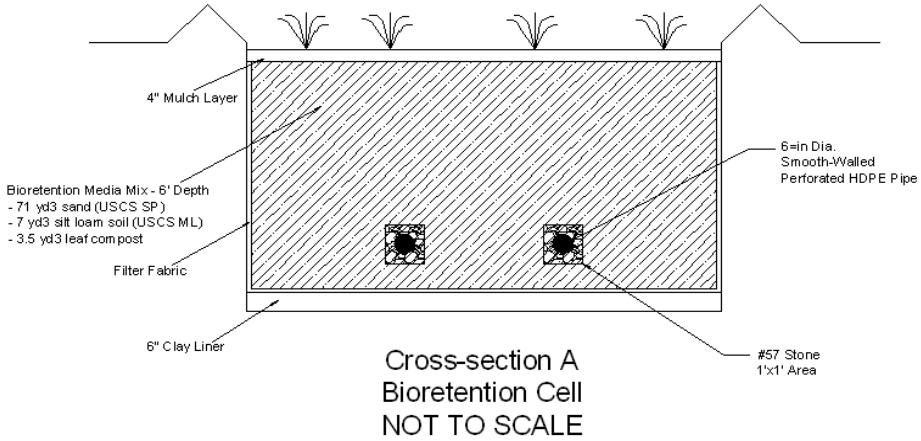

Figure 3-2. Aquatics Center cell cross-sectional view (Morin and Debusk 2008)

Surface runoff is collected by two storm drains in the parking lot and piped approximately 50 m via a 45.72 cm smooth walled corrugated pipe from the existing stormwater drainage system. This cell was designed to have a maximum ponding depth of 15 cm with a 91.4 cm by 91.4 cm manhole serving as the overflow drain, giving the cell a maximum ponding volume of approximately 5.2 m^3 (DeBusk and Wynn 2011; Willard et al. 2017). As recommended by Hunt and Lord (2006), when constructed the cell had a bioretention media consisting of 88% washed sand, 8% clay and silt fines and 4% organic material (leaf compost), by volume (DeBusk and Wynn 2011). This media was not compacted during construction to maximize the infiltration rate, with the assumption that the material would settle over time to the designed ponding depth. In addition, a 10 cm layer of mulch was added to the surface of the cell to promote the growth of the planted vegetation and to prevent surface crusting of the bioretention media. This vegetation included hardy native perennials, shrubs and trees; however, by the time monitoring began only

two Eastern Redbud trees (*Cercis canadenis*) and one Shadbush (*Amelancher canadenis*) were remaining.

Of the three trees in the cell, the Shadbush in the north east corner provided the most shading. This tree was approximately 3.7 m tall and had a 4.9 m canopy diameter at the widest point. The two Eastern Redbud trees were significantly smaller. The Redbud on the northern side of the cell was the smaller of the two, measuring 2.1 m tall with a 1.2 m maximum canopy diameter. The second Redbud on the southern side of the cell was slightly larger, measuring 2.7 m tall with a 1.8 m maximum canopy diameter. The location of the trees provided the cell with ample shading during the morning hours and minimal shading in the afternoon and evening hours (Figure 3-3). The broad leaves and dense canopy provide the cell nearly complete coverage at 8:30 AM (Figure 3-4 A). As the day progressed the shading diminished substantially. By 11:30 AM shading coverage was approximately 60% (Figure 3-4 B) and by 4:00 PM shading was approximately 10% (Figure 3-4 C). Finally, by the end of the day there was virtually no shading provided by the vegetation (Figure 3-4 D). To summarize, during the afternoon, when direct solar radiation is greatest, the cell had an estimated minimum and maximum shading of 10% and 60%, respectfully.

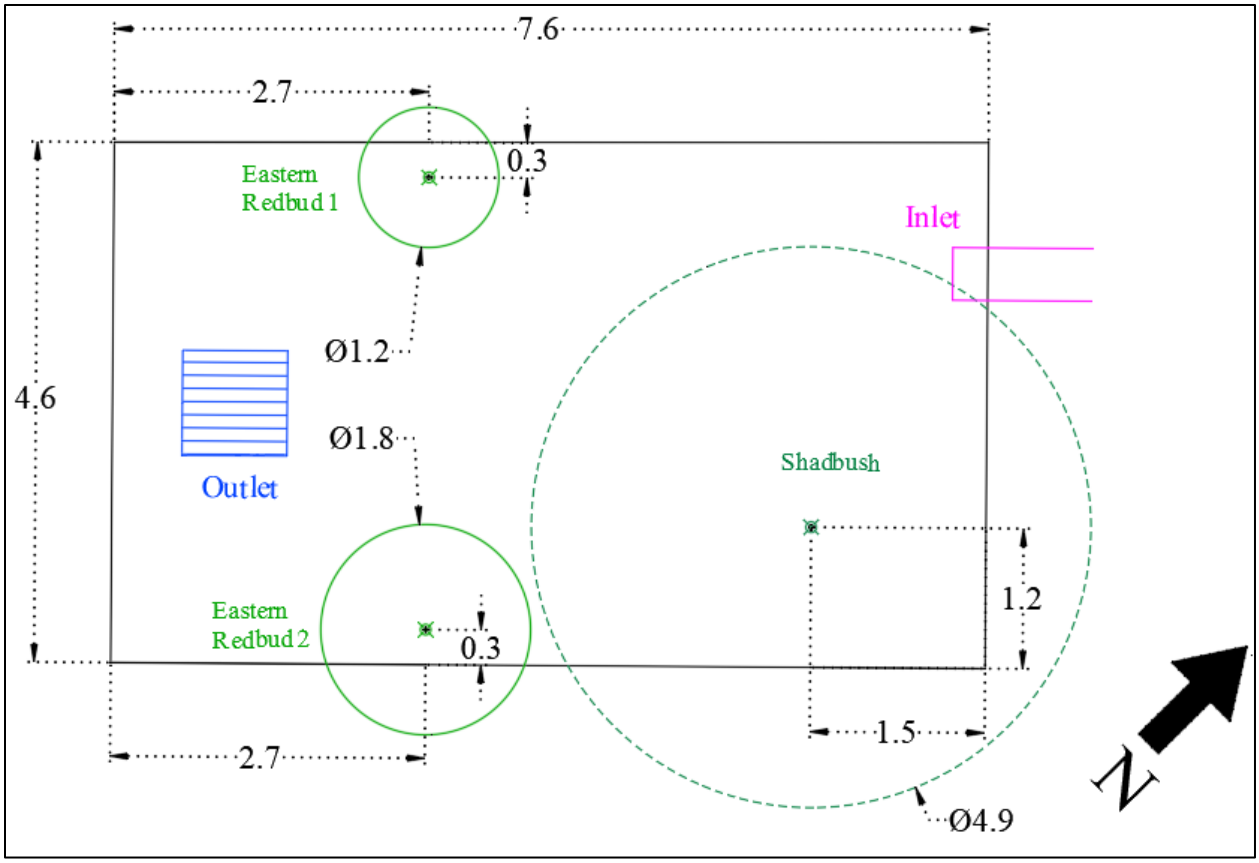

Figure 3-3. Aquatics Center vegetation location

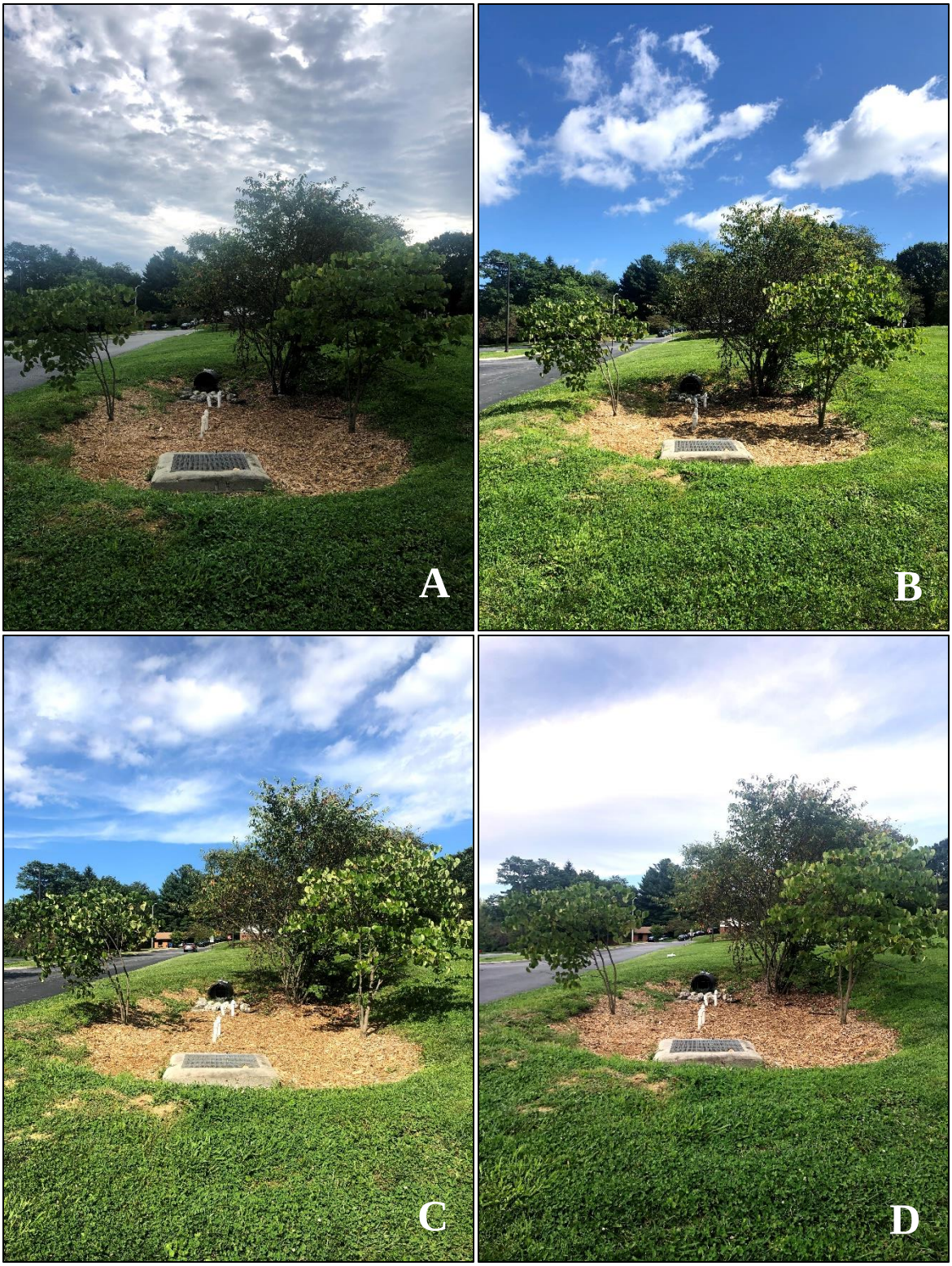

Figure 3-4 A-D. Aquatics Center cell shading on 08/30/2020. A) 8:30 AM, B) 11:30 AM, C) 4:00 PM, D) 7:00 PM

Due to the local karst topography, a 15 cm compacted clay liner was installed at the bottom of the cell to minimize concentrated ground water recharge which could result in the formation of a sinkhole. As a result, the cell has two parallel 10 cm perforated pipes spaced 1.52 m apart. Each pipe was wrapped in filter fabric and encased in a 0.304 m by 0.304 m area with #57 stone to prevent clogging. These pipes are connected to the outflow structure and located 30 cm above the bottom of the cell to provide internal water storage (IWS). Post-construction monitoring indicated the cell was effective in reducing flow volume and peak flow from the parking lot by 97% and 99%, respectively (DeBusk and Wynn 2011).

3.4 Campus Cell Design

The second bioretention cell monitored in this study is located on the main Virginia Tech campus, adjacent to the Smithfield Road parking lot at the intersection of Duck Pond Drive and Smithfield Road (37° 13’ 23” N, 80° 23’ 47” W). This cell was constructed as part of a parking lot expansion in 2006 and drains an approximately 3,500 m^2 portion of the upper Smithfield Road parking lot, which is asphalt (Figure 3-5). Again, the asphalt color was determined using the Cam Palette mobile app. Like the Aquatics Center site this lot was also weathered but there were only two distinct colors identified (Table 3-2). Surface runoff from the parking lot was collected by one curb inlet storm drain in the northern corner of the lot and piped approximately 24 m via a 38 cm diameter pipe to a pretreatment basin. This 20 m long and 5 m wide pretreatment basin was implemented to promote settling of sediment from the initial pulse of runoff inflow. The runoff collected in this pretreatment area was then piped into the bioretention cell by six 4.5 m long, 20.32 cm diameter corrugated plastic pipes. Trapezoidal in shape with sides slopes of 3:1, this cell has a surface area of approximately 240 m^2 and a media depth of 86.36 cm resulting in a cell volume of

approximately 207.3 m^3 This cell has a surface area to drainage area ratio of approximately 6.5% which falls into the standard range set by Hunt and Lord (2006).

Table 2-2. Campus cell parking lot color description with estimated area coverage.

Hexadecimal Number	RBG Number	Percent of Area Covered
#b5a8a0	R:181 G:168 B:160	30%
#35363b	R:53 G:54 B:59	70%

The media composition was unclear from the design plans but based on the standards set in the *1999 Virginia Stormwater Management Handbook*, the media should be 50% sand, 30% topsoil, and 20% leaf compost, by volume (VADCR 1999). The outlet structure is a 76 cm by 76 cm precast concrete square, with three 10 cm smooth wall polyethylene pipe orifices set at 13.7 cm above the cell surface to serve as the overflow drain. However, due to soil compaction, settling and degradation of the organic material in the cell media since construction, the ponding depth was 45.72 cm at the time of monitoring. This resulted in an approximate ponding volume of 109.7 m^3. For higher flow volumes this outflow structure had a 61 cm by 61 cm top grate as an additional measure to prevent the parking lot from flooding. Debris racks were installed around these orifices to prevent clogging. The outflow from this cell connects to the preexisting storm drain system and is piped approximately 90 m to Stroubles Creek.

The underdrain system consists of three parallel rows of 10 cm perforated corrugated pipes, trenched in a 10 cm deep layer of filter stone (VDOT No.1 Aggregate) wrapped in geotextile fabric.

The drainage pipes are connected to the outlet structure by a perpendicular 10 cm perforated corrugated pipe (Figure 3-6). The on-campus cell has a 15 cm clay liner below the drainage system to prevent infiltration into underlying soil. A geotextile fabric layer was placed between this clay liner and the bioretention soil mixture or stone aggregate above it. Unlike the Aquatics Center SCM there is no IWS included in this design; the drainage system is directly above the clay liner.

The cell was originally designed to have a 10 cm layer of mulch but when monitored, the mulch layer had decomposed and a layer of grass and weeds had developed (Figure 3-7 and 3-8). Prior to monitoring, the understory vegetation shown in Figures 3-7 and 3-8 was mowed by Virginia Tech Facilities to allow for equipment installation. This vegetation grew relatively fast as was mowed again towards the end of the monitoring period. The original planting consisted of 12 Monarch River Birch (*Betula nigra)* and 42 Sheep Laurel (*Kalmia angustifolia*) planted on the cell surface and 13 Witch Hazel (*Hamamelis virginiana*) planted on the outer rim between the cell and adjacent parking lot. These trees along with multiple large White Oak (*Quercus alba)*, American Beech (*Fagus grandifolia*) and Sugar Maple (*Acer saccharum*) around the cell provide more consistent shading throughout the day, as compared to the Aquatics Center Cell. During the morning and evening hours cell shading is nearly 100% (Figure 3-9 A and 3-9 D). However, due to the tree species and poor health, the River Birch in the cell does not have a dense canopy. As a result, shade cover over the cell is moderate during the middle of the day. The minimum shading was approximately 50% coverage at 11:30 AM (Figure 3-9 B), and the maximum shading was approximately 70% at 4:00 pm (Figure 3-9 C).

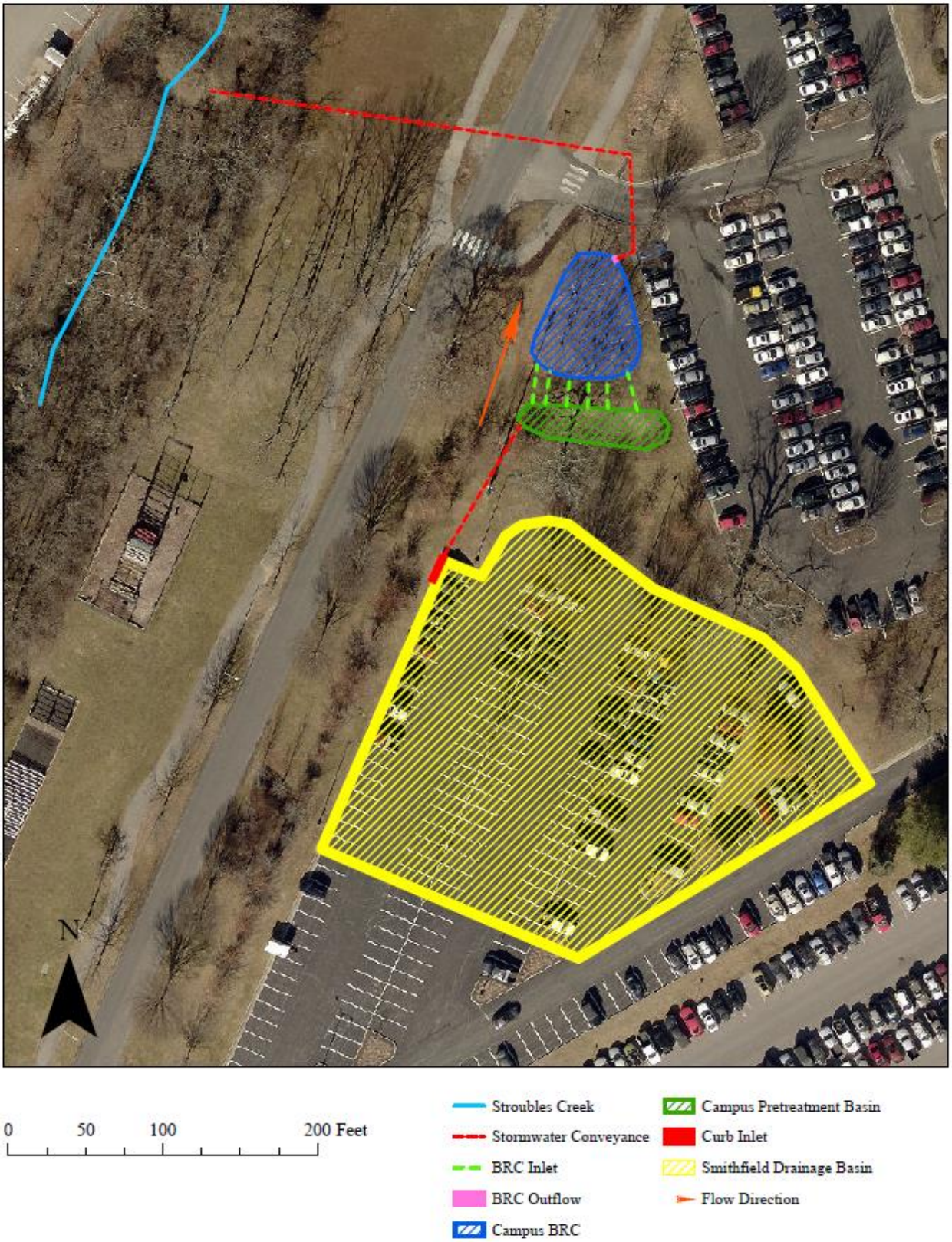

Figure 3-5. Campus cell plan view

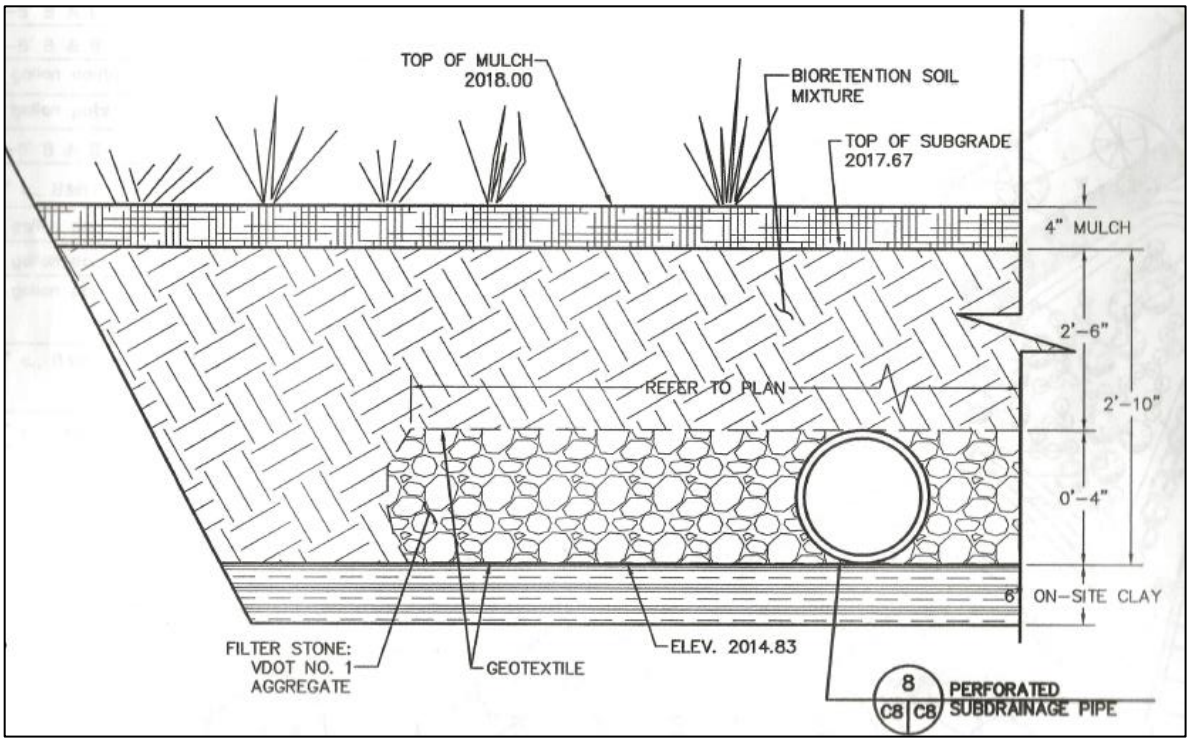

Figure 3-6. Campus cell cross section view (Draper Aden Associates 2005)

Figure 3-7. View of the Campus cell looking south

Figure 3-8. View of the Campus cell looking west

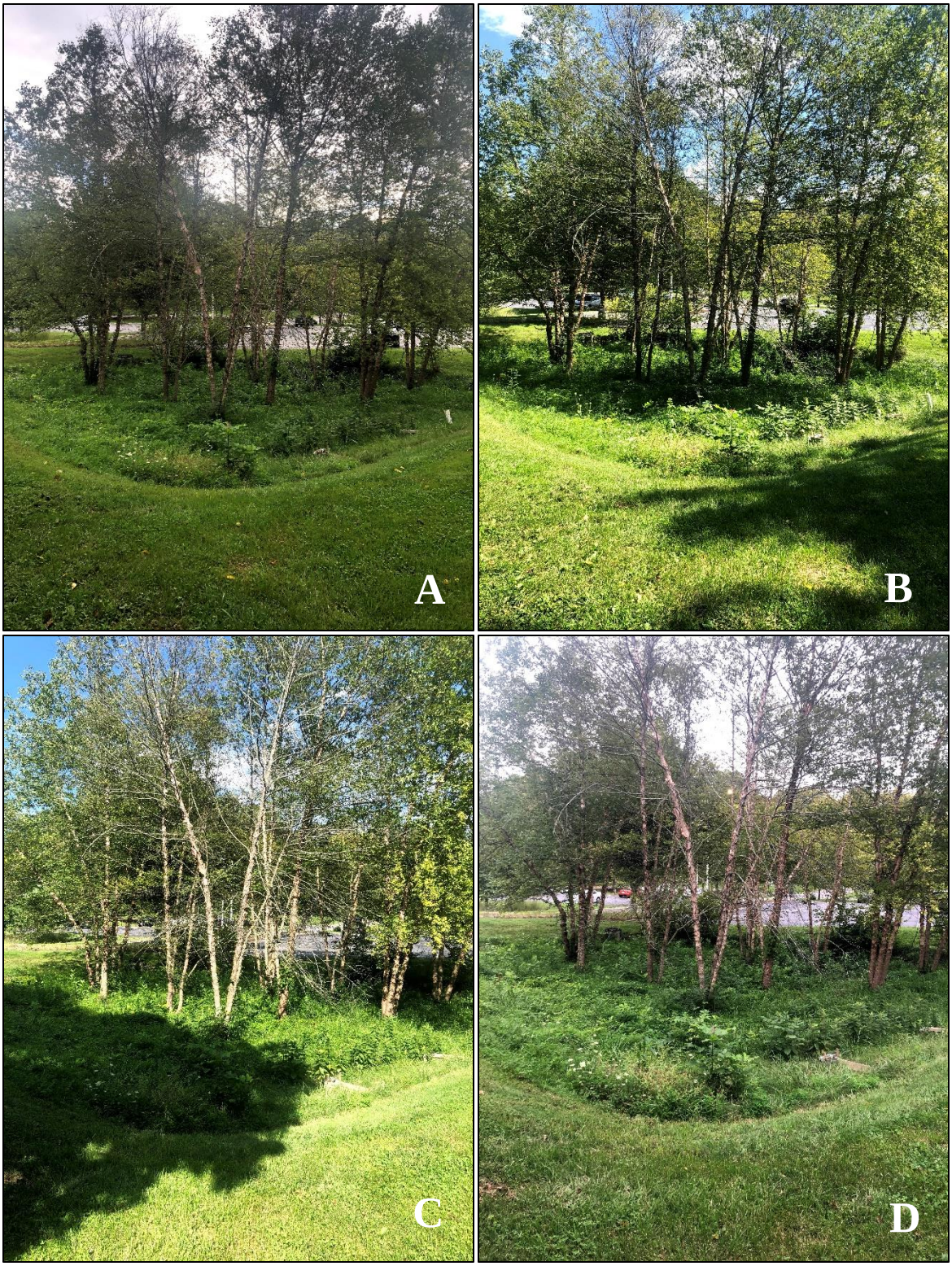

Figure 3-9 A-D. Campus cell shading on 08/30/2020. A) 8:30 AM, B) 11:30 AM, C) 4:00 PM, D) 7:00 PM

3.5 Parking Lot Characteristics

Parking lot characteristic are another aspect that should be explored when assessing thermal pollution potential within a watershed. Since the impervious surfaces are one of the driving forces increasing runoff temperatures; higher inflow temperatures to a bioretention cell will affect the outflow temperatures. Although Janke et al. (2009) found that heat load export and runoff temperatures from impervious surfaces are not as sensitive to the physical properties of the pavement as the storm characteristics, some highlighted contrast may explain potential differences between inlet thermal load to each cell. Cell shading was discussed, but parking lot shading may be just as important for reducing runoff temperatures entering and ultimately leaving the cell. Neither parking lot has much shading and the lots are exposed directly to solar radiation during most of the day. However, the Aquatics Center lot has a row of large broadleaf trees on the eastern side of the lot which provided shading in the morning. Comparatively, the Campus cell has multiple large broadleaf trees on the northern border as well as two smaller broadleaf trees within the lot; however, given the size of this lot and tree location, these provide minimal shading throughout the day.

Pavement color is another important aspect to consider when comparing inflow temperatures. As stated earlier, both parking lots are weathered and effectively lighter than when initially installed. This is typical with asphalt as the dark petroleum derivatives used as a binder oxidize over time, exposing more of the lighter stone aggregate (EPA 2012). Representative pavement colors were determined for each parking lot. The RGB number systems indicates the composite layers of red, green, and blue found in an image pixel. For example, pure black would have the coding R:0, G:0, B:0, so effectively the lower the number associated with the RGB coding the darker the pigment. As indicated in Tables 3-1 and 3-2, the Campus cell lot has a darker

pigment than the Aquatics Center. The darker lot will have a lower albedo and may absorb more solar radiation resulting in higher surface temperatures. Again, this may be a possible explanation for any differences in influent runoff temperatures.

Flow length is the last parking lot characteristic that may lead to differing runoff temperatures between the sites. The maximum flow length, or the furthest linear distance in the drainage area from the outlet, will ultimately affect the time the surface runoff is in contact with the pavement. The longer the runoff is in contact with the pavement, greater amount of thermal energy the runoff can absorb. As stated earlier, the Campus cell has a larger drainage area, nearly twice that of the Aquatics Center. Despite having a larger drainage area, there is only one curb inlet to collect storm water runoff from the lot. Meanwhile, the Aquatics Center has two curb inlets, providing shorter travel distances to the storm drain system that eventually lead to the bioretention cell. The maximum travel distance for the Campus lot is approximately 81.2 m, and for the Aquatic Center this distance is approximately 35.3 m. Slope will also impact flow velocity across the lot surface but the difference in slope between the two parking lots is negligible.

3.6 Monitoring

Monitoring began on July 10th, 2020 and was completed September 30th, 2020. Due to restrictions caused by the COVID-19 pandemic, monitoring began later than originally intended, so, early summer storms were not included in this study. Prior to monitoring equipment installation, cell maintenance was performed at each site. The Aquatics Center cell had accumulated nearly 10 cm of sediment since construction and the surface of the cell was nearly level with the overflow drain, resulting in almost no available ponding volume. A maintenance crew from the Town of Blacksburg removed this accumulated sediment and reapplied the mulch layer to return the cell to its originally designed condition (Figure 3-10, 3-11 and 3-12). However,

during this maintenance process all of the native perennial grasses were removed from this cell, leaving behind only the shrubs from the original planting plan. The campus cell and corresponding pretreatment cell were completely overgrown with poison ivy and dense grasses. Virginia Tech Facilities mowed the site to allow for easier equipment installation.

Figure 3-11. Aquatics Center cell prior to sediment removal

Figure 3-10. Aquatics Center cell after sediment removal

Figure 3-12. Aquatics Center Cell after mulch layer applied

3.7 Aquatics Center Bioretention Cell

To measure inflow at the Blacksburg Aquatics Center BRC, a 38.1 cm Thelmar compound v notch/rectangular weir with a 45.7 cm pipe adapter was installed in the inlet pipe (Thel-Mar LLC, Brevard, North Carolina). A HOBO U20 (Onset Corp., Cape Cod, Massachusetts) unvented pressure transducer was use to record water level and water temperature upstream of the weir, recording on 5-minute intervals throughout the monitoring period. The weir was set 28 cm upstream of the pipe outlet and the pressure transducer was set 22 cm upstream of the weir, as shown in Figures 3-13 A and 3-13 B. Due to limitations with the outflow structure, a Thelmar weir could not be placed to monitor outflow rate. The two drainage pipes from the cell were too small

to use a Thelmar weir and the outflow pipe from the outflow structure was partial obstructed by concrete. Furthermore, the outlet of the outflow system was located at a junction of the existing stormwater conveyance system (Figure 3-14 A). With a concern of backwater effects from the existing drainage system interfering with the weir and pressure transducer combination, this location was not used either. To circumvent these limitations, a pressure transducer was placed in the outflow structure to record water height and water temperature (Figure 3-14 B). Using the water height in the structure, outflow pipe dimensions and pipe slope, pipe flow calculations were conducted to verify the stage discharge relationship determined during flow calibration.

Soil temperature measurements within each cell were recorded using a HOBO U12-008 4-channel external data logger with 4 HOBO TMCx-HD air, water and soil temperature sensors. These sensors were placed in four different soil locations to measure the soil thermal profile. Two sensors were placed on the cell surface just below the media surface and much layer, one in an area of the cell that was mainly shaded and one in an area of the cell that was mainly exposed to direct sunlight (Figure 3-14 C). The two remaining soil temperature sensors were set at depth using nested piezometers that were installed during cell construction (Figure 3-14 D). One sensor was placed at 0.91 m and the other was placed at 1.8 m.

Figure 3-13 Aquatic Center cell inflow monitoring A) Thelmar weir B) HOBO-U20 pressure transducer

Figure 3-14 A-D. Additional Aquatics Center cell monitoring set up. A) Cell outflow drainage junction. B) Outflow structure HOBO U-20. C) Soil media temperature probe installation. D) Nested piezometer used to place temperature probe at depth.

3.8 Campus Cell

As stated previously, surface runoff from the parking lot was directed into a pretreatment basin prior to flowing into the campus BRC. Six 4.5 m long, 20.32 cm diameter corrugated plastic pipes connected the pretreatment basin to the bioretention cell. For monitoring purposes, metal plot borders were trenched into the pretreatment basin to restrict pooling to half of the basin (Figure 3-15 A). This barrier eliminated three of the inflow pipes from conveying water into the bioretention cell. One of the remaining inflow pipes was capped to allow only two inflow pipes to convey water into the cell. Two 15-cm H flumes were installed at the outlet of these pipes to measure inflow into the bioretention cell (Figure 3-15 B and 3-15 C). HOBO U20 pressure transducers were used to record water level and water temperature in each H-flume stilling basin, recording on 5-minute intervals throughout the monitoring period.

Outflow was originally planned to be measured using a 38 cm Thelmar compound v-notch/rectangular weir with an ISCO 6712 bubble level sampler placed in the outlet pipe of the outflow structure. Due to device malfunctions this system did not continuously log for the entirety of the monitoring period. However, a HOBO U20 datalogger was again used to record water level and water temperature in the outflow structure, so this was used to determine out flow rates at the Campus cell (Figure 3-15 D).

Like the Aquatics Center cell, soil temperature measurements were recorded using a HOBO U12-008 4-channel external data logger with 4 HOBO TMCx-HD soil temperature sensors. Temperature sensors were placed just below the surface of the cell in both sunny and shaded locations. Since this cell was not as deep, both sensors placed at depth were located at the bottom of the cell (86.31 cm) within 2.54 cm PVC pipes. One soil temperature sensor was placed near the inflow and one was placed near the cell outlet. Both barometric pressure and air temperature were

recorded at this site using a HOBO U20 transducer to correct water depth sensor readings at each site.

Figure 3-15 A-D. Campus cell flow monitoring equipment. A) Plot borders used to section off pretreatment basin. B) 15-cm H-Flume 1. C) 15-cm H-flume 2. D) Outflow HOBO-U20 pressure transducer

3.9 Onset HOBO Data Loggers

All sensors used during cell monitoring were manufactured by Onset Computer Corporation (Onset, Cape Cod, Massachusetts). Prior to installation all six HOBO-U20 pressure transducers were calibrated by the manufacturer. All data retrieved from the dataloggers was processed using HOBOware, a graphing and analysis software package developed by Onset. The HOBO-U20 pressure transducers had a water level typical and maximum error of ±0.075%, 0.3 cm of water and ±0.15%, 0.6 cm of water, respectively. For raw pressure the transducers had an accuracy of ±0.3%, with a maximum error 0.43 kPa. For water and air temperature, the sensors had an accuracy of ±0.44°C from 0°C to 50°C. Eight HOBO TMCx-HD air, water, and soil temperature sensors were used with two HOBO 4-Channel External Dataloggers to measure soil temperature. This combination had an accuracy of ±0.25°C from 0°C to 50°C.

3.10 H Flumes

As shown in Figures 3-26 and 3-27, 15-cm H flumes were used to determine inflow rates at the Campus Cell, as seen in Figures 3-26 and 3-27. These flumes were 29.2 cm wide, 106.7 cm long and the side walls were 15.24 cm tall. In addition, the flumes had a stilling basin attached to the side of the flume that were used to determine flow depth and flow temperature through the flume. To determine flow rate, Equation 3 below was used. However, a flow calibration was performed to determine the accuracy of this equation with the flume set up.

$$\frac{L}{s} = 0.003171487 - 0.10001658H_m^{0.5} + 28.15410639H_m^{1.5} + 894.3863793H_m^{2.5} \qquad (3)$$

where H_m = head (m).

3.11 Calibration of Flow Monitoring Equipment

At the Aquatics Center, water was discharged over a range of flow rates to the parking lot from a fire hydrant located on site. Flow rates from the hydrant were measured using a using a Sensus 125-w 6.35 by 6.35 cm fire hydrant flow meter (Xylem, Inc., Rye Brook, New York). The flow meter attached to the hydrant was used to determine the total volume of water used and to track the total flow volume input into the cell. Although not included in the monitoring plan due to backwater concerns during storm events, a 38 cm Thelmar weir was installed at the cell outlet pipe to determine flow rates leaving the cell. Visual flow readings from the both Thelmar weirs at the inflow and outflow were compared HOBO-U20 depth readings (Figure 3-16). From there, a power curve relationship was developed in order to determine the flow rates for all the storms during the monitoring period, as seen in Figures 3-17 and 3-18. Comparing total inflow volumes based on the flow meter readings and the weir readings, it was observed that the inflow to the bioretention cell was 3.79 m^3 lower than the volume measured at the flow meter. Given that there were losses between the fire hydrant discharge and the inflow to the bioretention cell, the discharge readings from the inflow weir were used to develop the inflow rating curve.

Figure 3-16. Example visual reading from Aquatics Center BRC calibration

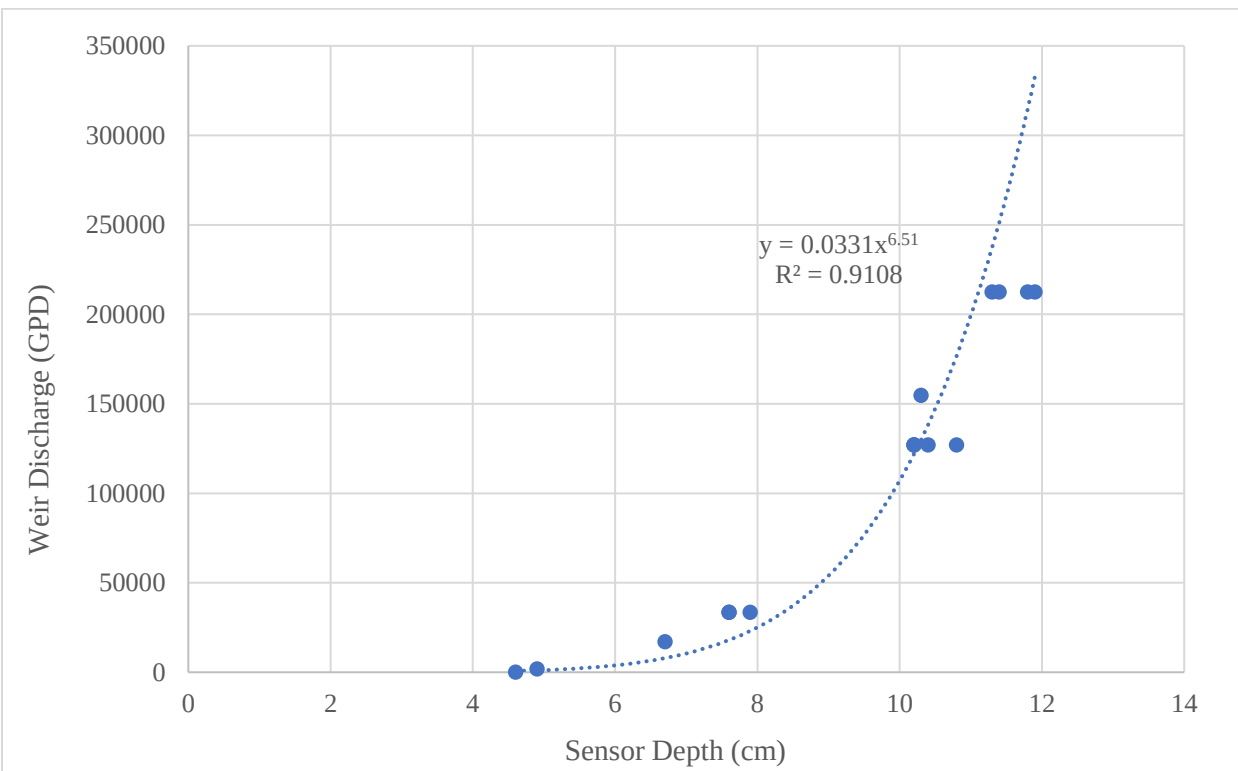

Figure 3-17. Aquatics Center cell inflow calibration curve

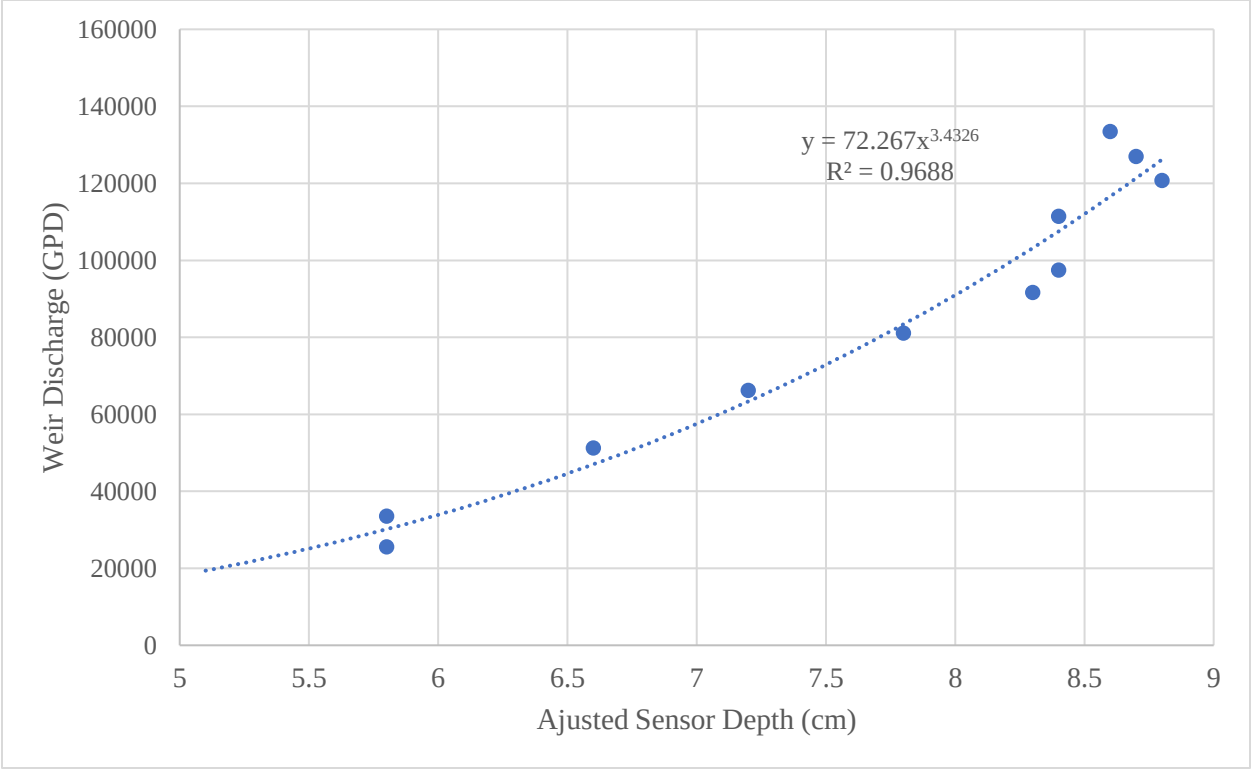

Figure 3-18. Aquatics Center cell outflow calibration curve

The calibration for the campus cell was completed in two parts. Using a Berkeley B71149 air cooled gas pump (Pentair, Golden Valley, Minnesota), water was pumped from Stroubles Creek to the campus cell. Visual flow readings from the Thelmar weir were compared to water depth readings from the HOBO U20 datalogger located in the outflow structure. The water pumped from Stroubles Creek was directed to the bioretention cell near the outflow structure and allowed to infiltrate into the cell media (Figure 3-19). After water began to flow through the outflow structure, visual flow readings were recorded. A power curve relationship was created from the water depth in the outflow structure and the visual flow readings from the Thelmar weir (Figure 3-21).

The H-flume calibration was performed using a 300-gallon tank (Figure 3-20): water was fed into each H-flume and flow was measured using a P3 International P0550 garden hose water

meter (P3 International Corp., Sanford, North Carolina). Head measurements were measured directly from the flume spillway and compared to sensor data for a range of flows rates. When measured flow rates were compared to calculated flow rates using Equation 3 it was determined that the H flume equation overpredicted flow rates for this given installation (Figure 3-22 and 3-23).

Figure 3-20. Campus cell outflow calibration

Figure 3-19. H-flume flow calibration tank and pump

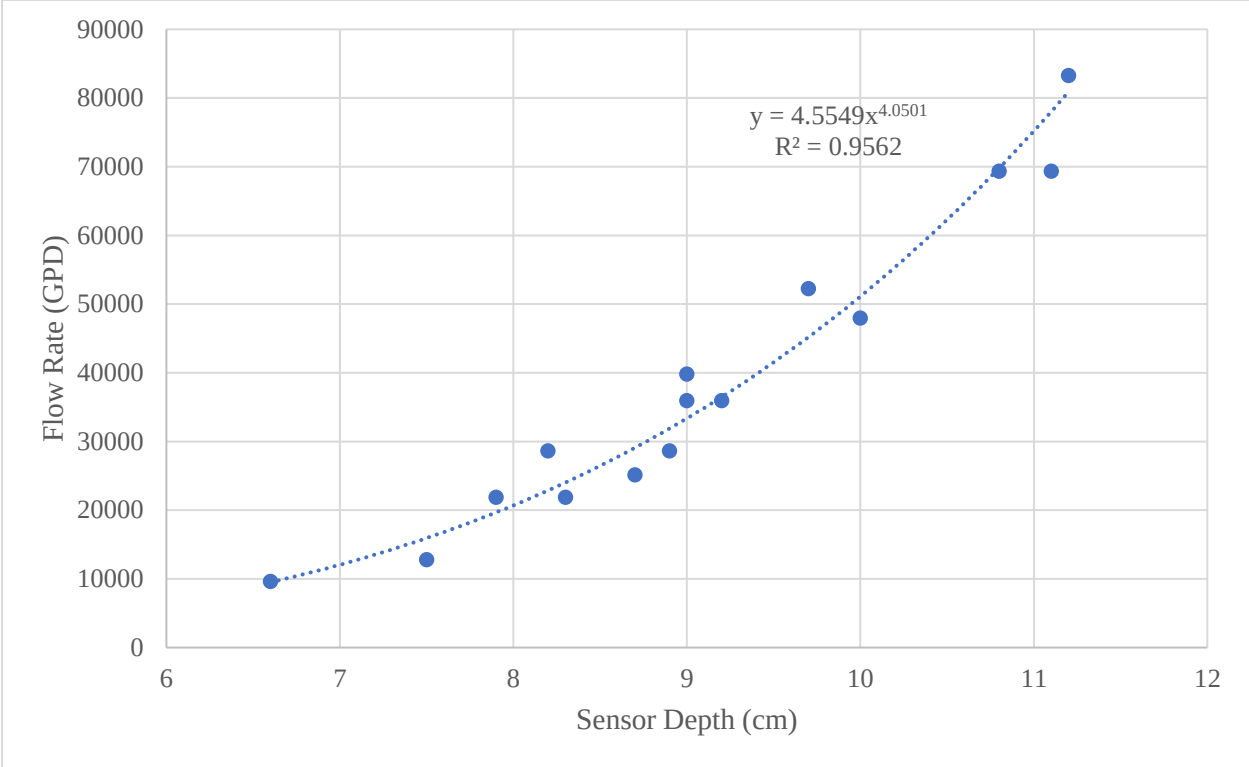

Figure 3-21. Campus cell outflow calibration curve

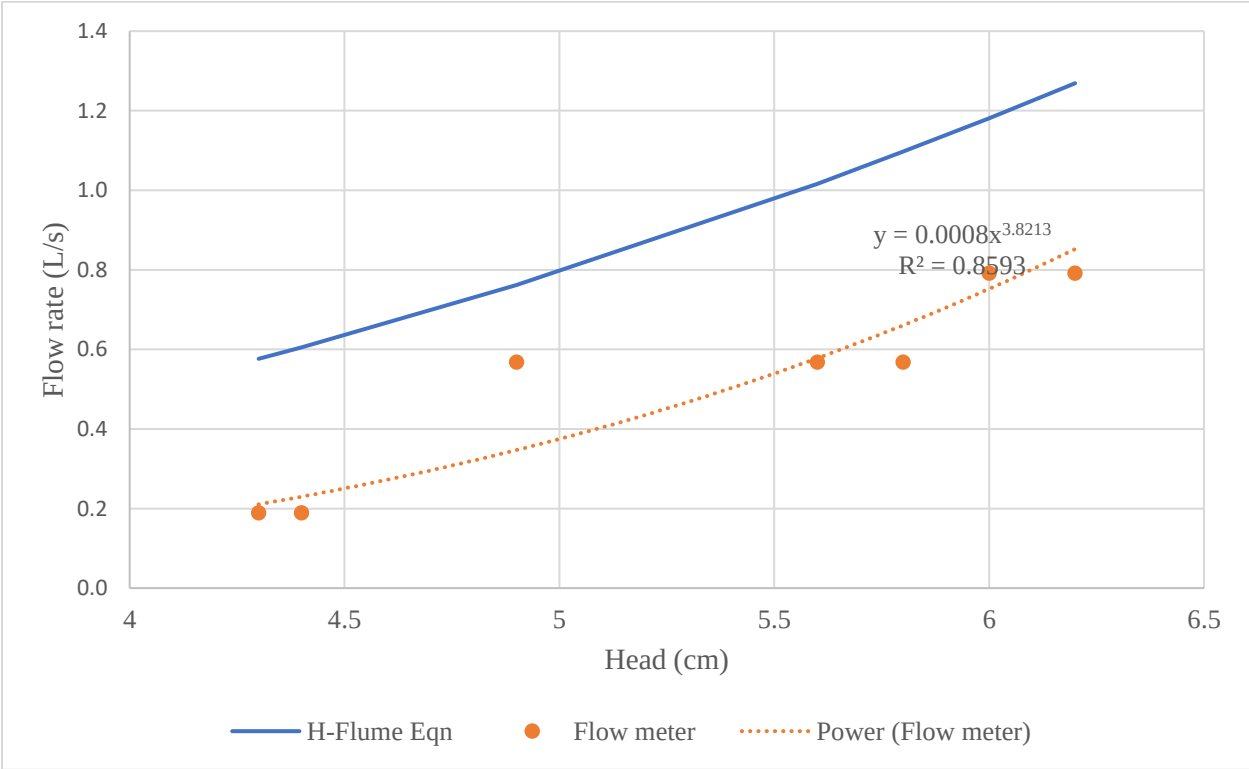

Figure 3-22. Campus cell inflow H-flume 1 calibration curve

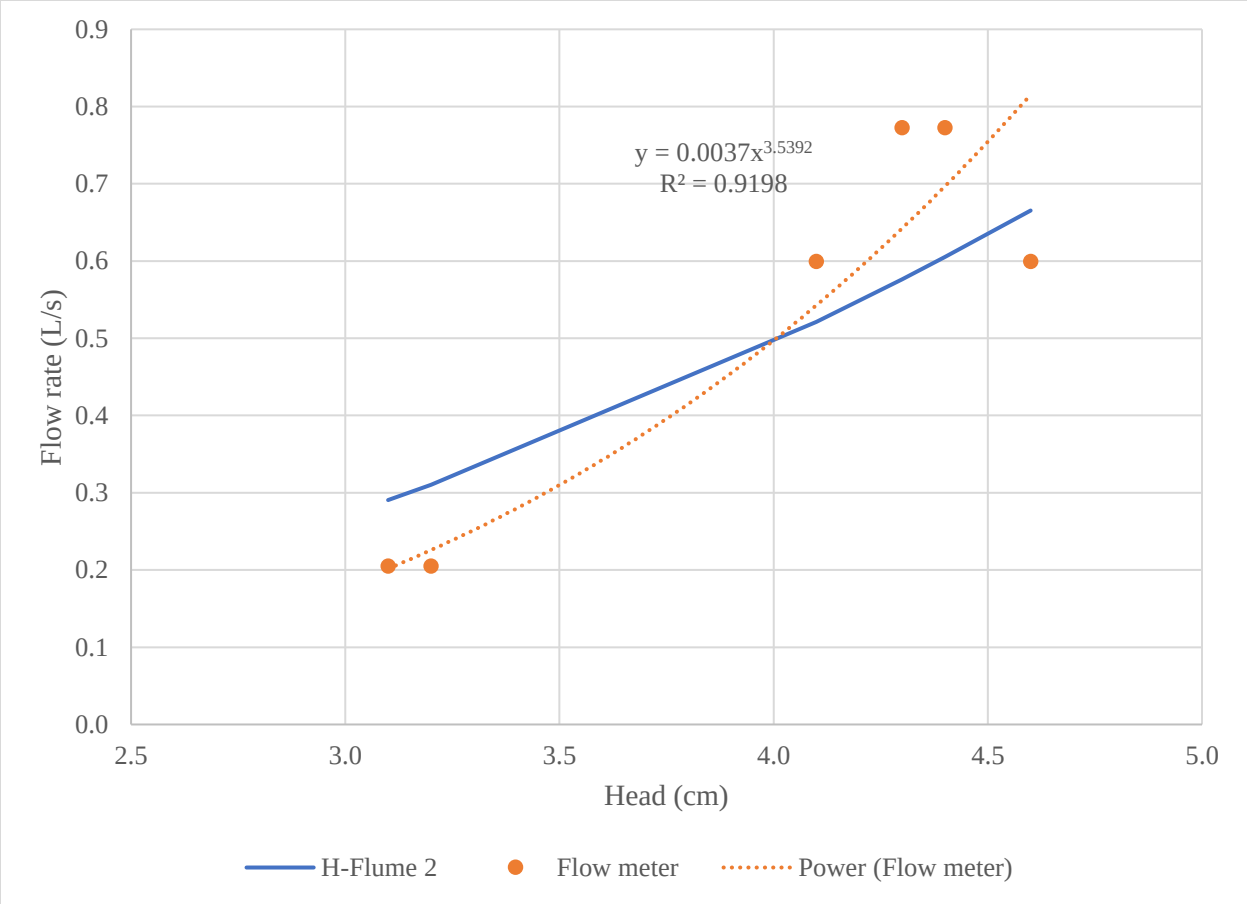

Figure 3-23. Campus cell inflow H-flume 2 calibration curve

3.12 Climate Data

To isolate storm events and to compare cell response to different intensity storms, precipitation data was retrieved from the Virginia Tech StREAM (Stream Research, Education, and Management) Lab weather station (37° 12’ 23.3” N, 80° 26’ 48.8” W). A Campbell Scientific TE525METS-L rain gage (Logan, Utah) with a 15.24 cm orifice was used to record precipitation on a 30-minute interval. This system included a tipping bucket magnetic reed switch sensor with an accuracy up to 1.0% up to 50 mm per hour. Solar radiation and air temperatures were also retrieved from this station; they were both measured on 30-minute intervals during the monitoring

period. Solar radiation readings were measured using an Apogee Instruments CS300 pyranometer (Logan, Utah), with an absolute accuracy of ±5% for daily total solar radiation. Air temperature readings were measured using a Campbell Scientific CS215 temperature and relative humidity probe which has an air temperature accuracy of ±0.4°C from 5° to 40°C and an accuracy of ±0.9°C from -40° to 70°C.

The weather station is located 2.38 km away from the Campus cell and 5.15 km away from the Aquatics Center cell (Figure 3-37). Similar to methods describe in Debusk and Wynn (2011), individual storm events were identified as storms with 6-hour intervals between recorded precipitation. Storms were identified using the precipitation data from the StREAM Lab weather station. Flow was attributed to a precipitation event if flow occurred three hours prior to the first recorded rainfall and three hours after the last recorded rainfall for a storm event. To ensure that no outflow was excluded from the storm monitoring period, each storm was checked to make sure there was no outflow outside this 3-hr time frame, if so, the monitoring period was extended to include these data points.

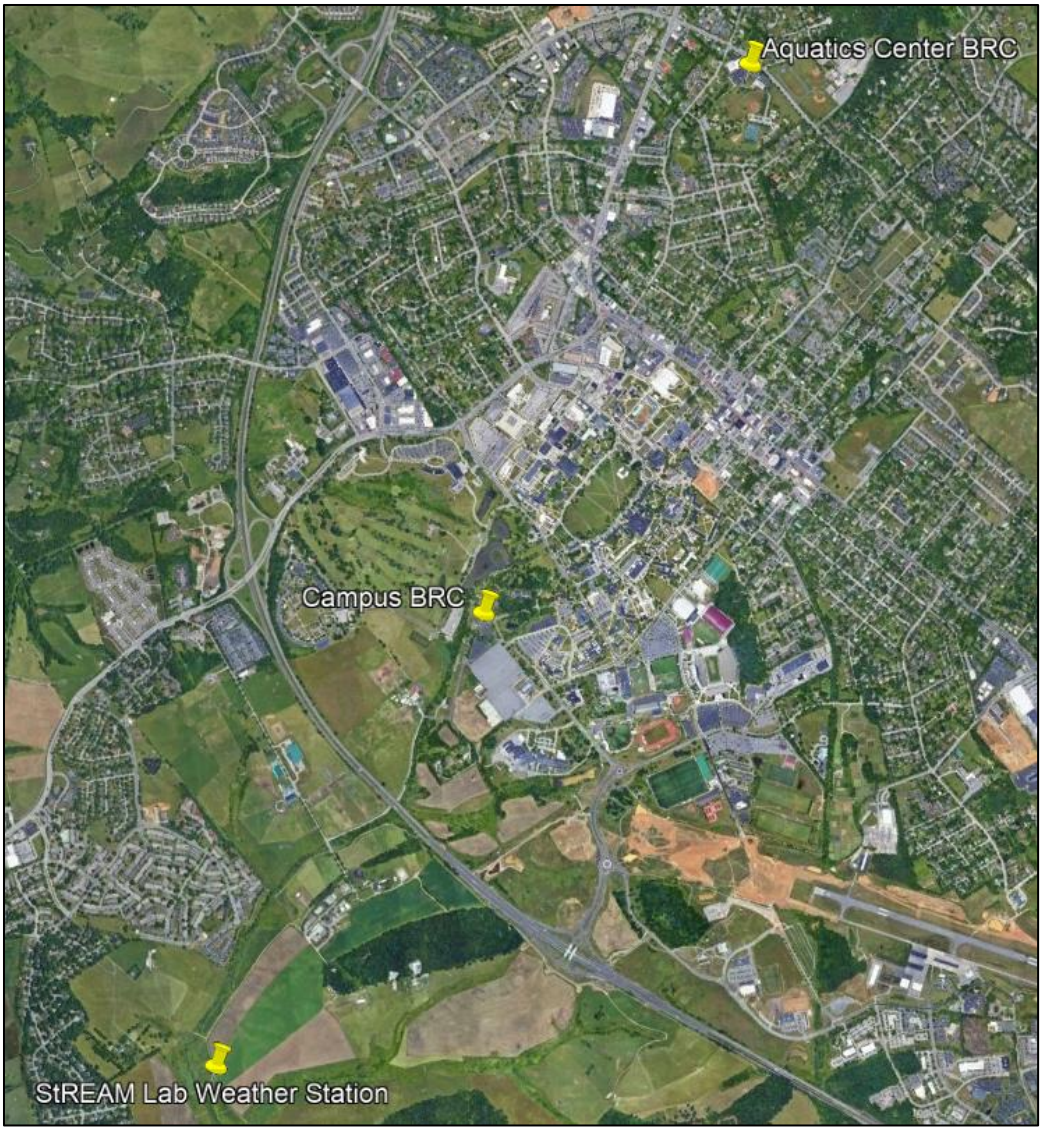

Figure 3-24. StREAM Lab Weather Station location in reference to both BRC

3.13 Quantifying Temperature and Heat Load

The primary objective of this research was to quantify the changes in temperature and heat loads in stormwater due to bioretention. The two metrics used to quantify these changes in thermal pollution between the inlet and outlet of the two bioretention cells were Event Mean Temperature (EMT) and Heat Load (HL). The flow-weighted temperature or EMT was calculated using

Equation 1. This event mean temperature is consistent with the event mean concentrations (EMCs) calculated for other stormwater pollutants monitored when assessing SCM performance (Delctic 1998; Kieser et al. 2003; UNHSC 2011, Wardynski et al. 2014). This metric was used because it offers a more representative temperature because instantaneous temperature measurements are weighted by flow volume.

The second metric calculated was the heat load, which was calculated using Equation 2. Heat load was used in addition to the EMT to quantify the impact bioretention has on thermal energy, equivalent to a chemical pollutant load reduction. The primary role of bioretention is runoff volume reduction; even if EMT reduction between the inlet and outlet was negligible the heat load would quantify the thermal reduction due the flow reduction through the cell (Wardynski et al. 2014). This metric can also be used to assess the impact of this flow volume on the receiving stream network.

3.14 Data Analysis

After calculating the EMT and heat load for each storm event, data analysis was performed using the statistical software MiniTab (MiniTab, LLC, State College PA). The EMT and heat load datasets for each cell were tested for normality using both the Ryan-Joiner Test and Anderson-Darling tests. For data that was determined to be non-normal, transformations following the ladder of powers were performed to normalize the data sets, as required for parametric tests (Helsel et al. 2020). For negatively skewed data sets, the transformation x^3 was used. For positively skewed data, the transformation *Log10(x)* was used. To account for zero values present in the data sets in this in the transformation, the addition of a constant (*+10 or +100*) was used. To determine the statistical significance of the difference in EMT and heat load entering and leaving the cell two statistical tests were performed. A non-parametric 1-Sample Sign test was used to test for

significance (median > 0) of the difference between EMT and heat load entering and leaving the cell (Inflow – Outflow). Since 21°C was identified as the temperature threshold where trout begin to experience stress, a 1-Sample Sign Test was performed for the outlet EMT to determine if there was a significant difference between the outlet EMT median and this threshold (H_0: M = 21, H_1: M > 21). Finally, a paired t-test was used to test for a significance difference between inlet and outlet EMT and heat load. A significance level of $\alpha = 0.05$ was assumed. For this parametric test, the null hypothesis (H_0) was difference = 0, while the alternative hypothesis (H_1) was difference ≠ 0.

Multivariable regression was used to identify explanatory variables for the high EMT and heat loads entering the cells. Variables explored included: maximum air temperature (MAT) prior to or during the storm, maximum solar radiation (MSR) prior to the storm, maximum rainfall intensity (MRI), total rainfall depth (TR) and storm duration (SD). Using Minitab, a best subset analysis was conducted to identify storm characteristics that correlated significantly with high inflow EMT and heat load into the cells. By comparing the R-squared, adjusted R-squared and predicted R-squared for each best subset analysis the most significant predictor variables were identified and regression models were created to assess which storm parameter had the most significant impact on EMT and heat load into the bioretention cells. An alpha value of 0.05 was used for statistical significance and for regressions, only coefficients with p-values < 0.05 were include in this discussion.

Lastly, Soil temperature profiles were created for each storm events and for the entirety of the monitoring period. For continuous data through the monitoring period, maximum daily temperatures were plotted for each sensor at each cell location. For storm events, instantaneous temperature measurements on five-minute increments were plotted for periods of recorded inflow

and outflow. These profiles were visually analyzed for trends in response to inflow events and daily weather patterns.

4 Results and Discussion

4.1 Monitoring Period Overview

During the 83-day monitoring period from July 10th 2020 to September 30th 2020 there were 38 storm events which resulted in 291 mm of precipitation over the study area. On average, the maximum daily temperature was 26.2°C, while the minimum daily temperature was 14.9°C during the monitoring period. The maximum 30-minute rainfall intensity recorded during the monitoring period was 21.8 mm/hr (Storm 15); the recurrence interval for this storm event was 1-2 years (NOAA 2021). The largest total rainfall from a single storm event was 31 mm (Storm 32), over a 17-hour period; the recurrence interval for this storm was less than 1 year (NOAA 2021).

Figure 4-1 shows the maximum and minimum air temperatures and the daily precipitation during the monitoring period. As evident in the plot, storms with greater volume, tended to coincide with dips in both maximum and minimum air temperatures. The same holds true for Figure 4-2, which shows a similar trend with decreases in daily maximum solar radiation coinciding with larger storm events. These larger storm events are associated with frontal events and have greater cloud cover for a larger portion of the day. Figure 4-3 shows a frontal event. This event was a longer storm event with more cloud coverage throughout the day, resulting lower solar radiation and lower air temperature throughout the day. Comparatively, Figure 4-4 shows a shorter more convective storm event. This convective storm event had less cloud cover prior to precipitation resulting in higher solar radiation and air temperatures prior to and during the storm event. As visible in the figures the inflow EMT, in this case at the Campus cell, were significantly higher during the convective event than during the frontal event, 28 °C and 23.3 °C, respectfully.

Figure 4-5 shows that some high intensity storms coincide with relative peaks in daily maximum solar radiation. This highlights that shorter, more intense convective storms may have a greater impact on runoff temperatures. If there is less cloud cover prior to the storm, surface temperatures will be greater and could result in higher runoff temperatures. Initially, the trends in these three plots illustrate that the quantity of precipitation may not have as large of an impact on runoff temperatures as the rainfall intensity. These storm characteristics will be discussed in more detail later in this section. A comprehensive list of storm characteristics and weather data is presented in Appendix A (Table A-1 and A-2)

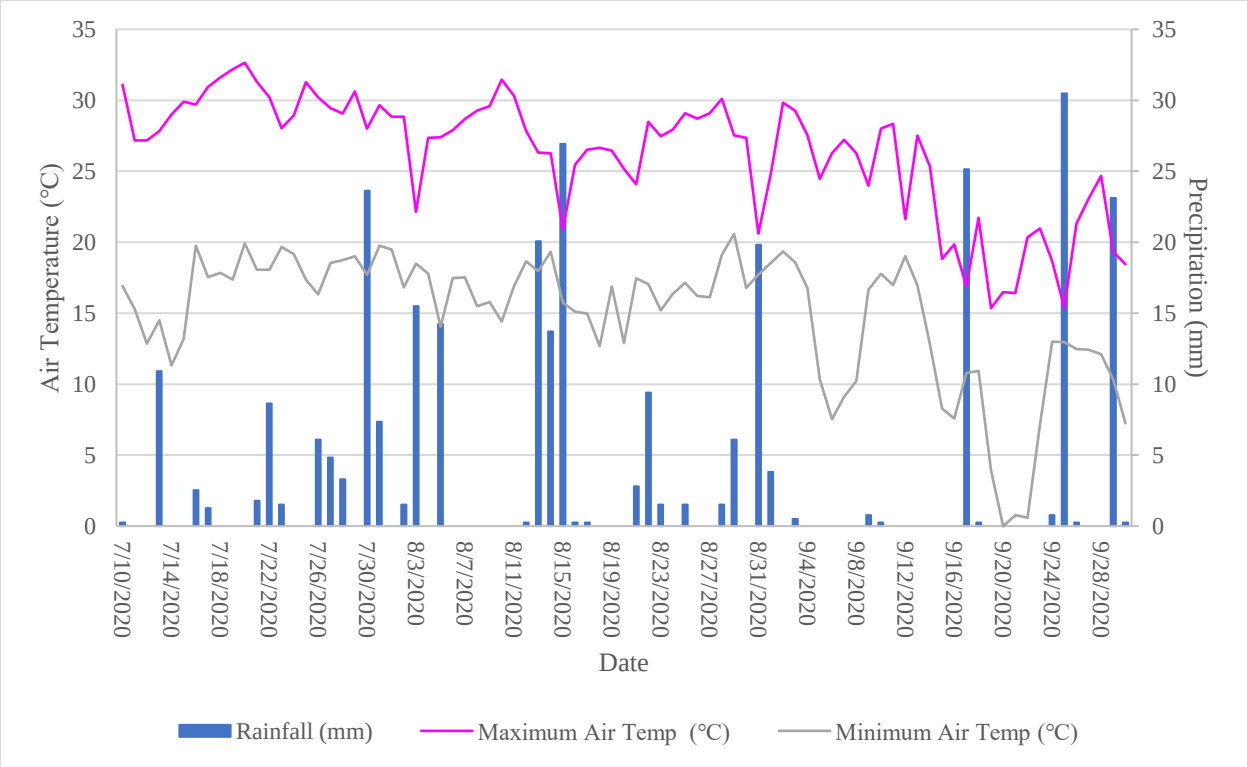

Figure 4-1. StREAM Lab air temperature and daily total precipitation data

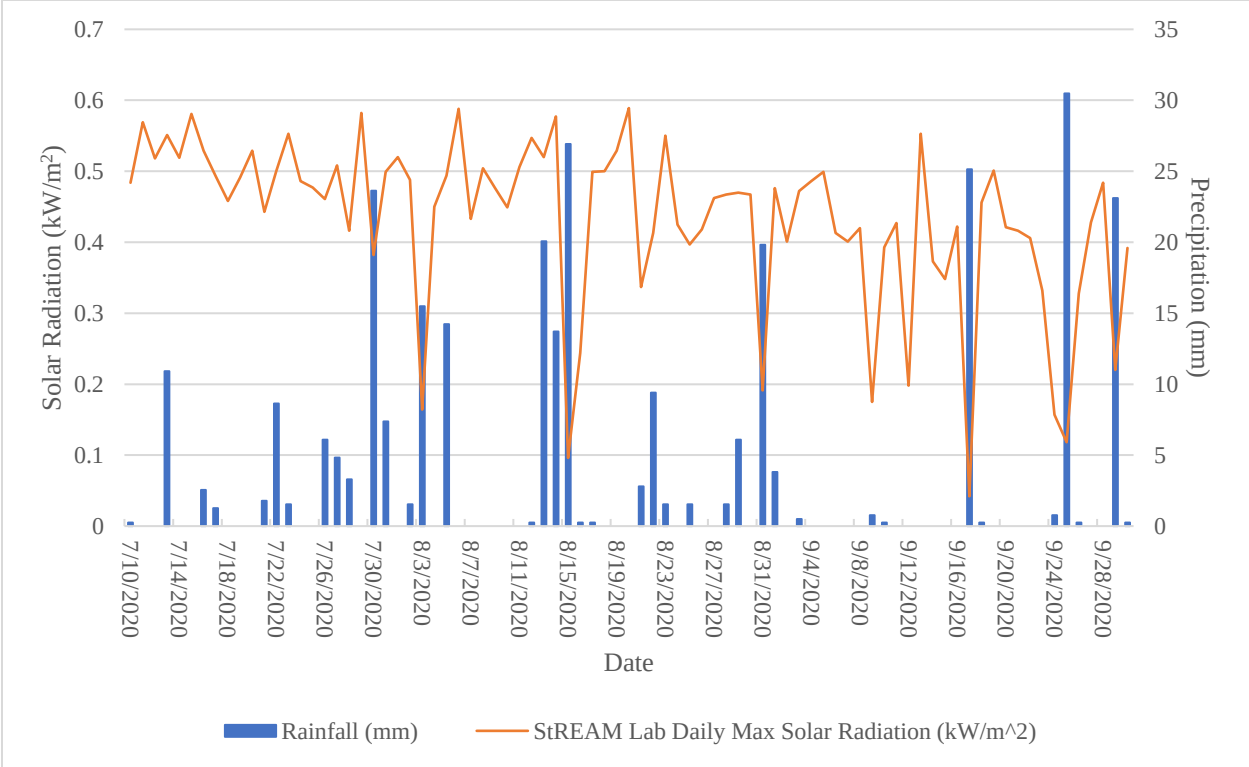

Figure 4-2. Solar radiation and daily total precipitation

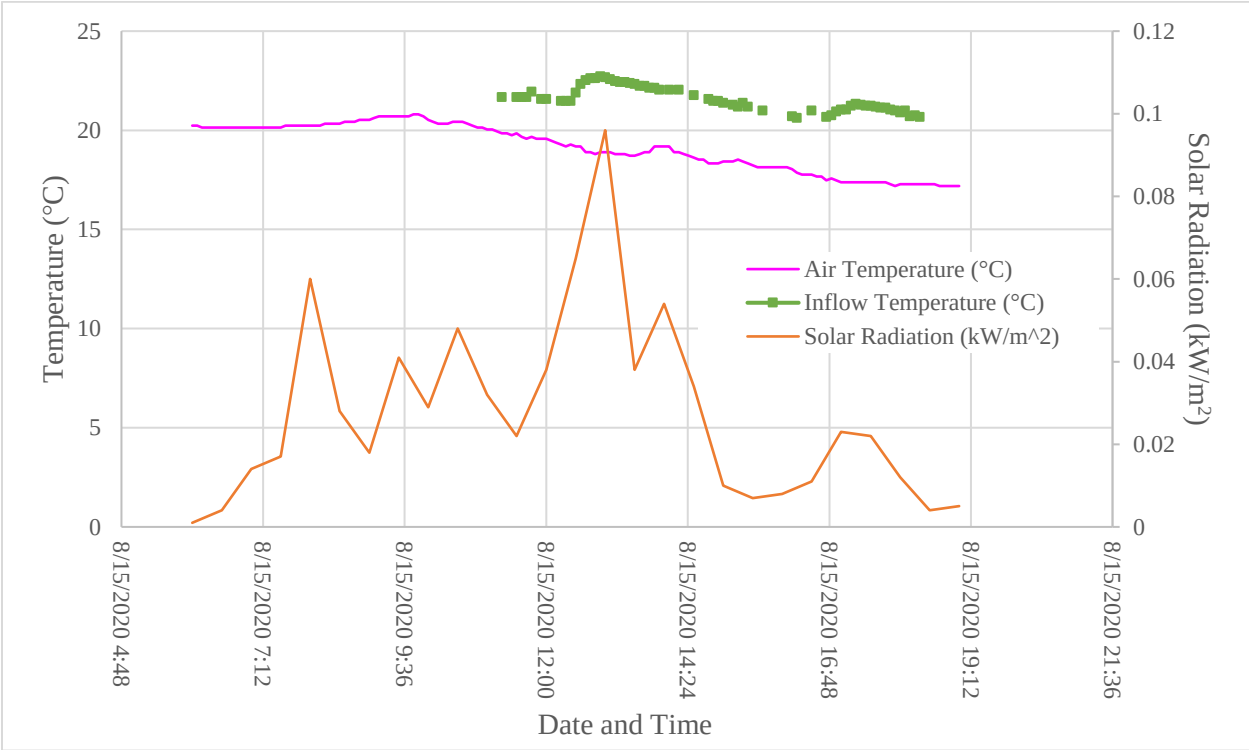

Figure 4-3. Air temperature, solar radiation and Campus cell inflow EMT associated with a frontal storm. Storm 19, 08/14/2020.

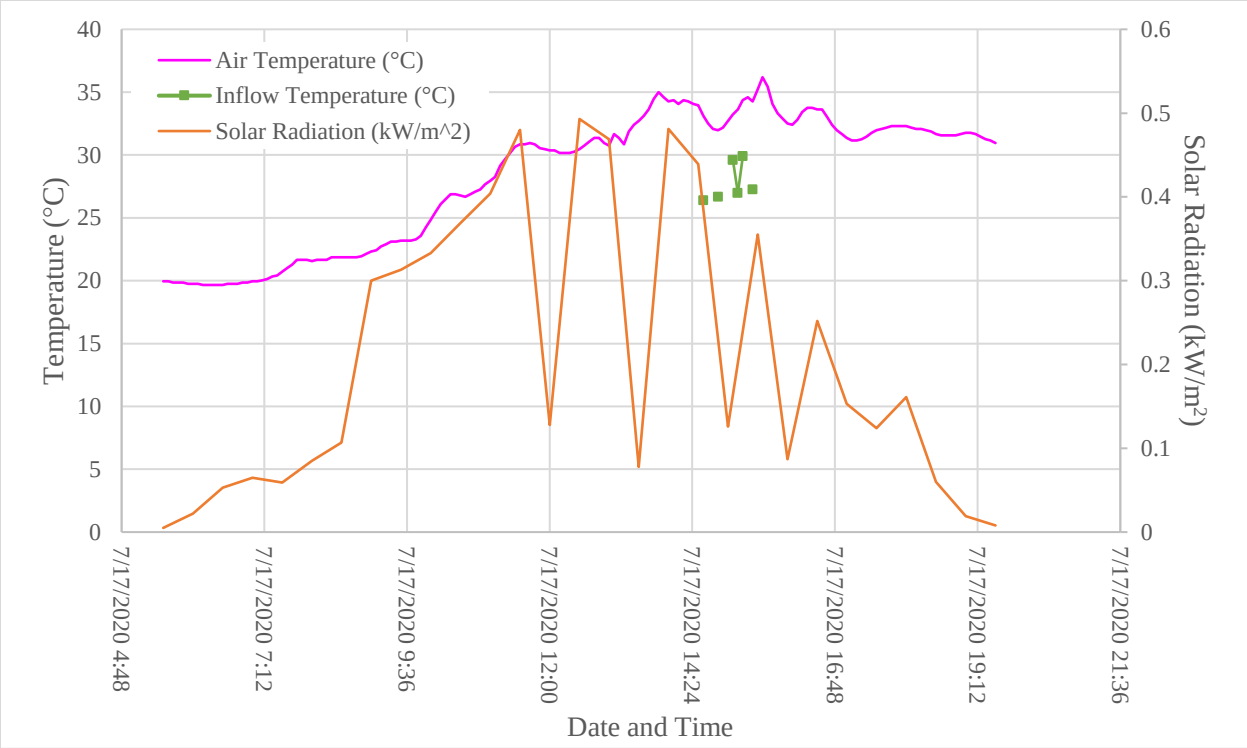

Figure 4-4. Air temperature, solar radiation and Campus cell inflow EMT associated with a convective storm. Storm 3, 07/17/2020.

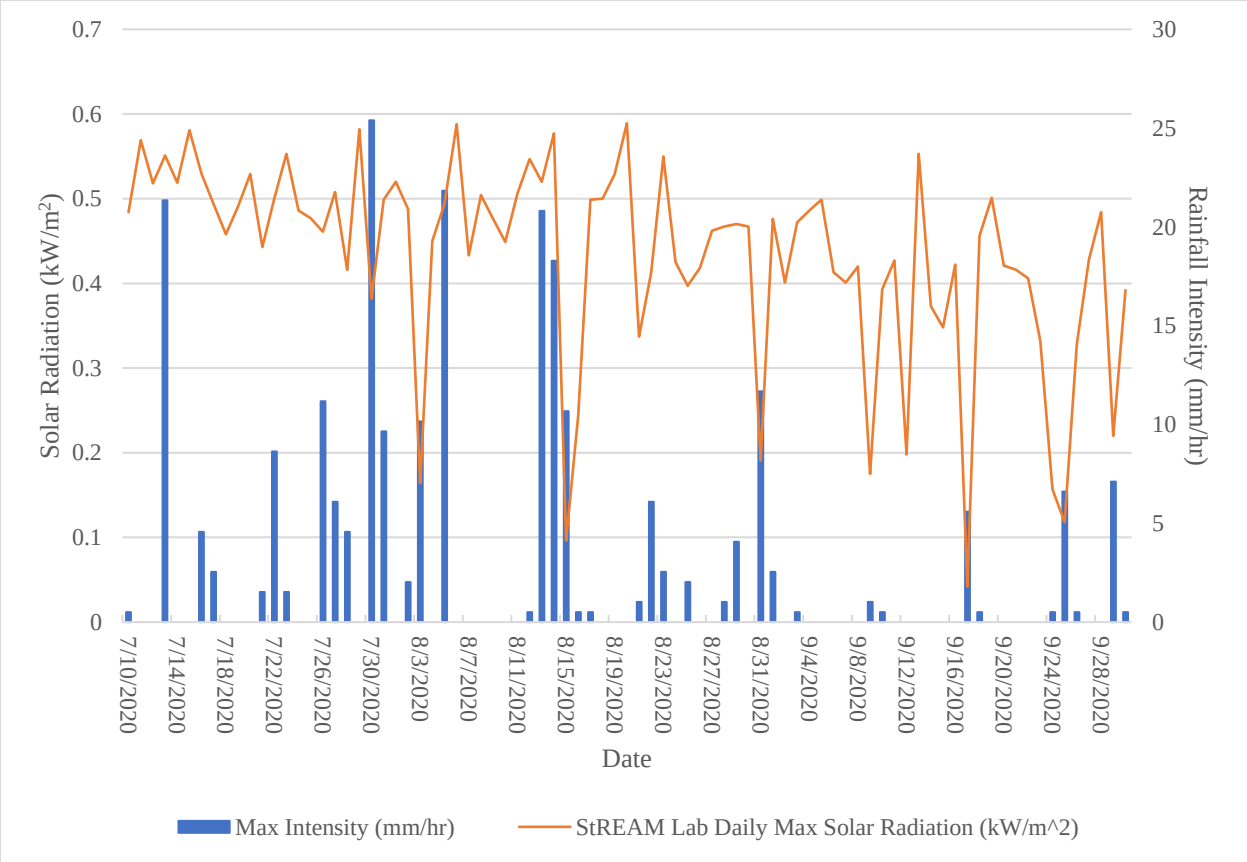

Figure 4-5. Solar radiation and daily maximum rainfall intensity

Comparing the air temperature data from the Campus cell and StREAM Lab illustrates the urban heat island effect (Figure 4-6). The StREAM Lab weather station was located in the floodplain of the StREAM Lab which is completely undeveloped, meanwhile, the Campus cell is surrounded by impervious pavement and built surfaces which absorb more solar radiation and emit this as heat. The average daily maximum temperature over the monitoring period was 26.2°C and 29.1°C at the StREAM Lab and Campus cell, respectfully. Furthermore, peak daily temperatures were nearly 8°C warmer at the Campus cell which indicates the effect that built surfaces can have on localized air temperatures.

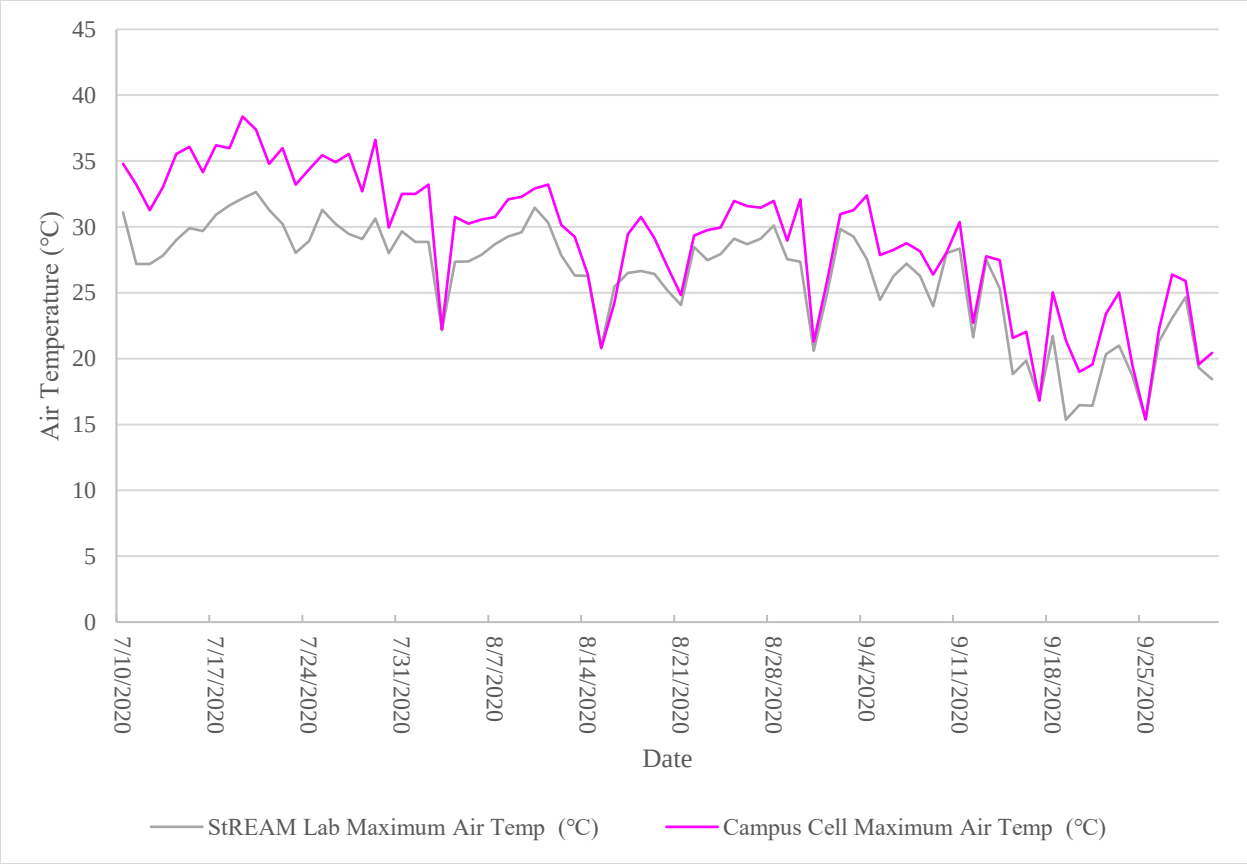

Figure 4-6. Maximum air temperature comparison between the StREAM Lab and Campus cell

4.2 Storm Characteristics

After identifying the potential best subsets for predicting EMT temperatures for each cell location a linear regression model was fit for each group of predictor variables. Maximum air temperature was identified as the most influential storm characteristic and was included in both subsets for regression modeling. The strong relationship between maximum air temperature and runoff temperature is unsurprising, as the dew point temperature is frequently used to estimate

rainfall temperature and the air temperature must be close to the dew point temperature for precipitation to occur.

Although there was a nonlinear relationship between EMT and maximum air temperature (Table 4-1), a multiple linear regression was also conducted to evaluate the relative impact of the weather parameters on inflow EMT. The first linear regression equation developed was for inlet EMT included max air temperature (MAT, °C) and max rainfall intensity (MRI, mm/hr). The coded coefficients were 3814 for maximum air temperature and 1474 for maximum rainfall intensity (p-value < 0.001 and < 0.001, respectfully). The magnitude of the coded coefficients indicates that maximum air temperature is nearly three times as influential as maximum rainfall intensity. Furthermore, the adjusted R^2 indicates that this equation for 70.4% of the variance within the data for this relationship. The second regression equation included max air temperature and maximum daily solar radiation (MSR, kW/m^2). Again, the coded coefficients indicate that maximum air temperature (3121) is nearly three times as influential as maximum daily solar radiation (1122), although the p-values indicate that this regression is not as significant as the first equation (p-value < 0.001 and 0.029, respectfully). Lastly, the adjusted R^2 indicates that this equation accounts for 64.4% of the variance within the data for this relationship.

For heat load, maximum rainfall intensity was identified as the most influential predictor variable and was used in both regression equations developed. The first equation for heat load included total rainfall (TR, mm) and max rainfall intensity. The coded coefficients, 0.336 for total rainfall and 0.408 for maximum rainfall intensity, show that maximum rainfall intensity is a slightly more influential predictor variable (p-value = 0.002 and < 0.001, respectfully). The adjusted R^2 shows that this model account for 62.3% of the variance within the data. The second heat load regression included storm duration (hr) and max rainfall intensity. The coded

coefficients, 0.229 for storm duration and 0.555 for maximum rainfall intensity, show that maximum rainfall intensity is twice as influential as a predictor variable in this model (p-value = 0.009 and < 0.001, respectfully). The adjusted R^2 shows that this model account for 60% of the variance within the data.

Table 4-1. Regression equations, p-value and adjusted R-squared values for EMT and heat load predictor variables

Regression equation	Equation p-value	Adjusted r^2
Inlet EMT (°C) = -9133 + 0.3168 MAT + 13686 MRI	< 0.001	70.4%
Inlet EMT (°C) = 6144 + 0.2593 MAT + 18433 MSR	< 0.001	64.4%
Inlet Heat Load (MJ) = -3.726 + 1.663 TR + 3.786 MRI	< 0.001	62.3%
Inlet Heat Load (MJ) = -5.069 + 1.604 SD + + 5.155 MRI	< 0.001	60%

In a simulation study of runoff temperatures and heat loads from paved surfaces, Janke et al. (2009) found that runoff temperatures and heat loads were strongly correlated to rainfall parameters and initial pavement temperatures. The physical properties of the paved surfaces (slope, roughness and length) had little influence on the simulated runoff temperatures and heat load (Janke et al. 2009). In this study, simulated mean runoff temperatures were lowest during storm events with high rainfall intensities, however, highest heat load exports values were associated with the highest rainfall intensities. As a result, the researchers suggested mean runoff temperature alone is not a good indicator of the thermal impact of a storm event (Janke et al. 2009). Furthermore, increased storm duration was associated with increased total heat load export, especially for higher intensity storm events (Janke et al. 2009). In other modeling studies, Roa-Espinosa et al. 2003 found that model sensitivity was associated with choice of rainfall temperature

and solar radiation during storm events (Arrington 2004). Lastly, Picksley and Deletic (1999) found a strong correlation between runoff temperatures and both air temperature and rainfall duration in two small watersheds in Sweden and Yugoslavia.

Although properties of the drainage areas were not included in this analysis, these equations highlight factors influencing thermal loads from impervious surfaces. It was expected that the maximum daily solar radiation would have a greater influence on EMT and heat load entering the cell, which would lead to the suggestion that increasing shade cover to impervious surfaces may lower runoff temperatures and heat loads. Although increased shading of impervious surfaces will reduce EMT, the strong relationship between EMT and air temperature indicates that reducing the air temperature in urban areas overall could help mitigate the impacts of urbanization on stream temperatures. However, due to climate change and increasing global temperatures runoff temperatures may continue to increase, further stressing already impaired stream networks.

4.3 Flow Events

During the monitoring period, there were 33 inflow events at the Campus cell and only 14 inflow events at the Aquatics Center cell (Appendix B Table A-3 and A-4). Despite the distance in location between both cells and the distance between the weather station, it is assumed that the cells experienced similar precipitations amounts and intensities during each storm. As mentioned earlier, during the calibration of the Aquatics Center flow equipment, there was a significant loss in flow volume from the fire hydrant to the inlet of the cell of approximately 12%. Considering the cell was constructed as a retrofit to a preexisting drainage system it is assumed that these losses may be attributed to leaks in this existing system. In general, storms that produced more than 6 mm in total precipitation or had a maximum rainfall intensity greater than 10 mm/hr resulted in measurable inflow at the Aquatics Center cell.

Of the 33 inflow events at the Campus cell, 26 produced outflow (79%) while 11 of the 14 inflow events at the Aquatics Center produced outflow (78%). It should be noted that there was a smaller storm sample size at the Aquatics Center Cell and a possible under representation of smaller storms. Smaller storms are more likely to be completely retained by the cell media, as compared to larger storms. As a result, the total flow volume reduction was greater at the Campus cell. Despite receiving a nearly three times the amount of inflow volume than the Aquatics Center cell, the Campus cell was slightly more effective at reducing the total stormwater (Figure 4-7). After normalizing this inflow volume by drainage area size the Campus cell still received 24% more inflow volume than the Aquatics Center cell. The Campus cell had a flow volume reduction of 86% while the Aquatics Center cell had a flow reduction volume of 83%. Despite having deeper soil media and an IWS, the Aquatics Center cell did not reduce flow volumes as much as reported in previous research. When monitoring the same site in 2011, Debusk and Wynn reported flow reductions of 97% over a nine-month period from October 2007 to July 2009. During this study 28 precipitation events were monitored and only five produced measurable outflows. In a similar study of the Aquatics Center cell, Willard et al. (2017) monitored 23 runoff events, 10 of these inflow events produced outflow through the bioretention cell. On a storm basis, flow volume reduction ranged from 37 to 100%. In general, studies have reported flow volume reduction through bioretention cells upwards of 50% (Hunt et al. 2009; Li et al. 2009).

Although the Aquatics Center cell was more than twice as deep as the Campus cell, the Aquatics Center was had a significantly smaller surface area (35 m^2) compared to the Campus cell (240 m^2). Despite having a shallower depth, the Campus cell had a much larger soil media volume-to-drainage area ratio, over three times larger, which previous studies have indicated is a beneficial characteristic for flow reduction (Li et al 2009; Jones and Hunt 2009). Furthermore, the Aquatics

Center has a greater potential for overflow given its smaller ponding volume, which would clearly decrease treatment performance. Of the 11 outflow events, at least four overflow events were observed at the Aquatics Center. Storms 1, 11, 19 and 27 were overflow events. These were either observed on site or noted through large temperature spikes in the outflow temperature readings during the middle of an outflow event. However, there was no monitoring equipment explicitly used to monitor potential overflow events so there could potentially be more that were undetectable from the monitoring data. No overflow events were observed at the Campus Cell. This overflow potential may be a crucial design characteristic as any stormwater volume leaving the cell as overflow is effectively bypassing the soil media, leaving the cell as untreated.

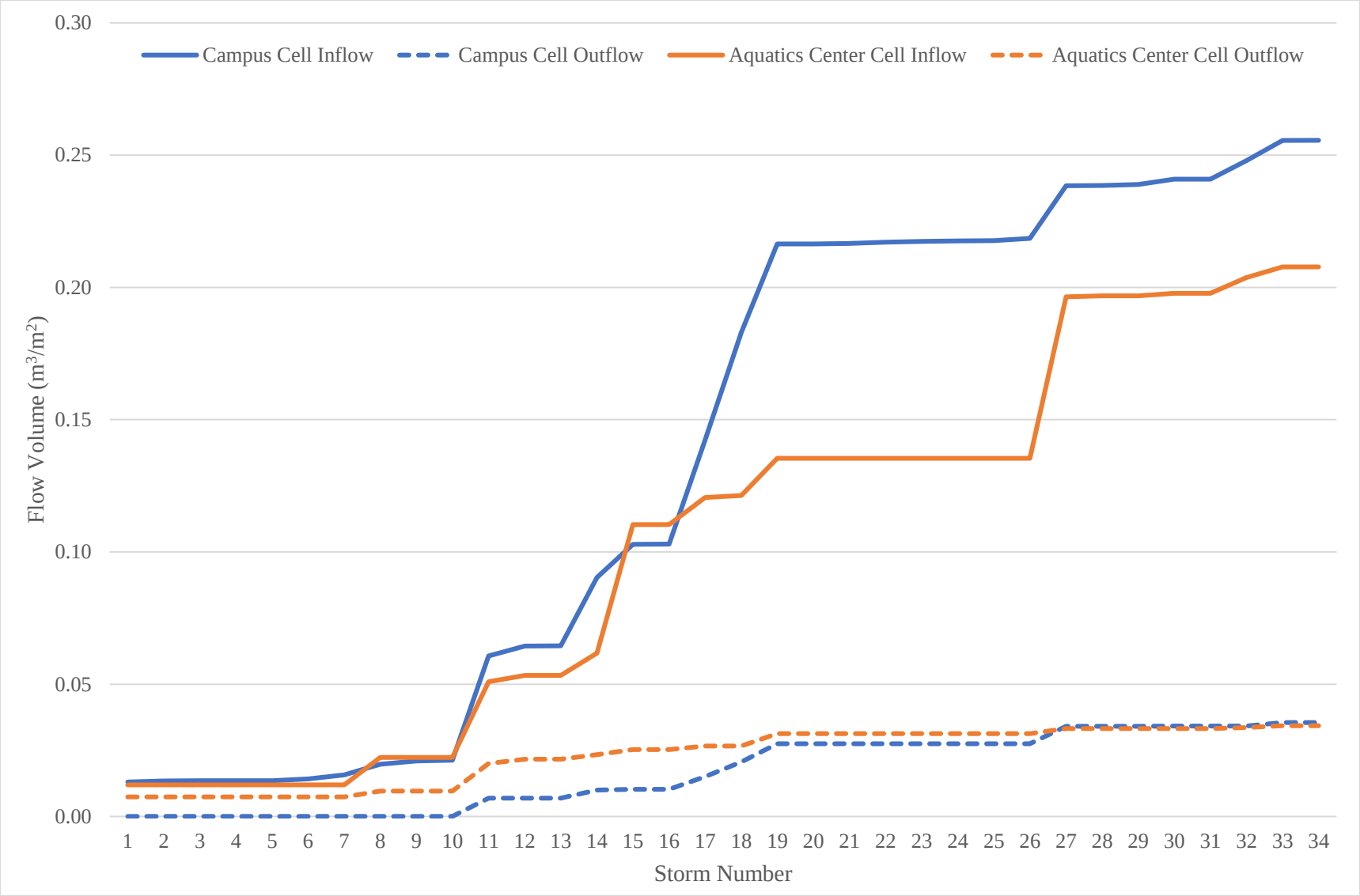

Figure 4-7. Cumulative inflow and outflow volumes for both cells standardized by drainage area. Storm 1 occurred on June 13th 2020

4.4 Changes in EMT and Heat Load

The first objective of this study was to quantify thermal load reduction though bioretention cells. EMT and heat load were used because they offer a more representative metric of the thermal reduction capabilities of bioretention cells than temperature alone (Wardynski et al. 2014). EMT was calculated to determine overall effective discharge temperature leaving the cell (Equation 1). This metric provides a flow-weighted average temperature that is representative of the entire stormwater volume entering and leaving the cell (Wardynski et al. 2014). Aquatics Center cell inlet EMTs ranged from 17.1-27.5°C with a mean and median inlet EMT of 22.9°C and 23.3°C, respectfully (Table A-3). At the Campus cell, inlet EMTs ranged from 16.1-28°C and the mean and median inlet EMT were 23.1 and 23.7°C, respectfully (Table A-4). Heat load was used to quantify the overall thermal energy reduction through the bioretention cell as it indicates the thermal impact a stormwater volume will have on a receiving water body (Equation 2). This metric will illustrate the thermal impact reduction through both stormwater temperature reduction as well as through stormwater volume loss through exfiltration and storage. The Aquatics Center cell inlet heat loads ranged from 50 to 9119 MJ with a mean and median inlet heat loads of 2360 and 1565 MJ, respectfully (Table A-3). At the Campus cell, inlet heat loads ranged from 3 to 8203 MJ and the mean and median inlet heat loads were 1802 and 513 MJ, respectfully (Table A-4).

To test for significance between inflow and outflow EMT and heat load two statistical test were performed: a one sample sign test and a paired t-test were used. The one sample sign test was used to determine if the median difference in EMT and heat load entering and leaving the cell (Inflow-Outflow) was greater than zero. The results from this test indicated that there was a significant difference between the EMT and heat load values entering and leaving the cell ($p = 0.994$, $p = 1$, respectfully). The median change in EMT at the Aquatics Center cell and Campus

cell were 2.5°C and 3.4°C, respectfully. This finding indicates that the Campus cell was more effective at reducing EMT as the difference between the inlet and outlet was about a degree greater than the Aquatics Center cell. In terms of heat load, the median difference at the Aquatics Center and Campus cell were 950 MJ and 512.6 MJ, respectfully ($p = 1$, $p = 1$, respectfully). EMT reduction was greater at the Campus Cell while heat load reduction was greater at the Aquatic Cell. Again, the median heat load reduction was greater at the Aquatics Center due to larger heat load associated with the large flow volumes needed to generate inflow into the cell. The Campus cell experienced inflow events from smaller storms, ultimately driving this heat median down.

EMT reduction was evident at both sites, but the greatest EMT reduction was seen at the Campus cell with an average of 6.6°C reduction (28.6% reduction) for all storms during the monitoring period (p-value < 0.001). This reduction value is skewed because it includes storms that did not produce outflow, so EMT reduction for storms with no outflow is 100%. Removing these storms from the calculation, the average EMT reduction for storms that produced outflow at the Campus cell was 3°C (13% reduction, p-value <0.001). Similarly, the average EMT reduction at the Aquatics Center cell was 6°C (26.2% reduction, p-value = 0.027) for all storms that produced inflow during the monitoring period. For storms that produced outflow at the Aquatics Center cell the average EMT reduction was 1.6°C (7% reduction, p-value = 0.019) which is significantly less than the reduction at the Campus cell. As stated earlier, there were four overflow events at the Aquatics Center cell during the monitoring period. The average EMT reduction for storms that produced outflow, but not overflow, at the Aquatics Center cell was 1.9°C (8.3% reduction). Although the difference in EMT reduction is minimal (1.3%) after removing overflow events, this difference illustrates the importance of designing cells to minimize overflow events. Despite having similar EMT reduction percentages for all inflow events at each cell, the Campus cell

demonstrated higher EMT reduction for storms that produced outflow when compared to the Aquatics Center cell.

Figures 4-8 and 4-9 shows the inlet and outlet EMT for each storm event. As evident in these figures, outlet EMT generally increased over the course of the summer and peaked at the end of July for the Aquatics Center cell and during the middle of August for the Campus Cell. Despite having similar EMT inflow ranges during the summer, this EMT outlet increase indicates that thermal reduction potential decreased as soil temperatures increase during the monitoring period. It should be noted that the Campus cell experienced slightly higher inflow EMTs. This may be due to the parking lot characteristics, discussed later in this section, or potentially due to the monitoring equipment set up at this site. The parking lot for this cell is larger and has less shading and a longer flow path. Additionally, the flow path for the Aquatics Center cell included a 50 m long pipe, twice as long as the inflow pipe at the Campus cell, in which the runoff could have cooled before reaching the bioretention cell. The stilling wells set up for the H-flumes resulted in higher initial inflow temperatures as any water that was already in the wells was warmer than the inflowing water, particularly for afternoon storm events. However, temperatures typically stabilized within the first few monitoring intervals. Despite having higher inflow EMT, the outflow EMT was, on average, over half a degree cooler than the EMT at the Aquatics Center cell over the course of the monitoring period. Given past literature suggesting that deeper cells enable greater runoff temperature reduction (Jones and Hunt 2009), this finding may suggest that cell media depth may not be the most influential design characteristic for temperature reduction.

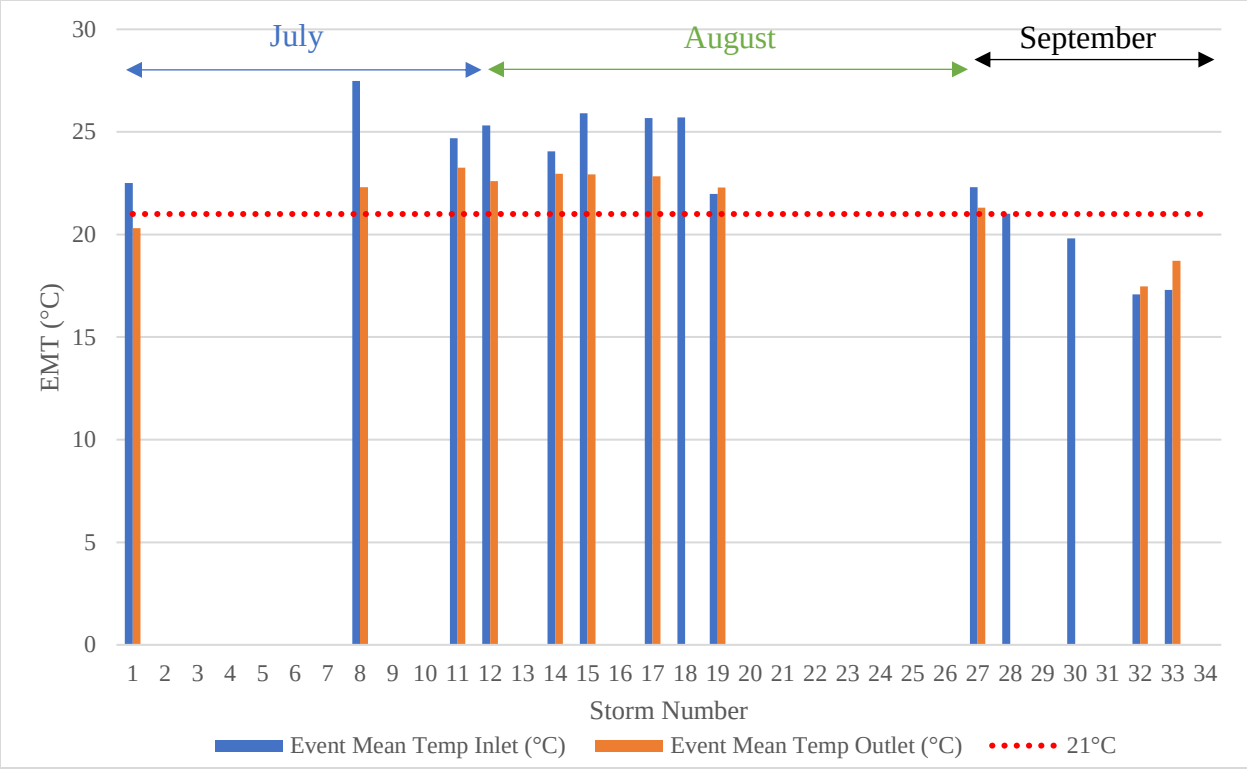

Figure 4-8. Aquatics Center cell inlet and outlet EMT.

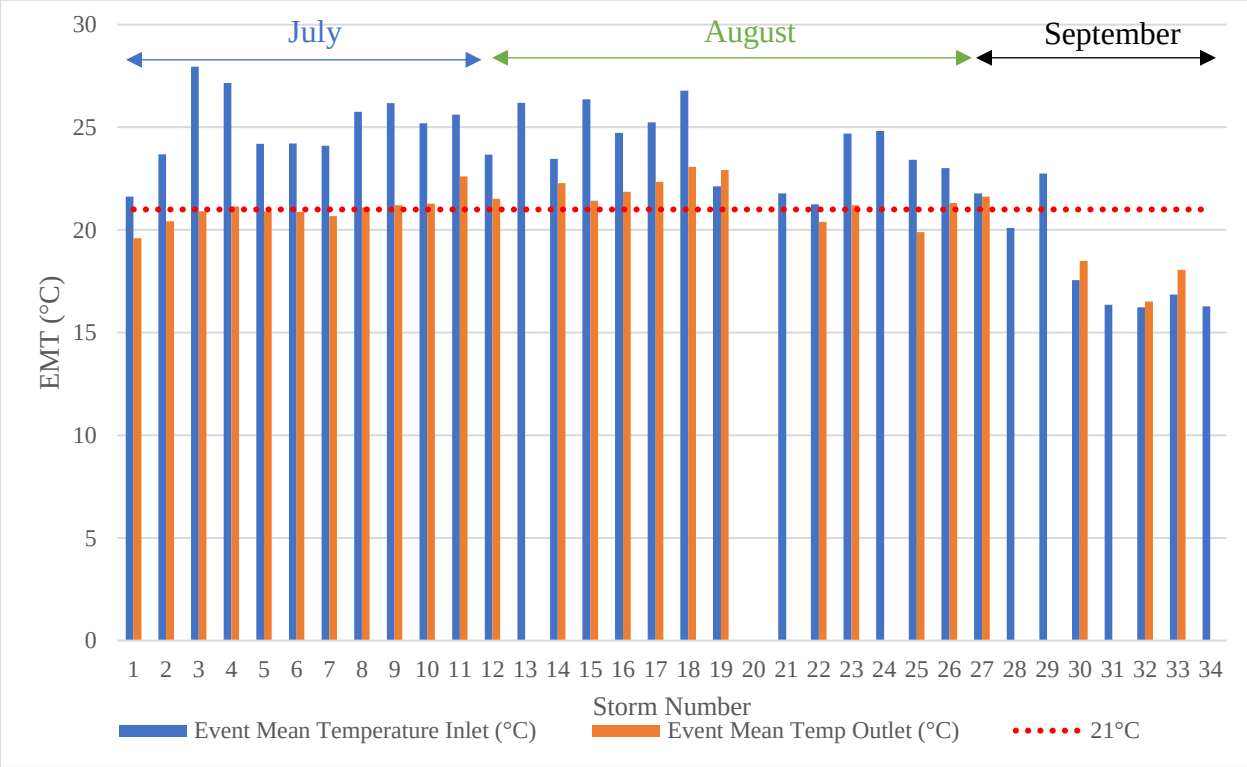

Figure 4-9. Campus cell inlet and outlet EMT

EMT increase through the bioretention cells was observed on seven occasions during the monitoring period, four times at the Campus cell and three instances at the Aquatics Center cell. Similar to results of previous studies, most EMT increase was observed during late summer when soil temperatures were increasing and air temperatures were decreasing. Dietz and Clausen (2005) observed similar trends during fall and winter months in Connecticut when runoff temperatures were significantly lower. In these cases, the bioretention media acts as a heat source transferring stored thermal energy to the colder runoff. This a potential concern during the fall as this coincides with Brook Trout spawning season (Jones and Hunt 2009). Despite the increase in outflow EMT for these storms, the EMT leaving the cell remained below than the 21°C stress threshold for cold-water fish species. Storm 19 on 08/15/2020 was the only event that resulted in an increase in EMT during the middle of the summer. This EMT increase was observed at both cells and was due impart to the lower inlet EMT associated with this storm event. Storm 19 was an all-day storm event with a majority of the inflow and outflow occurring in the afternoon and evening. Air temperatures were lower during this storm event than any other storm event July and August which may explain the lower inflow EMT to the cells. The minimum and maximum air temperatures during this storm were 15.4°C and 20.8°C, respectfully.

During the monitoring period both cells showed similar heat load reduction potential (Table 4-2). Although the average heat load entering and leaving the Aquatics Center was greater than those values at the Campus cell, this is due mainly to the types of storms that generated inflow at the Aquatic Center site. As stated earlier, only larger, more intense storms generated inflow at the Aquatics Center. As a result, these storms included larger stormwater volumes entering and leaving the cell, resulting in higher thermal load values. In general, storms with large flow volumes

resulted in large heat loads entering and leaving the cells, indicating that heat load is more of a function runoff volume than runoff temperature (Table A-3 and A-4). Figure 4-10 shows the cumulative influent and effluent heat loads at each cell during the monitoring period.

Table 4-2. Campus Cell Average Heat Load and Reduction

Site	**Average Heat Load Inflow (MJ)**	**Average Heat Load Outflow (MJ)**	**Average Heat Load Reduction (MJ)**	**% Decrease**
Campus	1802	471	1431	79
Aquatic Center	2360	461	1997	85
*Average Heat load taken for storms that produced inflow				

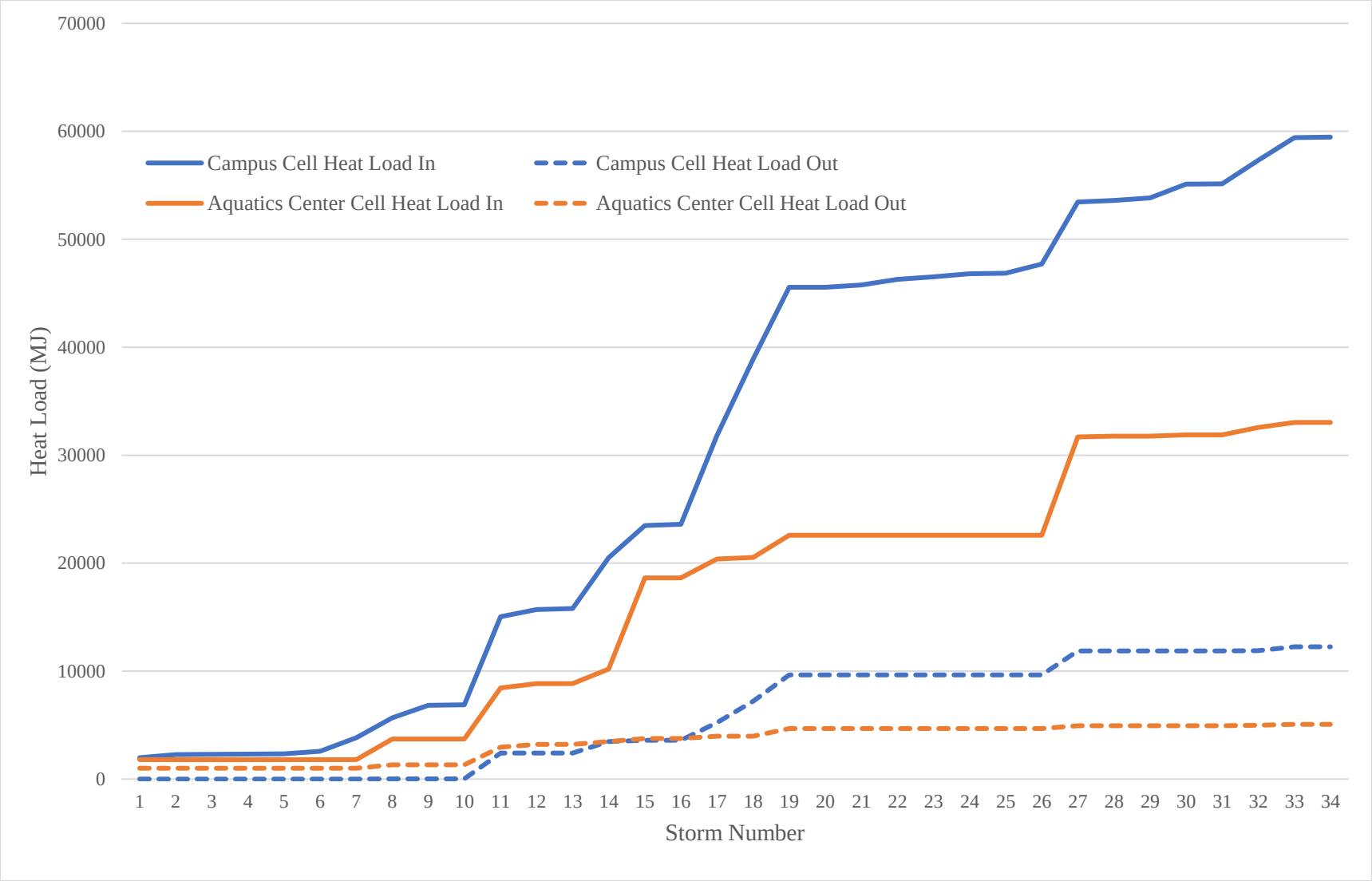

Figure 4-10. Cumulative influent and effluent heat load at each cell. Storm 1 occurred on July 13th, 2020

In order to assess the significance of temperature reduction below the 21°C stress threshold for trout a one sample sign test for median was conducted using 21°C as the test median. Only flow events that generated outflow were used for this analysis. The median outflow EMT at the Aquatics Center cell was 21.8°C ($p = 0.967$) and the median outflow EMT for the Campus cell was 20.9°C ($p = 0.837$). The p-values from both cells indicate that there was no significant difference between outflow EMT and this 21°C threshold. This is consistent with the findings of Jones and Hunt (2009); this study also observed significant temperature reduction in runoff temperature but no significant difference between outflow temperatures and the 21°C threshold.

Streams are more susceptible to thermal pollution during summer months because air temperature and solar radiation are highest and and stream base flow is typically lowest (Arrington et al. 2004). However, for runoff to cause thermal pollution the runoff temperature needs to exceed the stream temperature. Temperature and stage readings for the entirety of 2020 from Bridge 1 at the StREAM Lab indicate that stream temperatures are highest during the summer months (Figure 4-1). Based on the daily maximum stream temperature readings it is likely that there are no trout populations within this section of Stroubles Creek, as daily maximum temperatures reach over 37°C during the summer months, which is well above the 30°C lethal temperature threshold for trout (Elliot and Elliot 1995; Wehrly et al 2007). However, this monitoring station and the approximately 800 m reach upstream of Bridge 1 is largely unshaded, which likely the primary cause of the high water temperatures. As a result, storm events indicated by the increase in stage appear to decrease stream temperature in this section of Stroubles Creek. Cell outflow EMTs were lower than the daily maximum stream temperature for 97% of the study period. Storm 19 on 08/15/2020 was the only storm event that resulted in outflow EMT greater than the maximum daily stream temperature. For this storm event, outflow EMT at the Campus cell was 22.9°C while the

maximum Stroubles Creek stream temperature was 22.6°C for this day. The Aquatics Center cell did not have outflow EMTs greater than the Stroubles Creek daily maximum temperature at any point during the monitoring period. Lastly, stream stage was also lowest during summer months into the fall, which may be of concern as the fall is Brook trout spawning season. This lower baseflow will make the stream more susceptible to thermal pollution during a crucial life stage of the Brook Trout.

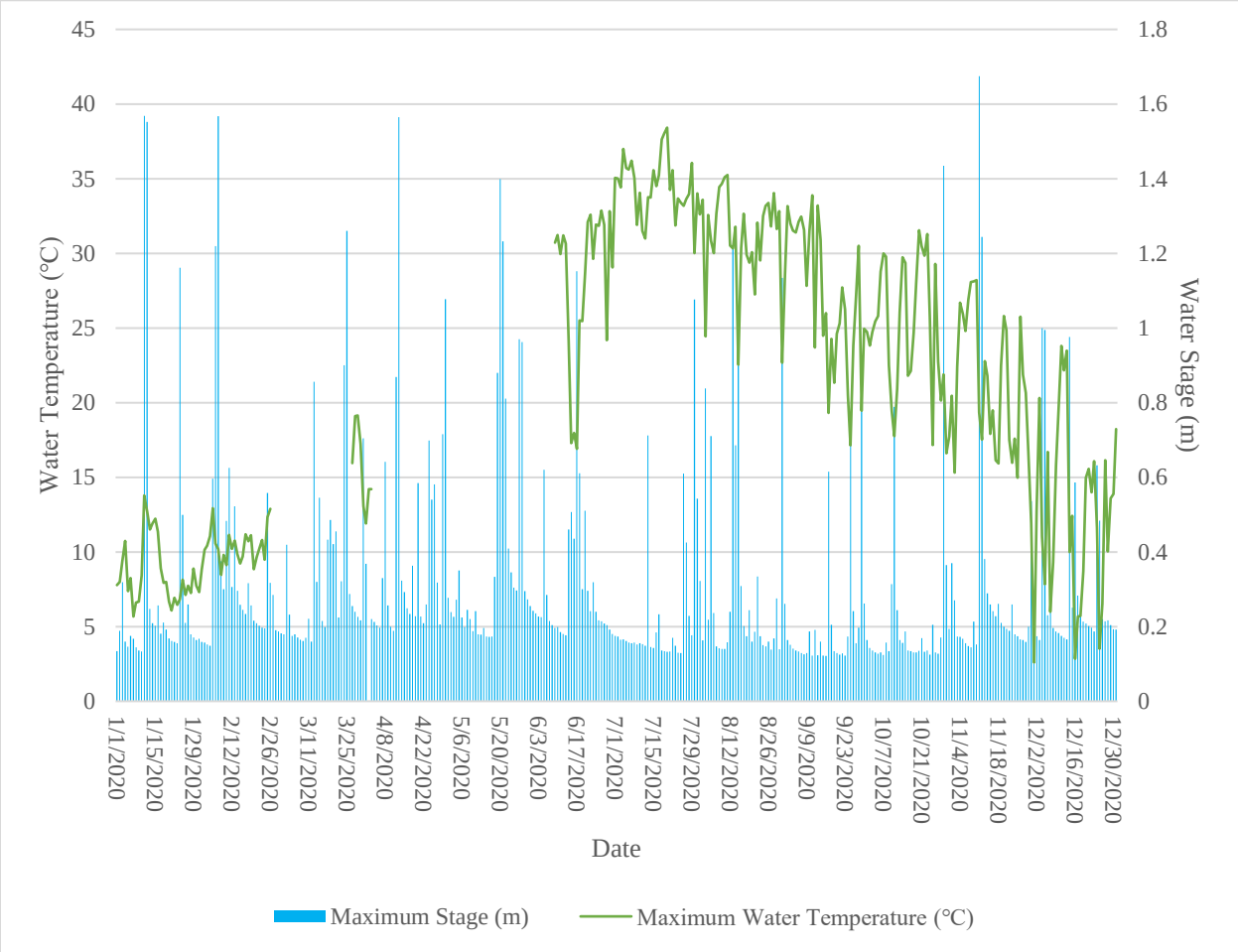

Figure 4-11. Stroubles Creek maximum daily stage and water temperature at Bridge 1

4.5 Comparison of Cell Designs

The second objective of this research was to identify beneficial design characteristics for thermal reduction. Originally, the plan was to monitor multiple bioretention cells in the area to draw from a larger range of design characteristics. Due to the Covid-19 pandemic, monitoring set up was delayed and travel was limited by the university. As a result, monitoring defaulted to these two local bioretention cells. Although, monitoring was limited to these two cells, there were stark contrasts between the cell designs which may highlight design characteristics that promote runoff temperature reduction. Design characteristics of each cell along with cell media composition are listed in Tables 4-3 and 4-4.

To highlight some of the contrasting design characteristics it should first be noted that the drainage area for the Campus cell was more than twice that of the Aquatics Center Cell. In addition, the Aquatics Center cell was built as a retrofit to a preexisting stormwater drainage system so design was limited by preexisting conditions, such as underground utilities. Furthermore, the design approach for each cell differed. The Campus cell was designed following specifications described in the *1999 Virginia Stormwater Management Handbook*, while the Aquatics Center Cell was designed to meet the peak flow and volume reductions using flow routing through the cell (Morin and Debusk 2008). As a result, the surface area to drainage area ratio at the Aquatics Center was 2.1%, which is lower than the minimum ratio of 2.5% suggested by the state of Virginia and lower significantly lower than the 5-7% suggest by other literature (VADCR 1999; Lord and Hunt 2006). Comparatively, the Campus cell has a ratio of 6.5%, which follows both recommendations. With less surface area for infiltration and less ponding volume, the Aquatics Center experiences more overflow events during higher intensity storms. Any overflow during a storm event will effectively bypass the bioretention cell, which negatively impacts the temperature

and heat load reduction potential of the cell. This design limitation at the Aquatic Center Cell may be offset by a soil media composition comprised of mostly sand, which has higher infiltration rates (Table 4-3). However, Hunt et al. (2012) suggested that hydraulic retention time, especially at deeper soils layers, may be crucial for temperature reduction. In this case at the Aquatics Center cell, the soil media may be too porous and stormwater may infiltrate to the subsurface drainage before temperature equilibrium is reached with the cell media.

Another difference between the two cells is in the ponding depth and resulting ponding volume. The Aquatic Center has a maximum ponding depth of 15 cm. This is on the lower end of the 15.2 to 30.5 cm range recommended in both the *1999 Virginia Stormwater Management Handbook* and the updated VADEQ Stormwater Design Specification NO. 9 (VA DCR 1999; VA DEQ 2011). In contrast, the Campus cell was originally designed to have a ponding depth of 13.7 cm which again was slightly lower than the design specifications but due to soil compaction and organic material decomposition since construction, the cell had an actual ponding depth of 45.7 cm during monitoring. This depth is 50% larger than the design specification. As a result, the ponding volumes are 5.24 m^3 and 109.7 m^3 for the Aquatic Center and Campus cells, respectfully. Despite having a smaller drainage area, the ponding volume-to-drainage area ratio at the Aquatics Center is over eight times smaller than that of the Campus cell. This lack in ponding volume leads to overflow events during large and high intensity storm events.

Another contrast between the cells is the media depth. The Aquatic Center cell has a media depth of 1.8 meters, while the Campus Cell has a media depth of 0.86 m. The State design specifications suggest that the cell media depth should be 0.61 m - 1.82 m, so each design is towards the extrema of the design specification (VA DCR 1999; VA DEQ 2011). However, the drainage system at the Aquatic Center was set 30 cm above the cell bottom so it effectively had a

discharge depth of 1.5 m. Previous research has indicated that that optimal depth for runoff temperature reduction is between 90 and 120 cm (Jones and Hunt 2009). Although neither cell is in this range the Campus cell drainage system is closer to this suggested range and may perform better than the Aquatics Center. After a certain depth, soil temperatures may not decrease further and remains relatively constant, so runoff temperature reduction below this soil temperature may not be possible.

A deeper cell may aid in water storage and overall flow reduction; however, despite the differences in cell depth, the larger surface area of the Campus cell led to a greater media volume when compared to the drainage area size. Li et al. (2009) observed that cells with a greater soil volume-to-watershed size ratio were more effective at reducing outflow. Flow reduction was indicated as the key component to reducing the overall thermal impact of storm water (Jones and Hunt 2009). In addition, a deeper media layer will have a more stable temperature as it is removed from the temperature fluctuations caused by air temperature and direct solar radiation. Deeper layers in the cell media were observed to generally be cooler than the upper media layers (Jones and Hunt 2009).

Both cell designs included an underdrain system and a clay liner to prevent the formation of sinkholes. However, the Aquatics Center cell includes an internal water storage area (IWS) as the drainage system is raised 30 cm above the bottom of the cell. This IWS results in a cell media storage volume of approximately 10.5 m^3 below the drainage system, which may assist in overall flow volume reduction through the cell. The drainage system at the Campus cell was installed directly above the clay liner at the bottom of the cell. However, comparing linear distance of subsurface drainage piping between the cells, the Aquatics Center has approximately 12 m within the cell compared to 55 m at the Campus cell. Additional runoff temperature cooling was observed

through drainage piping (Jones and Hunt 2009), so greater linear distance of subsurface drainage may aid in temperature reduction. Lastly, even though there was a clay liner installed during construction it should be noted that root growth as the vegetation matured may have broken through this clay liner resulting in flow volume loss through the bottom of the cell. Due to the cell media depths this has likely occurred at the Campus Cell but it is assumed the Aquatics Center liner remains intact, given the cell depth. Furthermore, there was no clay liner placed on the sides of either cell so lateral flow loss is also possible.

The last characteristics that should be addressed are the mulch layer and canopy shading present at each cell. The Aquatics Center Cell had a 5 cm layer of cypress woodchip mulch added prior to monitoring while the Campus Cell did not have a mulch layer. Although the design plans for the Campus Cell included a layer of mulch, the bowl of the cell was not maintained and was overgrown with vegetation by the time of monitoring. This mulch layer may reflect solar radiation, reduce soil temperatures and act as an insulator and regulator of the soil temperature. Finally, canopy cover is significantly greater at the Campus Cell which has multiple large, mature Monarch River Birch, Sheep Laurel and Witch Hazel in the bowl and along the edge of the cell. This cell has a minimum and maximum shade coverage of 60% and 70%, respectfully, during the middle of the day. In contrast, the Aquatics Center only has two Redbud trees and one Shadbush located along the edge of the cell, leaving more than half of the cell surface exposed to direct sunlight through the day. This resulted in a minimum and maximum shade coverage of 10% and 60%, respectfully, during the middle of the day. Direct sunlight to the surface of the cell increases the soil temperature and may reduce the potential for thermal reduction during infiltration.

Table 4-3. Cell design comparison

Cell Design	Aquatics Center Cell	Campus Cell
Drainage Area (m^2)	1600	3700
Cell Surface Area (m^2)	35	240
Surface Area/Drainage Area (m^2/m^2)	2.1	6.5
Ponding depth (cm)	15	45.7
Ponding Volume (m^3)	5.2	109.7
Cell Depth (m)	1.8	0.86
Media Volume (m^3)	62.9	207.3
Mulch Layer	Yes	No
Internal Water Storage (IWS)	Yes	No

Table 4-4. Cell media composition

Aquatics Center Cell		Campus Cell	
Cell Media Composition	**Percent by Volume**	**Cell Media Composition**	**Percent by Volume**
Washed Sand	88%	*Sand*	50%
Clay and Silt Fines	8%	*Topsoil*	30%
Organic Matter	4%	*Leaf Compost*	20%

4.6 Soil Temperature Profiles

Comparing the soil profiles for each site illustrates trends discussed previously in literature. Jones and Hunt (2009) observed that soil temperatures near the surface experienced more daily temperature fluctuation and soils at greater depths were generally cooler and maintained a more stable temperature. Analyzing the daily minimum and maximum soil temperatures at each depth at each site shows that surface soil temperatures had greater diurnal fluctuations when compared to soil temperatures at greater depths (Figure 4-12 and 4-13). Furthermore, generally speaking, sensors located on the surface in shaded areas experienced lower maximum temperatures during the first half of the monitoring period. This trend flips during the second half of the monitoring period as shaded areas show a higher daily maximum at both sites. This may be due to the change in the angle of the sun over time which may have resulted in the area being exposed to more direct sunlight than when initially installed. However, this indicates the importance of adequate canopy shading on soil temperature reduction. On clear nights, generally in September, the surface of the bioretention cell becomes significantly cooler than the bioretention media due to radiative cooling.

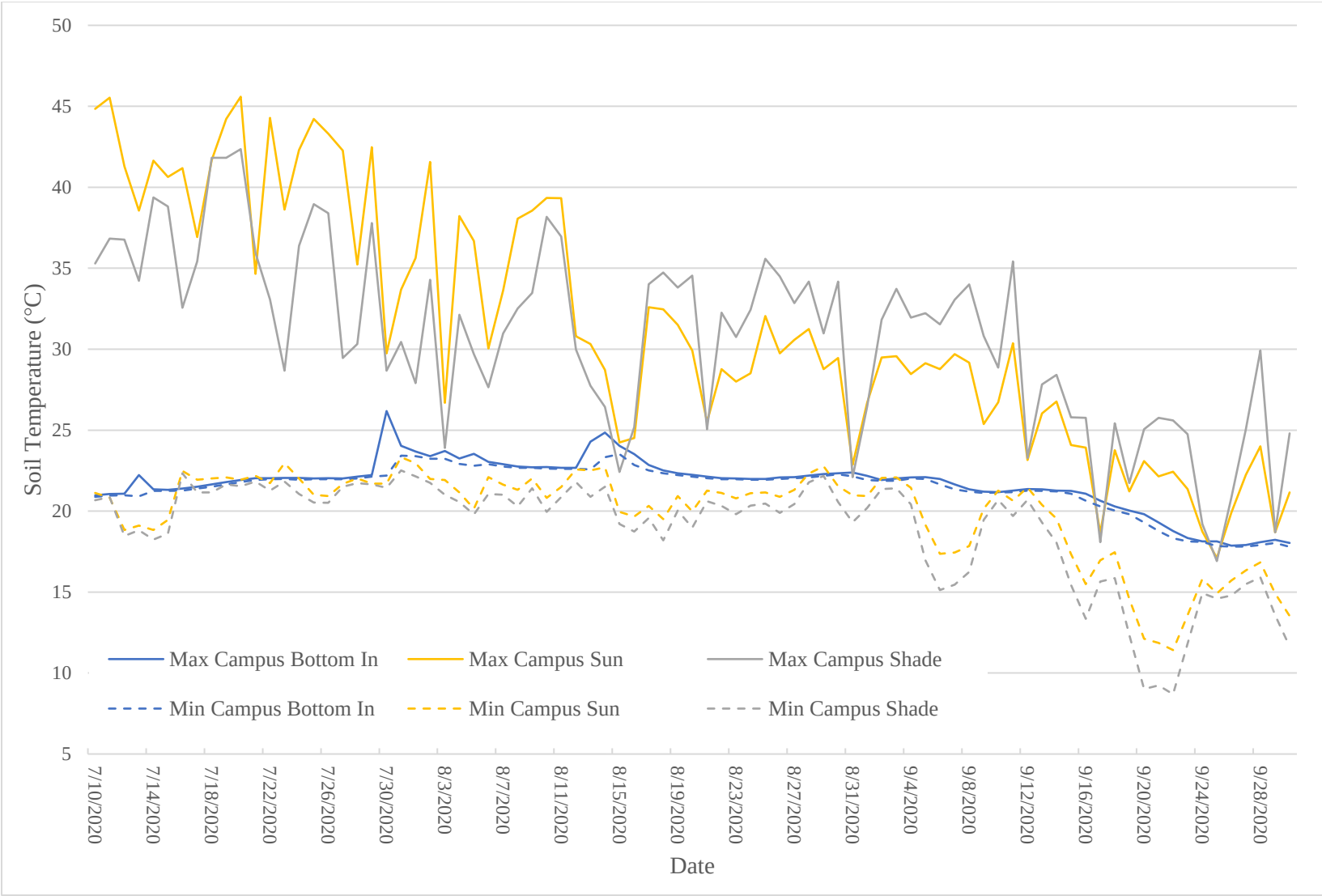

Figure 4-12. Campus Cell soil profile for entirety of monitoring period

At depth, both sites show similar temperature trends. Soil temperatures were less affected by the diurnal temperature changes due to air temperatures, direct solar radiation and radiation loss at night. Sharp increases in the soil thermal profile at depth were associated with precipitation events, showing the soil is gaining temperature in response to the infiltration of warmer runoff. Both sites showed a lagged response in soil temperature increase, indicating that once the deeper soil increased in temperature it takes multiple days for the soil to return close to the temperature before a storm event (Figure 4-12 and 4-13). For example, this occurred on 07/29/2020 at the Campus cell (Figure 4-12) and 08/15/2020 at the Aquatics Center cell (Figure 4-13). This intermittent heating will affect the ability of the cell to reduce runoff temperatures if storms occur closer together as soil temperature will be higher for the sequential storm. Comparing the average maximum temperature at the bottom of the Campus cell (86 cm) to the drainage depth of the Aquatic Center cell (150 cm) indicated that the deeper cell was warmer than the shallower cell over the course of the monitoring period. The average maximum temperature at 86 cm near the inlet at the Campus cell was 21.7°C. The temperature at this depth near the outlet was almost a degree lower but this sensor malfunctioned for an extended period during monitoring, which would explain this lower average daily maximum temperature. Comparatively, the sensor at the 90 cm depth at the Aquatics Center reported an average daily maximum temperature of 22.5°C (Table 4-6).

Given the accuracy of the soil temperature sensors of ±0.25°C from 0°C to 50°C, these temperature differences are not that significant. However, the proximity of the Aquatics Center cell to the parking lot may explain these temperature differences. The Aquatics Center cell is located immediately next to parking lot and the surface of the cell media is level with this paved surface. The Campus cell is spaced further from the adjacent parking lot and top of the cell media

is significantly lower than the parking lot. Furthermore, the soil temperatures were coolest at the bottom of the Aquatics Center Cell, at 1.8m. Although this depth was below the underdrain system inflowing water may mix with the cooler runoff stored in the IWS from previous storm events. During this mixing, the cooler stored water could potentially be flushed out, providing additional thermal reduction benefits.

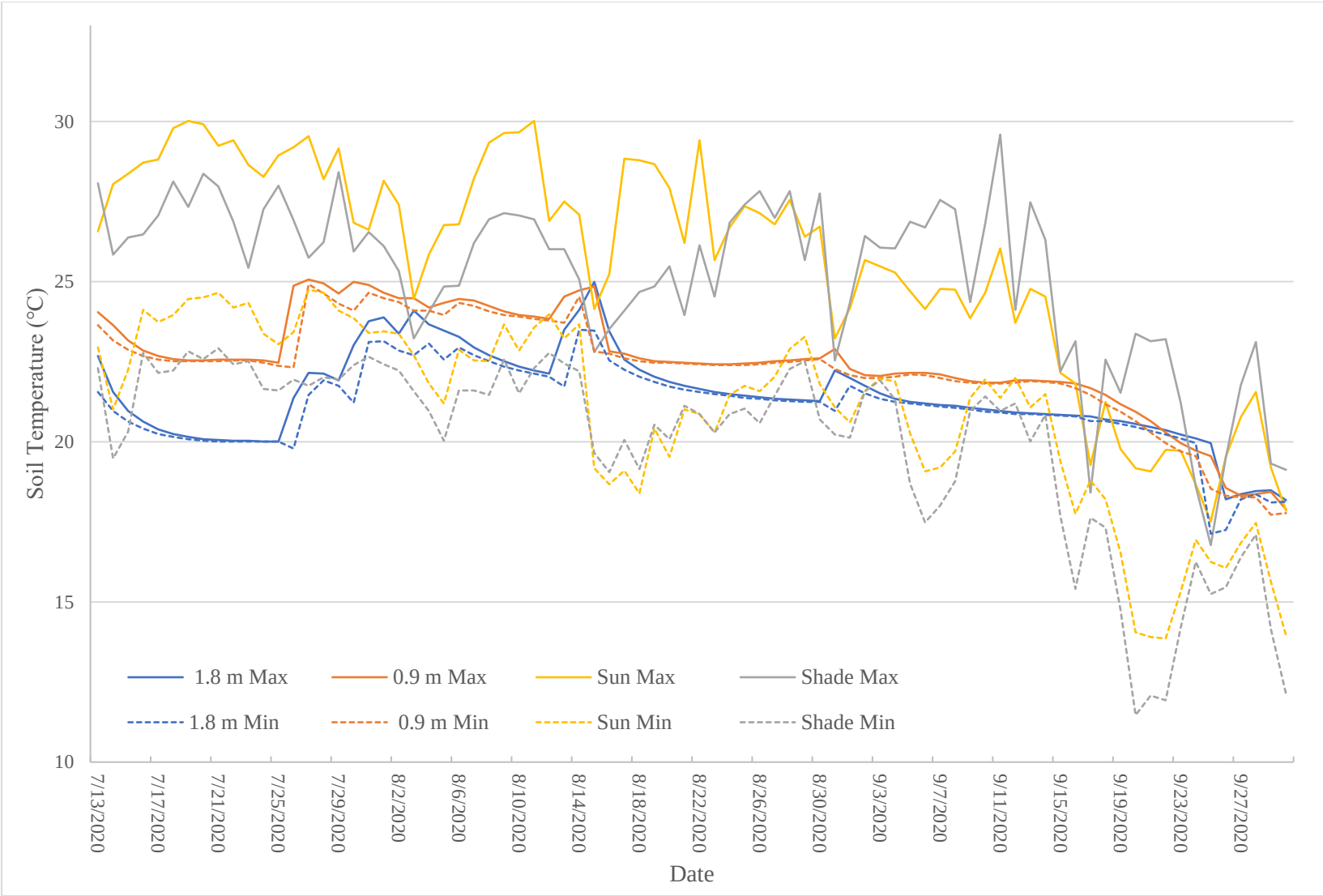

Figure 4-13. Aquatics Center cell soil profile for entirety of monitoring period

Comparing the average daily maximum temperatures from both cell locations illustrates that despite having more shading the cell surface as the Campus cell experienced greater temperature maximums (Table 4-5). However, at the outflow depth of 0.86 m the Campus cell was nearly a full degree cooler than the similar depth reading at the Aquatics Center. Figures 4-14 and 4-15 further show this observation, in both these figures the orange line represents a one to one relationship. Comparing the daily maximum surface temperatures between the cells indicate that throughout the monitoring period surface temperatures were greater at the Campus cell (Figure 4-12). Despite having more shading, these higher maximum temperatures may be due to the lack of a mulch layer at this cell. Comparing the daily maximum temperatures at a similar depth (0.9 m vs 0.86 m) at both cell locations indicates that for almost the entirety of the monitoring period the Aquatics Center cell had greater daily maximum temperatures. This may be due to the proximity of the cells to surrounding parking lots. The Aquatics Center cell is closer to the adjacent parking lot which may result in the higher soil media temperatures at this depth. Although The bottom of the Aquatics Center (1.8 m) was coolest there was no sensor set up at the outflow depth of the Aquatics Center (1.5 m) so it is difficult to compare outflow depth temperatures between the cells. However, the mean maximum daily temperatures reported in Table 4-5 and the maximum and minimum daily temperatures shown in Figures 4-12 and 4-13 indicate that for a majority of the monitoring period soil temperatures were above 21°C. In terms of thermal equilibrium, this is an important consideration as runoff temperature reduction below 21°C is impossible if soil media temperatures remain above this temperature.

Table 4-5. Average Daily Maximum Soil Temperatures

Site	**Sensor Location**			
Aquatic Center	**Surface Sun**	**Surface Shade**	**1.8 m**	**0.9 m**
Mean Max Temp (°C)	25.7	25.2	21.4	22.5
Campus	**Surface Sun**	**Surface Shade**	**0.86 m Inlet**	
Mean Max Temp (°C)	31.4	30.7	21.7	

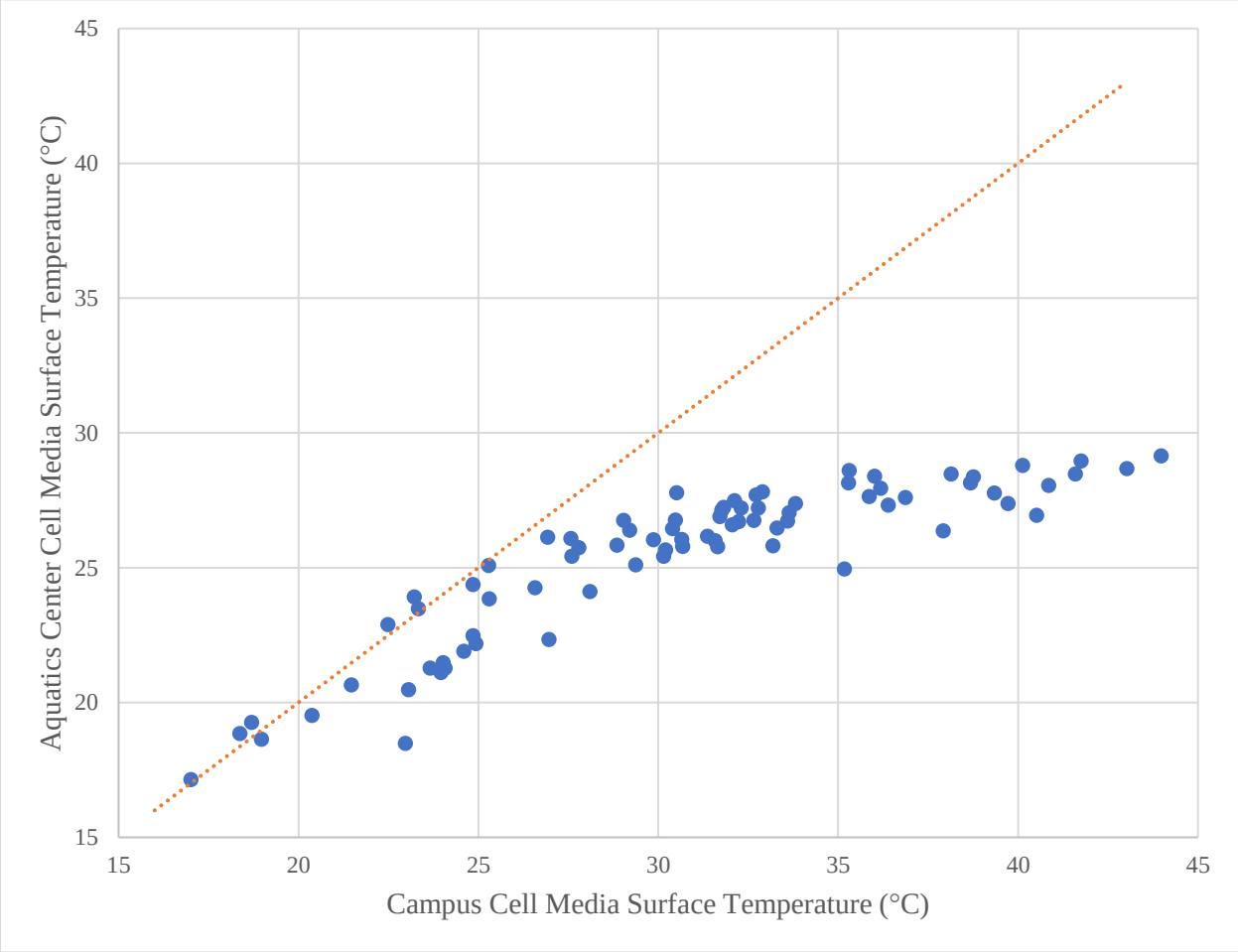

Figure 4-14. Comparison of daily maximum cell surface temperature between the cells

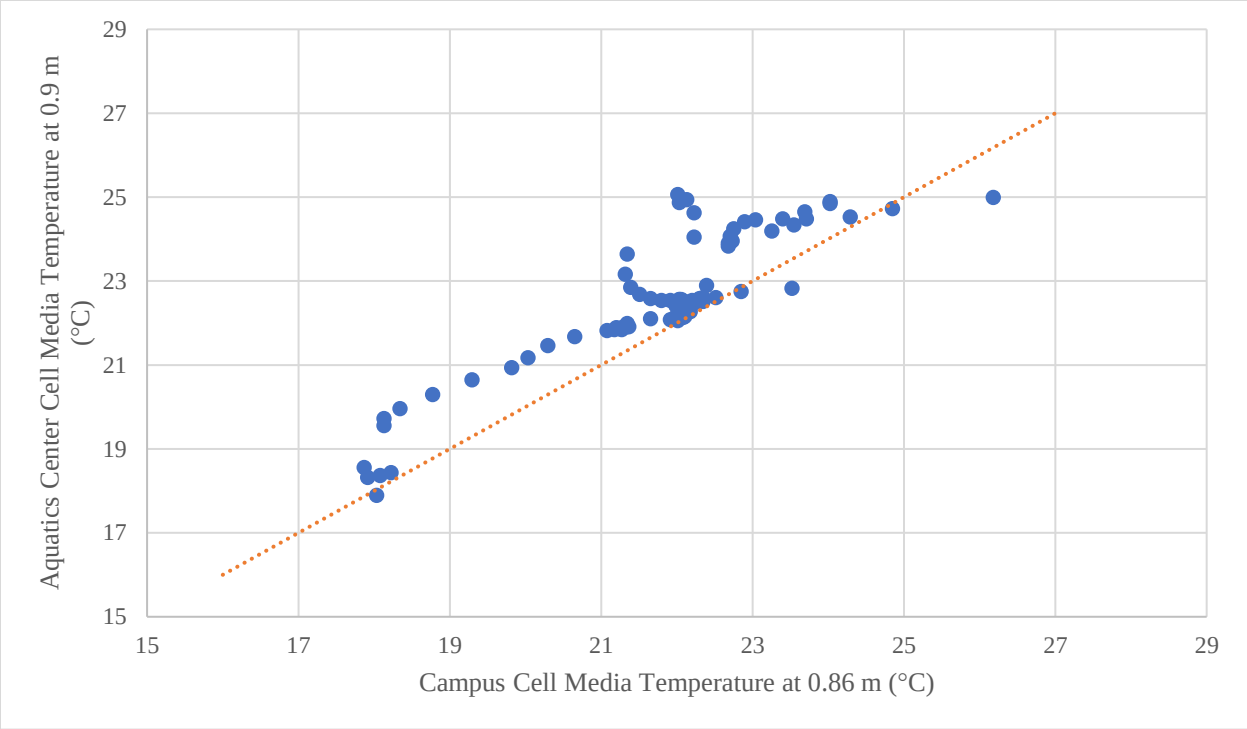

Figure 4-15. Comparison of daily maximum cell media temperature between the cells at similar depths

Despite having more shading, the Campus cell experienced great maximum soil temperatures during the monitoring period. Previous research has suggested that vegetative cover and broad leaf vegetation in particular will have a greater effect on a soil and flow temperatures through a bioretention cell (Hunt, Davis and Traver 2012; Jones and Hunt 2007). Even though the Campus cell had more shading throughout the day, these results indicate that it still was not adequate for reducing and stabilizing soil surface temperatures. The Aquatics Center cell recorded lower daily maximums and overall more stable surfaces temperatures throughout the monitoring period (Figure 4-16). On average the daily maximum surface soil temperature was nearly 6°C cooler and the Aquatics Center cell surface soil temperature, on average, only fluctuated 4.9°C degrees per day compared to 11.6°C at the Campus cell (Table 4-6). Despite having significantly

less vegetative shading throughout the day this may indicate the significance of a mulch layer for regulating and stabilizing soil temperatures. Jones and Hunt (2007) suggested that lighter mulch will reflect solar radiation, reducing soil temperatures.

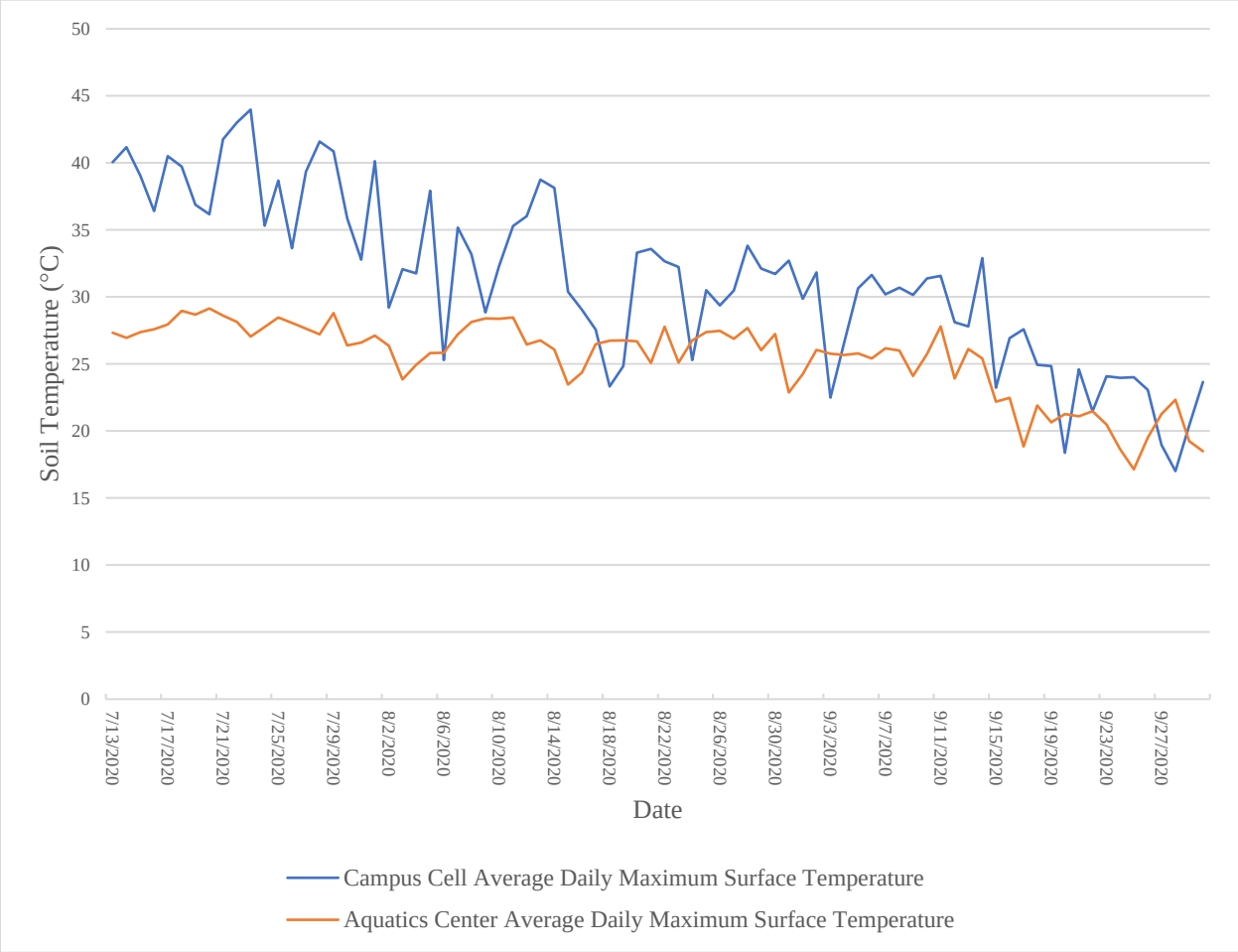

Figure 4-16. Soil Surface Temperature Comparison

Table 4-6. Average Daily Soil Temperature Fluctuation

Aquatics Center	**Surface Sun**	**Surface Shade**	**1.8 m**	**0.9 m**
Diurnal Temperature Range (°C)	4.7	5.2	0.3	0.2
Campus	**Surface Sun**	**Surface Shade**	**0.86 m Inlet**	
Diurnal Temperature Range (°C)	11.5	11.8	0.3	

Soil temperature profiles were created for all storm events. To compare the temperature responses within each bioretention cell during the same storm events, the temperature profiles from each cell for two separate storm events are shown in Figures 4-17, 4-18, 4-19 and 4-20. These two storm events were selected for comparison because both storms produced similar amounts of total rainfall, but had differing durations and maximum rainfall intensities. The first storm event, storm 14 which occurred on 08/03/2020, was a longer storm event. First rainfall occurred early in the morning, 5:00 am, and scattered rainfall occurred throughout the rest of the day with the last recorded rainfall at 16:30 pm. This was all considered one storm as the rainfall events occurred within the three-hour range used for storm isolation, as described earlier. This storm produced a total of 15.5 mm of rain with a maximum 30-minute rainfall intensity of 10.2 mm/hr.

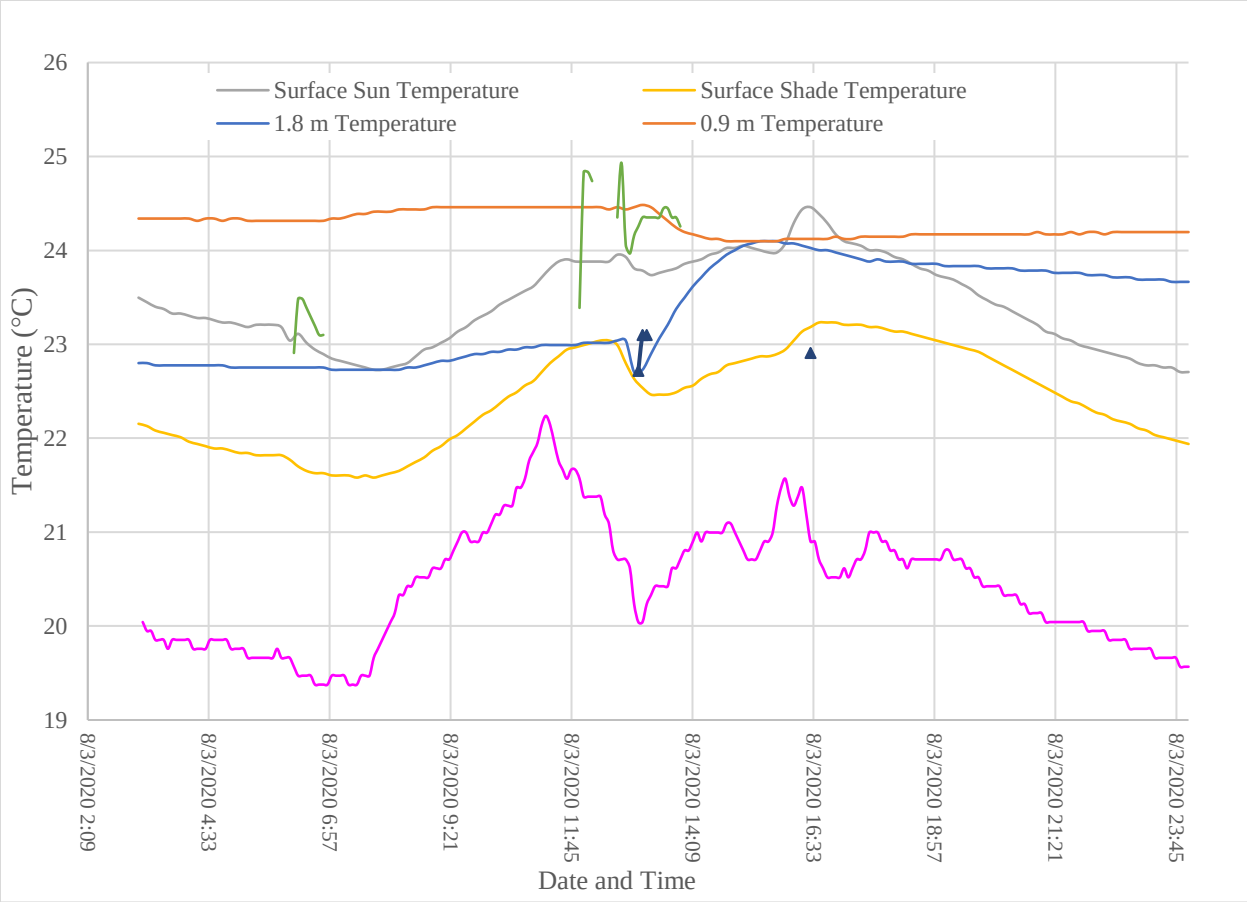

Figure 4-17. Aquatics Center cell storm 14, 08/03/2020, temperature profile

As evident in Figure 4-17, the initial inflow represented by the green line, generated no outflow within the cell. At this point, early in the storm event, the stormwater entering the cell was warmer than three of the four soil locations, with the 0.9 m sensor being the only location warmer than the inflowing storm water. Between the first and second inflow events, the soil temperature increase at all levels with the most drastic increase in the surface layers. This surface soil temperature increase is most likely due to the increase in air temperature, as the surface soil temperatures appear to mirror the air temperature readings throughout the storm event. It should be noted that air temperature readings were not directly retrieved from the Aquatics Center cell,

rather the air temperature readings were retrieved from the Campus cell under the assumption that temperature differences would be negligible. However, during the second inflow event runoff began leaving the cell as indicated by the navy triangles on the plot (Figure 4-17). After the initial outflow was generated, temperature increases at 1.8 m illustrate that stormwater had infiltrated to that depth, increasing the temperature of the surrounding media. At this depth, there was a slight temperature decrease prior the temperature increase, this may be due to cooler water stored in the cell being flushed out during initial infiltration. At 0.9 m, soil temperatures decreased and reached an equilibrium temperature with the surrounding soil layers at about 24°C.

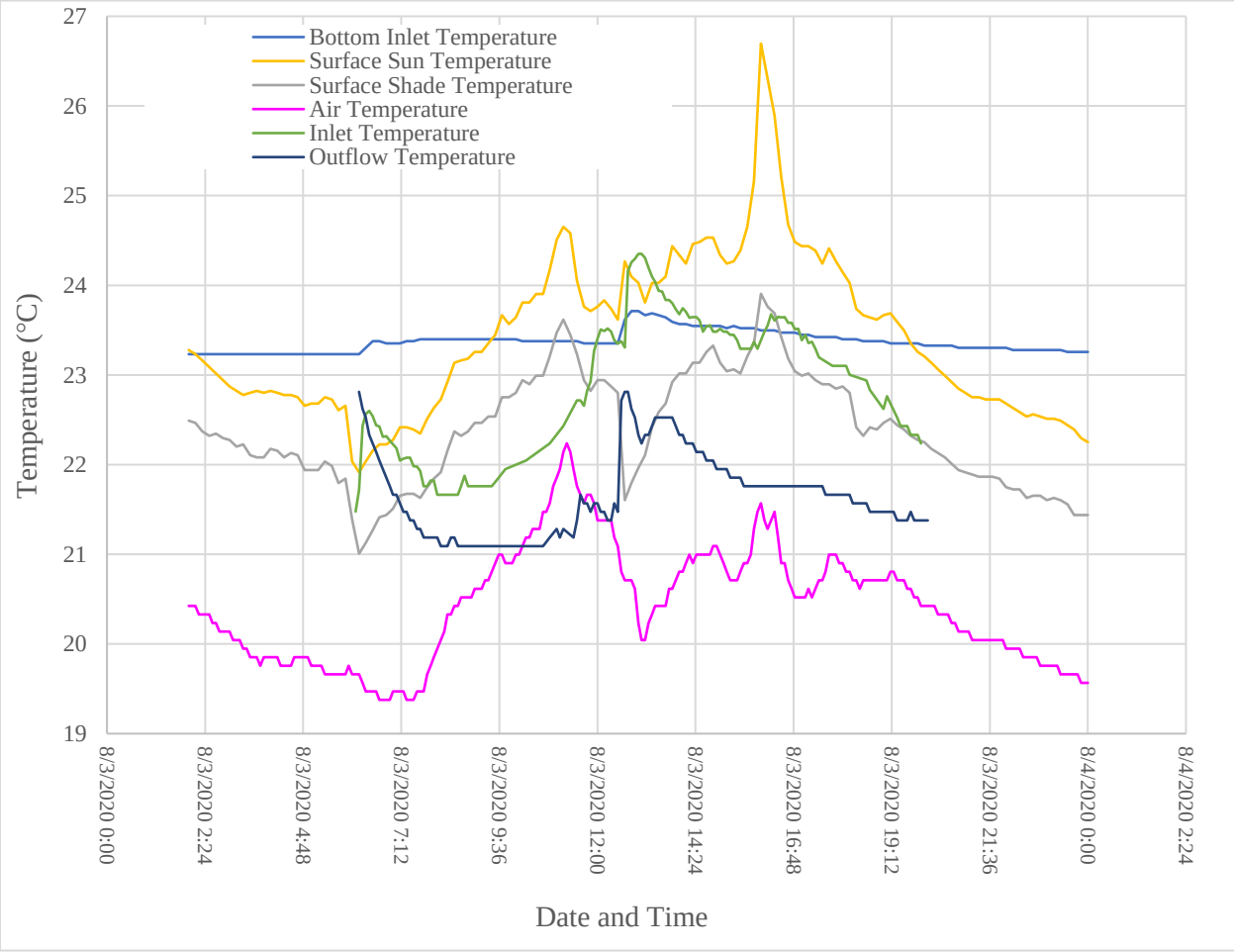

Figure 4-18. Campus cell storm 14, 08/03/2020, temperature profile

Comparing the Aquatics Center cell thermal profile (Figure 4-17) to the Campus cell thermal profile (Figure 4-18) for storm 14 shows similar trends to the Aquatics Center cell. Soil temperatures at the surface of the cell again mirrored the air temperature, while at depth, soil temperature spikes aligned with warmer inflow stormwater. At both cells the air temperature was cooler than the soil temperature, the surfaces layers responded quickly to changes in air temperature while the deep layers remained relatively stable. Like the Aquatics Center, soil temperatures on the shaded surfaces were cooler than the lower soil layers which may possibly provide some additional runoff cooling effects. The most interesting aspect of the Campus cell temperature profile is that outflow temperatures, aside from the initial outflow leaving the cell, is generally cooler than the deepest layer of soil media. Similar to findings by Jones and Hunt (2009), this suggests that additional cooling is occurring in the underdrain system as the infiltrated storm water is leaving the cell.

The second storm isolated for this comparison is storm 15 which occurred on 08/05/2020. This storm was a shorter more intense afternoon storm, starting at 16:00 pm and ending 17:30 pm, which produced a total rainfall of 14.2 mm and a maximum 30-minute rainfall intensity of 21.8 mm/hr. Similar cell responses discussed above are apparent for this storm at both sites (Figures 4-19 and 4-20). Most notably, the Campus cell outflow temperature was again cooler than the deepest soil layer which further supports the idea that additional cooling was occurring in the underdrain system.

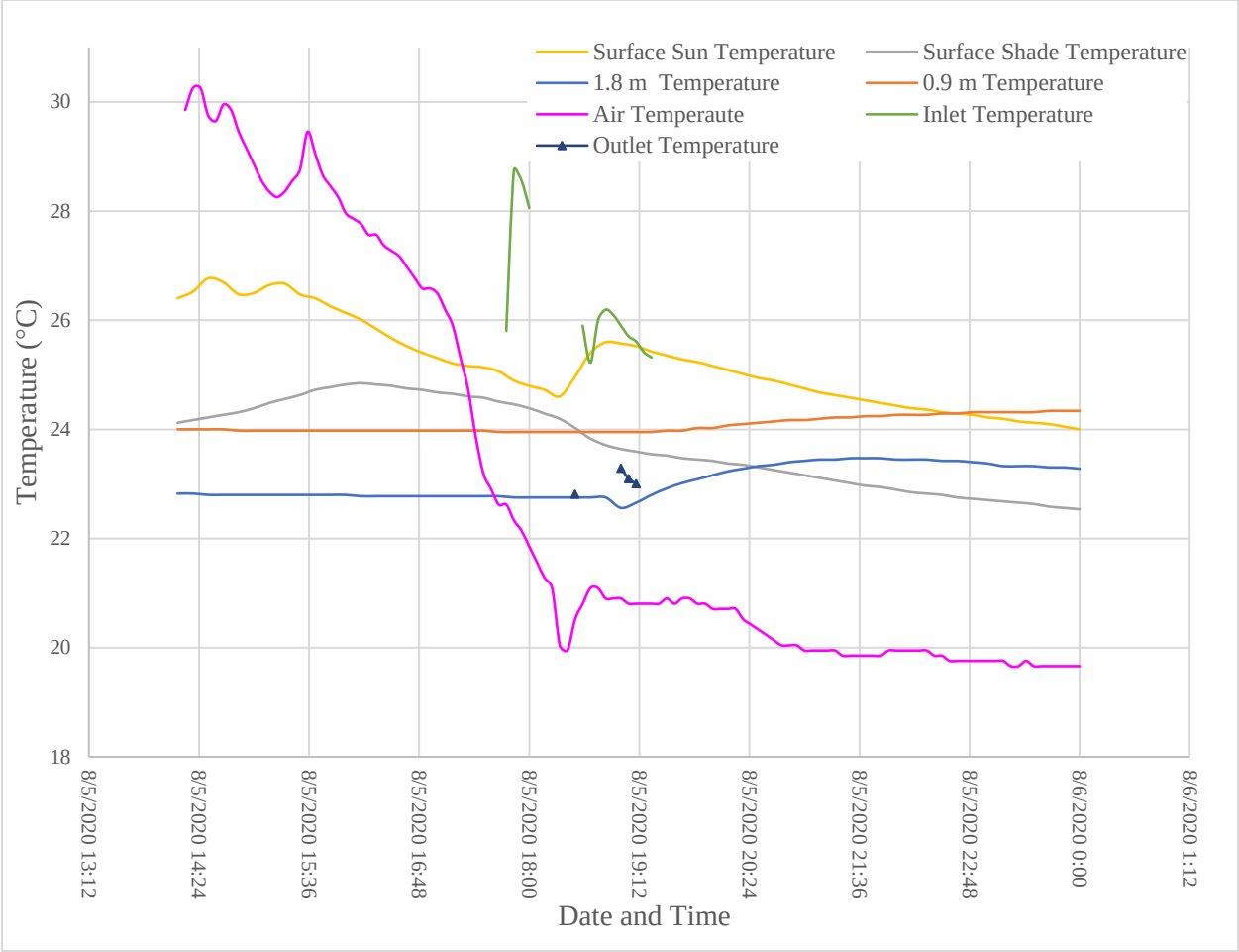

Figure 4-19. Aquatics Center cell storm 15, 08/05/2020 temperature profile

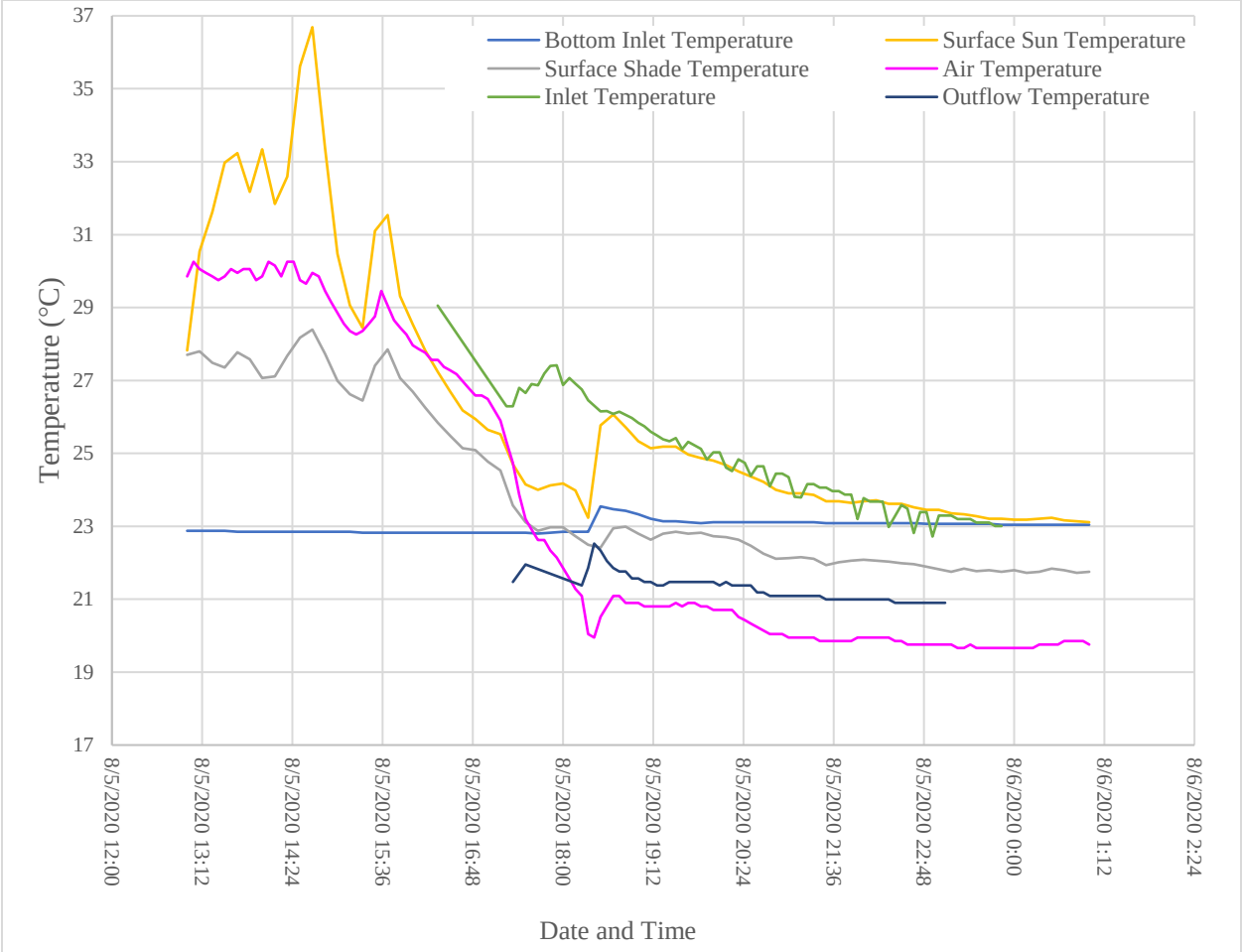

Figure 4-20. Campus cell storm 15, 08/05/2020 temperature profile

From these figures (Figures 4-17, 4-18, 4-19 and 4-20), it is clear that soil temperature is a major source of runoff temperature reduction, however the Campus cell plots indicate that additional cooling is occurring in the underdrain system. Soil temperatures at all depths for both sites were well above the 21°C temperature stress threshold from cold-water fish species, indicating the potential limitation of using bioretention cells in urban watersheds harboring these species. Despite this limitation, there is a clear runoff temperature reduction between inflow and outflow at both cells. Combined with flow volume reduction, the study findings indicate that

bioretention cells can effectively reduce storm water thermal loads. Furthermore, outflow from the Campus cell for the two storms shown in Figures 4-18 and 4-20 was substantially cooler than the bioretention media temperatures, suggesting that addition cooling is occurring after the stormwater infiltrates the cell media and proceeds to the outlet location. Jones and Hunt (2009) observed a similar trend when monitoring four bioretention cells in North Carolina and suggested that the submerged drainage system may be an addition source of cooling. At a larger scale, Hathaway et al. (2016) observed lower maximum and minimum runoff temperatures in larger watersheds that included more subsurface drainage infrastructure. Assuming that flow within the underdrain system is not fully inundated, meaning there is a free surface between the water and air, may allow for additional cooling.

During infiltration the heat exchange process between the stormwater and soil media is conduction. As the storm water begins to travel to the outlet location via subsurface drainage the addition of the water and air interface allows for additional cooling through convection, assuming that the air temperature in the drainage system is cooler than the runoff temperature. As evident in the figures (Figures 4-17, 4-18, 4-19 and 4-20), the ambient air temperature at the cell surface was cooler than both the soil and water temperatures during most of the monitored outflow events at the Campus cell. Although air temperature was not directly monitored within the drainage system it can be assumed that the air temperature within the pipe would be similar, if not cooler then the ambient air temperature. Given the difference in linear distance of subsurface drainage between the two sites, 12 m at the Aquatics Center cell and 55 m at the Campus cell, this may be a reasonable explanation for the cooler outflow temperatures evident at the Campus cell throughout the monitoring period. Lastly, by comparing peaks of inflow and outflow rates for each storm an average runoff travel time was determined for each cell. The average runoff travel time for the

Campus cell was 40 minutes, compared to 26 minutes at the Aquatics Center cell. This longer travel time from inflow to outflow may also provide an additional explanation for the cooler outflow temperatures at the Campus cell.

4.7 Cell Design and Maintenance

Based on the results of this study it is evident that bioretention cells can effectively reduce runoff temperatures and thermal heat load to receiving stream networks. However, as discussed in previous studies, consistent temperature reduction below the temperature stress threshold of cold-water aquatic species may be unachievable (Jones and Hunt 2009; UNHSC 2011). Cell media depth has been identified as the most influential design characteristic for thermal reduction (Jones and Hunt 2009), leading to the suggestion that media depths ranging from 90 – 120 cm are optimal for temperature reduction. The two cells monitored in this study were on both extremes of this range with the outflow depth of the Campus and Aquatics Center cells located at 86 cm and 150 cm, respectively. Although soil temperatures were similar at depth between the two cells, temperatures were consistently above 21°C indicating that temperature reduction below the biological temperature threshold via heat transfer to the cell media alone is unlikely. However, runoff temperature reduction below this temperature threshold was achieved more often throughout the monitoring period at the Campus cell. Considering the thermal profiles of the cell media it is apparent that additional cooling occurred after runoff infiltrated into the cell but before reaching the outflow point. Since outflow temperatures were cooler than the deepest soil layers in this cell, it is inferred that additional cooling occurred as the runoff traveled through the subsurface drainage system. This was also observed in previous studies and may be a beneficial design characteristic (Jones and Hunt 2009; Hathaway et al. 2016).

Although runoff temperature reduction was minimal, the greatest impact on thermal reduction was through stormwater volume reduction. Both cells experienced similar volume reduction, however, the Campus cell was slightly more effective at reducing flow volumes. It was initially hypothesized that the Aquatics Center would reduce flow volumes to a greater degree due to the incorporation of an IWS in the design as suggested by past studies (Lord and Hunt 2006). However, the smaller ponding volume and smaller cell media volume-to-watershed area may have been a limiting factor at this cell (Li et al. 2009). Although total flow volume reduction at the Aquatics Center was less than previous literature reported, (83% vs 99%) (Debusk and Wynn 2011), this may be due to an under representation of smaller storm events that did not generate inflow into the cell during the monitoring period. Of the 28 storms that generated inflow monitored by Debusk and Wynn (2011) during a seven-month period in 2007 and 2008, only four storm events produced outflow from the Aquatics Center cell. In this 2008 study, storms that produced as little as 2.5 mm of total precipitation generated inflow into the cell. In the current study, storms generally needed to produce at least 6 mm of total rainfall to generate inflow in the Aquatics Center cell. Furthermore, Debusk and Wynn (2011) only reported one overflow event during monitoring, compared to the four events reported in our study, which may further explain this difference in flow volume reduction. Lastly, the initial monitoring of the Aquatics Center cell occurred during a drought so there was likely greater exfiltration into surrounding soil which may explain this greater flow volume reduction reported (Debusk and Wynn 2011).

As mentioned earlier, it was clear that little maintenance had been completed on either cell prior to monitoring. Maintenance plans should typically be developed with the design plans and executive reports for cell construction. Although both cells were maintained to a degree, it was clear that regular and complete maintenance was lacking. It seemed that the maintenance

performed was merely cosmetic. The Aquatics Center cell had accumulated nearly 6 cm of sediments from the initial cell design, as a result, prior to monitoring the cell surface was nearly level with the outflow structure. With virtually no ponding volume it could be assumed that a majority of the inflow into the cell bypassed the cell completely and flowed directly into the outflow structure. In this event, the thermal reduction potential of this cell would be minimal. Even though mulch was removed and reapplied to the cell annually, there seemed to be no consideration regarding the accumulation of sediment. The last time this cell was monitored was in 2014; it is possible that the sediment accumulation had not been addressed since then. Furthermore, the Campus cell was originally design to have a mulch layer, but by the time of monitoring this mulch layer had decomposed and a dense layer of grass and weeds had developed. Although a mulch layer is typically used to promote vegetative growth, surface soil temperature measurement during the monitoring period indicated that surface temperatures can be reduced and regulated by the presence of a mulch layer. Even though temperature reduction was greatest at the Campus cell, the presence of a mulch layer may further increase this temperature reduction.

5 Conclusions

Bioretention cells can significantly reduce runoff temperatures and heat load, however, the application of this practice for protecting cold-water fish species may be limited. Although stormwater temperature reduction was observed, outflows from both cells were often greater than the 21°C stress threshold for many trout species. The greatest overall impact to thermal mitigation may be through stormwater flow volume reduction as a smaller volume of runoff entering a stream as surface runoff will have less thermal impact. Both cells monitored in this study proved to be effective in reducing stormwater flow volumes, upwards of 80% reduction throughout the monitoring period. Although stormwater temperature decreases were minimal, heat load

reductions over 80% were observed, indicating the thermal impact of this warmer stormwater volume was vastly reduced.

Comparing cell design for beneficial characteristics for thermal reduction was limited with only a two-cell sample size. Previous literature has indicated that a deeper cell design may provide better temperature reduction capabilities as soil temperatures are typically lower and more stable at greater depths. Of the two cells monitored in this study, the cell with the shallower depth to the outflow drainage system was able reduce run off temperatures more effectively than the cell with the deeper media. This suggest that cell depth alone is not the determining factor for runoff temperature reduction. During the monitoring period soil temperatures at all depths were generally above 21°C, meaning that runoff temperature reduction below the thermal stress temperature threshold for trout is very unlikely. There were only nine instances where inflow EMTs above 21°C were reduced to outflow EMTs less than 21°C. Of these nine occasions, eight occurred at the Campus bioretention cell. Leading up to this study it was hypothesized that the Aquatics Center bioretention cell would reduce runoff temperatures to a greater degree than the Campus cell due to the deeper cell media incorporated into this design. The main design difference between the cells that may have resulted in this greater temperature reduction at the Campus cell may be the linear distance of the underground drainage system. As stormwater enters the underdrain system and travels to the outflow point it can further cool through conduction between the water and pipe, as well as through convection at the free surface between the water and air, assuming the pipe is not completely full. Ultimately, this may be another crucial design characteristic for bioretention cells for runoff temperature reduction.

Of course, the sample size of this study was small. However, by using quantifiable and comparative metrics such as EMT, heat load and creating soil temperature profiles for the cell

media, future studies may be able to expand on this data. By monitoring more cells with different designs, a statistical approach may be used to further identify beneficial characteristics for temperature reduction. Recommendations for future research include monitoring the temperature of the soil surrounding the bioretention cell and measuring air temperature and precipitation at each site.

References

Alleman, J., Heitzman, M., 2019. Quantifying Pavement Albedo. National Concrete Pavement Technology Center Iowa State University, Ames, IA. 234 p.

Arrington, K., Norman, J.M., Roa-Espinosa, A., Ventura, S.J., 2004. Implementing a Thermal Urban Runoff Model (TURM), Journal of Water Management Modeling. https://doi.org/10.14796/jwmm.r220-20

Booth, D.B., Kraseski, K.A., Rhett Jackson, C., 2014. Local-scale and watershed-scale determinants of summertime urban stream temperatures. Hydrol. Process. 28, 2427–2438. https://doi.org/10.1002/hyp.9810

Broadmeadow, S.B., Jones, J. G., Langford, T.E.L., Shaw, P.J., and Nisbet, T.R., 2011. The Influence of Riparian Shade on Lowland Stream Water Temperatures in Southern England and their Viability for Brown Trout. River Res. Appl. 27, 226–237. https://doi.org/10.1002/rra

Brown, L.E., Hannah, D.M., 2007. Alpine stream temperature response to storm events. J. Hydrometeorol. 8, 952–967. https://doi.org/10.1175/JHM597.1

Castelli, E., Parasiewicz, P., Rogers, J.N., 2012. Use of Frequency and Duration Analysis for the Determination of Thermal Habitat Thresholds: Application for the Conservation of Alasmidonta heterodon in the Delaware River. J. Environ. Eng. 138, 886–892. https://doi.org/10.1061/(ASCE)EE.1943-7870.0000520

Chen, H.Y., Hodges, C.C., Dymond, R.L., 2021. Modeling Watershed-Wide Bioretention Stormwater Retrofits to Achieve Thermal Pollution Mitigation Goals. J. Am. Water Resour. Assoc. 57, 109–133. https://doi.org/10.1111/1752-1688.12894

Chesapeake Bay Program. Learn the Issues. Development [WWW Document]. Last Accessed: 03-27-2021 https://www.chesapeakebay.net/issues/development

Coutant, C. C.（1977）. Compilation of temperature preference data. J. Fish. Res. Board of Canada, 34, 740–745.

Davis, A.P., 2009. Bioretention Technology: Overview of Current Practice and Future Needs. J. Environ. Eng. 135, 109–112. https://doi.org/10.1061/(ASCE)0733-9372(2009)135(109)

Debusk, K.M., Wynn, T.M., 2011. Storm-water bioretention for runoff quality and quantity mitigation. J. Environ. Eng. 137, 800–808. https://doi.org/10.1061/(ASCE)EE.1943-7870.0000388

Delectic, A., 1998. The first flush load of urban storm runoff. Water Res. 32(8), 2462-2470. https://doi.org/10.1016/S0043-1354(97)00470-3

Diefenderfer, B.K., Al-Qadi, I.L., Diefenderfer, S.D., 2006. Model to predict pavement temperature profile: Development and validation. J. Transp. Eng. 132, 162–167. https://doi.org/10.1061/(ASCE)0733-947X(2006)132:2(162)

Dietz, M.E., Clausen, J.C., 2005. A field evaluation of rain garden flow and pollutant treatment. Water. Air. Soil Pollut. 167, 123–138. https://doi.org/10.1007/s11270-005-8266-8

Duan, S.W., Kaushal, S.S., 2013. Warming increases carbon and nutrient fluxes from sediments in streams across land use. Biogeosciences 10, 1193–1207. https://doi.org/10.5194/bg-10-1193-2013

Edinger, J.E., Duttweiler, D.W., Geyer, J.C., 1968. The Response of Water Temperature to Meteorological Conditions. Water Resour. Res. 4, 1137–1143. https://doi.org/10.1029/WR004i005p01137

Elliott, J.M., Elliott, J.A., 2010. Temperature requirements of Atlantic salmon Salmo salar, brown trout Salmo trutta and Arctic charr Salvelinus alpinus: Predicting the effects of climate change. J. Fish Biol. 77, 1793–1817. https://doi.org/10.1111/j.1095-8649.2010.02762.x

Elliott, J.M., Elliott, J.A., 1995. The effect of the rate of temperature increase onf the critical thermal maximum for parr of the Atlantic Salmon and brown trout. J. Fish Biol. 47, 917–919. https://doi.org/10.1111/j.1095-8649.1995.tb06014.x

Hathaway, J.M., Winston, R.J., Brown, R.A., Hunt, W.F., McCarthy, D.T., 2016. Temperature dynamics of stormwater runoff in Australia and the USA. Sci. Total Environ. 559, 141–150. https://doi.org/10.1016/j.scitotenv.2016.03.155

Helsel, D.R., Hirsch, R.M., Ryberg, K.R., Archfield, S.A., and Gilroy, E.J., 2020, Statistical methods in water resources: U.S. Geological Survey Techniques and Methods, Book 4, Chapter A3, 458 p., https://doi.org/10.3133/tm4a3.

Herb, W.R., 2008. Analysis of the effect of stormwater runoff volume regulations on thermal loading to the Vermillion River. University of Minnesota. St. Anthony Falls Lab, Minneapolis, MN. Proj. Reports 34 p. Retrieved from http://purl.umn.edu/115343

Herb, W.R., Weiss, M., Mohseni, O., Stefan, H.G., 2006. Hydrothermal Stimulation of a Stormwater Detention Pond on an Infiltration Basin, University of Minnesota. St. Anthony Falls Lab, Minneapolis, MN. Proj. Reports 34 p. Retrieved from http://purl.umn.edu/113685

Herb, W.R., Janke, B.D., Stefan, H.G., Mohseni, O., 2007. Estimation of Runoff Temperatures and Heat Export from Different Land and Water Surfaces. University of Minnesota. St. Anthony Falls Lab, Minneapolis, MN. Proj. Reports 34 p.

Huff, D.D., Hubler, S.L., Borisenko, A.N., 2005. Using Field Data to Estimate the Realized Thermal Niche of Aquatic Vertebrates. North Am. J. Fish. Manag. 25, 346–360. https://doi.org/10.1577/m03-231.1

Hunt, W., Lord, W., 2006. Bioretention Performance, Design, Construction, and Maintenance. North Carolina Coop. Ext. Serv. Raleigh, NC. 10 p.

Hunt, W.F., Davis, A.P., Traver, R.G., 2012. Meeting hydrologic and water quality goals through targeted bioretention design. J. Environ. Eng. (United States) 138, 698–707. https://doi.org/10.1061/(ASCE)EE.1943-7870.0000504

Janke, B.D., Herb, W.R., Mohseni, O., Stefan, H.G., 2009. Simulation of heat export by rainfall-runoff from a paved surface. J. Hydrol. 365, 195–212. https://doi.org/10.1016/j.jhydrol.2008.11.019

Jantz, P., Goetz, S., 2005. Urbanization and the Loss of Resource Lands in the Chesapeake Bay Watershed. Environ. Manage. 36, 808–825. https://doi.org/10.1007/s00267-004-0315-3

Johnson, J.P., Hunt, W.F., 2019. A retrospective comparison of water quality treatment in a bioretention cell 16 years following initial analysis. Sustain. 11. https://doi.org/10.3390/su11071945

Jones, M.B., 1975. Synergistic effects of salinity, temperature and heavy metals on mortality and osmoregulation in marine and estuarine isopods (Crustacea). Mar. Biol. 30, 13–20. https://doi.org/10.1007/BF00393748

Jones, M.P., Hunt, W.F., 2007. Stormwater BMPs for Trout Waters. North Carolina Coop. Ext. Serv. Raleigh, NC. 9 p.

Jones, M.P., Hunt, W.F., 2009. Bioretention impact on runoff temperature in trout sensitive waters. J. Environ. Eng. 135, 577–585. https://doi.org/10.1061/(ASCE)EE.1943-7870.0000022

Jones, M.P., Hunt, W.F., 2010. Effect of storm-water wetlands and wet ponds on runoff temperature in trout sensitive waters. J. Irrig. Drain. Eng. 136, 656–661. https://doi.org/10.1061/(ASCE)IR.1943-4774.0000227

Jones, M.P., Hunt, W.F., Winston, R.J., 2012. Effect of Urban Catchment Composition on Runoff Temperature. J. Environ. Eng. 138, 1231–1236. https://doi.org/10.1061/(asce)ee.1943-7870.0000577

Kaushal, S.S., Likens, G.E., Jaworski, N.A., Pace, M.L., Sides, A.M., Seekell, D., Belt, K.T., Secor, D.H., Wingate, R.L., 2010. Rising stream and river temperatures in the United States. Front. Ecol. Environ. 8, 461–466. https://doi.org/10.1890/090037

Ketabchy, M., Sample, D.J., Wynn-thompson, T., Nayeb, M., 2019. Science of the Total Environment Simulation of watershed-scale practices for mitigating stream thermal pollution due to urbanization. Sci. Total Environ. 671, 215–231. https://doi.org/10.1016/j.scitotenv.2019.03.248

Kieser, M. S., Spoelstra, J. A., Feng Feng, A., James,W., and Li, Y. (2004). Stormwater thermal enrichment in urban watersheds, Water Environment Research Foundation, Alexandria, VA. 212 p. https://doi.org/10.2166/9781780404332

LeBleu, C., Dougherty, M., Rahn, K., Wright, A., Bowen, R., Wang, R., Orjuela, J.A., Britton, K., 2019. Quantifying Thermal Characteristics of Stormwater through Low Impact Development Systems. Hydrology 6. https://doi.org/10.3390/hydrology6010016

Li, H., Sharkey, L.J., Hunt, W.F., Davis, A.P., 2009. Mitigation of Impervious Surface Hydrology Using Bioretention in North Carolina and Maryland. ASCE J. Hydrol. Eng. 14, 203–206. https://doi.org/10.1061/(ASCE)1084-0699(2009)14

Lieb, D.A., Carline, R.F., 2000. Effects of urban runoff from a detention pond on water quality, temperature and caged gammarus minus (say) (amphipoda) in a headwater stream. Hydrobiologia 441, 107–116. https://doi.org/10.1023/A:1017550321076

Long, D. L., Dymond R. L., 2013. Thermal Pollution Mitigation in Cold Water Stream Watersheds Using Bioretention. J. Am. Water Resour. Assoc. 50, 407-415. doi: 10.1111/jawr.12152.

Meisner, D.J., 1990 Effect of Climatic Warming on Southern Margins of the Native Range of Brook Trout, *Salvelinus fontinalis.* Can. J. Fish. Aquat. Sci. 47, 1065-1070. https://doi.org/10.1139/f90-122

Morin, C., Debusk, K., 2007. Reducing Urban Stormwater Impacts within the Stroubles Creek Watershed. (Senior Design Final Report). (Blacksburg): Virginia State and Polytechnic University; 64 p.

Natarajan, P., Davis, A.P., 2010. Thermal Reduction by an Underground Storm-Water Detention System. J. Environ. Eng. 136, 520–526. https://doi.org/10.1061/(asce)ee.1943-7870.0000172

National Climate Data Center (NCDC), 2010. Normal Annual/Seasonal Station Details (WWW Document). Last Accessed: 11-21-2020 URL https://www.ncdc.noaa.gov/cdoweb/datasets/NORMAL_ANN/stations/GHCND:USC00407766/detail

National Oceanic and Atmospheric Administration (NOAA), 2021. NOAA Atlas 14 Point Precipitation Frequency Estimates (WWW Document). Last Accessed: 05-13-2021 URL https://hdsc.nws.noaa.gov/hdsc/pfds/pfds_map_cont.html?bkmrk=va

Nelson, K.C., Palmer, M.A., 2007. Stream temperature surges under urbanization and climate change: Data, models, and responses. J. Am. Water Resour. Assoc. 43, 440–452. https://doi.org/10.1111/j.1752-1688.2007.00034.x

Picksley, W., Deletic, A., 1999. The Thermal Enrichment of Storm Runoff from Paved Areas - a Statistical Analysis. J. Water Manag. Model. 6062. https://doi.org/10.14796/jwmm.r204-07

Rice, K.C., Jastram, J.D., 2015. Rising air and stream-water temperatures in Chesapeake Bay region, USA. Clim. Change 128, 127–138. https://doi.org/10.1007/s10584-014-1295-9

Rossi, A., Renata, E., À, L.R., Hari, R.E., 2007. Screening Procedure to Assess the Impact of Urban Stormwater Temperature to Populations of Brown Trout in Receiving Water Screening Procedure to Assess the Impact of Urban Stormwater Temperature to Populations of Brown Trout in Receiving Water. Integr. Environ. Assess. Manag. 3, 383–392. https://doi.org/10.1897/1551-3793(2007)3(383:SPTATI)2.0.CO;2

Roy-Poirier, A., Champagne, P., Filion, Y., 2010. Review of Bioretention System Research and Design: Past, Present, and Future. J. Environ. Eng. 136, 878–889. https://doi.org/10.1061/(asce)ee.1943-7870.0000227

Rummel, S., Fesenmyer, K.A., Haak, A., Mayfield, M., Hudy, M., Williams, J.E., 2018. Identifying High-Value " Marginal " Brook Trout Populations Using a Conservation Portfolio Approach, in: Wild Trout Symposium XII - Science, Politics, and Wild Trout Management: Who’s Driving and Where Are We Going? West Yellowstone, MT. September 2017. 185–193.

Sansalone, J.J., Hird, J.P., Cartledge, F.K., Tittlebaum, M.E., 2005. Event-Based Stormwater Quality and Quantity Loadings from Elevated Urban Infrastructure Affected by Transportation. Water Environ. Res. 77, 348–365. https://doi.org/10.2175/106143005x51932

Smith, A.K., Sklarew, D., 2013. A Mid Atlantic brook trout (Salvelinus fontinalis) stream sustainability statistic for rating non-tidal streams. Sustain. Water Qual. Ecol. 1–2, 68–81. https://doi.org/10.1016/j.swaqe.2013.08.001

Steel, E.A., Beechie, T.J., Torgersen, C.E., Fullerton, A.H., 2017. Envisioning, Quantifying, and Managing Thermal Regimes on River Networks. Bioscience 67, 506–522. https://doi.org/10.1093/biosci/bix047

Strecker, E.W., Quigley, M.M., Urbonas, B.R., Jones, J.E., Clary, J.K., 2001. Determining Urban Storm Water BMP Effectiveness. J. Water Resour. Plan. Manag. 127, 144–149. https://doi.org/10.1061/(ASCE)0733-9496(2001)127:3(144)

University of New Hampshire Stormwater Center. 2011. Examination of Thermal Impacts From Stormwater Best Management Practices. Durham, NH. 148 p.

U.S. Environment Protection Agency. 2012. Cool Pavements. In Reducing Urban Heat Islands: Compendium of Strategies. Draft. Washington, DC. 37 p. https://www.epa.gov/heat-islands/heat-island-compendium

U.S. Environment Protection Agency. 2003. EPA region 10 guidance for Pacific Northwest state and tribal water quality standards. Region 10, Seattle, WA. EPA 910-B-03-002. 49 p.

Virginia Department of Environmental Quality (VADEQ), 2011. Virginia DEQ Stormwater Design Specification No.9 Bioretention. Richmond, VA. 54 p.

Virginia Department of Conservation and Recreation (VADCR), 1999. Virginia Stormwater Management Handbook, First Edition I. Richmond, VA. 619 p.

Virginia Department of Wildlife Resources (VADWR) (2021). (WWW Document) Last Accessed: 03-26-2021 URL https://dwr.virginia.gov/fishing/how-fishing-benefits-virginians

Vuocolo, Celia., Hofmann, Bryan., Benzing, T., 2019. Restoring Stream Habitat and Fish Passage (WWW Document). Virginia Conserv. Netw. Last Accessed: 01-20-2021 URL http://www.vcnva.org/restoring-stream-habitat-and-fish-passage/

Wahli, T., Knuesel, R., Bernet, D., Segner, H., Pugovkin, D., Burkhardt-Holm, P., Escher, M. and Schmidt-Posthaus, H. (2002), Proliferative kidney disease in Switzerland: current state of knowledge. J. of Fish Dis. 25, 491-500. https://doi.org/10.1046/j.1365-2761.2002.00401.x

Wardynski, B.J., Winston, R.J., Line, D.E., Hunt, W.F., 2014. Metrics for assessing thermal performance of stormwater control measures. Ecol. Eng. 71, 551–562. https://doi.org/10.1016/j.ecoleng.2014.07.068

Watson, E.C., Chang, H., 2018. Relation Between Stream Temperature and Landscape Characteristics Using Distance Weighted Metrics. Water Resour. Manag. 32, 1167–1192. https://doi.org/10.1007/s11269-017-1861-9

Wehrly, K.E., Wang, L., Mitro, M., 2007. Field-Based Estimates of Thermal Tolerance Limits for Trout: Incorporating Exposure Time and Temperature Fluctuation. Trans. Am. Fish. Soc. 136, 365–374. https://doi.org/10.1577/t06-163.1

Willard, L.L., Wynn-Thompson, T., Krometis, L.H., Neher, T.P., Badgley, B.D., 2017. Does it pay to be mature? Evaluation of bioretention cell performance seven years postconstruction. J. Environ. Eng. (United States) 143, 1–10. https://doi.org/10.1061/(ASCE)EE.1943-7870.0001232

Winston, R.J., Hunt, W.F., Lord, W.G., 2011. Thermal Mitigation of Urban Storm Water by Level Spreader–Vegetative Filter Strips. J. Environ. Eng. 137, 707–716. https://doi.org/10.1061/(asce)ee.1943-7870.0000367

Wynn, T., Hession, W.C., Yagow, G., 2010. Stroubles Creek Stream Restoration. Final Report. Biological Systems Engineering Department. Virginia Polytechnic Institute and State University. Blacksburg, VA. 19 p.

Appendices

Appendix A – Climate and Precipitation Data

Table A-1. Storm Data

Storm #	Time of First Rainfall	Time of Last Rainfall	Total Rainfall (mm)	Max. 30-min Rainfall Intensity (mm/hr)	Avg. Rainfall Intensity (mm/hr)
1	7/13/2020 1:30	7/13/2020 2:00	10.92	21.34	1.56
2	7/16/2020 22:00	7/16/2020 23:00	2.54	4.58	0.34
3	7/17/2020 12:30	7/17/2020 12:30	1.27	2.54	0.20
4	7/21/2020 13:30	7/21/2020 13:30	0.25	0.5	0.04
5	7/21/2020 21:00	7/22/2020 3:00	1.78	1.52	0.14
6	7/22/2020 15:30	7/22/2020 23:00	8.38	8.64	0.60
7	7/23/2020 15:30	7/23/2020 19:30	1.52	1.52	0.15
8	7/26/2020 21:00	7/27/2020 1:30	6.35	11.18	0.60
9	7/27/2020 16:30	7/27/2020 17:00	4.57	6.1	0.65
10	7/28/2020 11:30	7/28/2020 12:00	3.30	4.58	0.47
11	7/30/2020 12:00	7/30/2020 22:00	23.62	25.4	1.39
12	7/31/2020 23:00	7/31/2020 23:30	7.37	9.66	1.05
13	8/2/2020 18:00	8/2/2020 20:00	1.52	2.04	0.22
14	8/3/2020 5:00	8/3/2020 16:30	15.49	10.16	0.86
15	8/5/2020 16:00	8/5/2020 17:30	14.22	21.84	1.78
16	8/12/2020 15:30	8/12/2020 15:30	0.25	0.5	0.04
17	8/13/2020 14:30	8/14/2020 3:00	20.57	20.82	1.08
18	8/14/2020 13:30	8/14/2020 22:00	13.20	18.28	0.85
19	8/15/2020 5:30	8/16/2020 0:00	27.18	10.66	1.09
20	8/17/2020 6:30	8/17/2020 6:30	0.25	0.5	0.04
21	8/21/2020 7:30	8/21/2020 11:30	2.79	1.02	0.27
22	8/22/2020 3:30	8/22/2020 7:00	8.89	6.1	0.89
23	8/22/2020 17:30	8/22/2020 17:30	0.51	1.02	0.08
24	8/23/2020 15:00	8/23/2020 15:30	1.52	2.54	0.22
25	8/25/2020 20:30	8/25/2020 22:00	1.52	2.04	0.19
26	8/28/2020 16:30	8/29/2020 9:00	7.62	4.06	0.33
27	8/31/2020 4:30	8/31/2020 11:30	19.81	11.68	1.47
28	9/1/2020 0:30	9/1/2020 6:00	3.05	2.54	0.25
29	9/1/2020 16:00	9/1/2020 16:30	0.76	1.02	0.11
30	9/17/2020 6:00	9/18/2020 3:00	25.40	5.58	0.92
31	9/24/2020 11:30	9/24/2020 11:30	0.25	0.5	0.04
32	9/24/2020 23:00	9/25/2020 16:30	30.99	6.6	1.29
33	9/29/2020 3:30	9/29/2020 21:00	23.11	7.12	0.96
34	9/30/2020 15:00	9/30/2020 15:00	0.25	0.5	0.04

Table A-2. Solar Radiation and Air Temperatures

		Campus Cell Air Temperature			StREAM Lab Air Temperature		
Storm Number	**Max. Solar Radiation (kW/m^2)**	**Max Air Temp (°C)**	**Min Air Temp (°C)**	**Avg. Air Temp (°C)**	**Max Air Temp (°C)**	**Min Air Temp (°C)**	**Avg. Air Temp (°C)**
1	0.551	22.3	17.4	19.2	18.7	15.4	16.4
2	0.529	28.5	21.5	24.4	25.9	19.3	21.8
3	0.493	35.2	23.2	30.4	30.9	25.8	28.7
4	0.443	34.8	26.6	30.9	31.3	22.9	27.7
5	0.443	31.0	19.9	23.7	28.6	18.1	21.3
6	0.500	36.0	21.3	26.5	30.2	20.1	23.9
7	0.553	33.2	20.9	25.2	28.0	19.8	22.6
8	0.461	29.8	20.0	23.6	29.7	18.5	21.9
9	0.508	35.5	23.4	29.2	29.5	22.8	26.2
10	0.416	30.4	22.3	26.0	28.4	22.1	25.5
11	0.382	20.0	21.1	24.6	28.0	20.5	23.6
12	0.499	26.9	20.3	23.0	23.9	19.5	20.7
13	0.488	33.2	20.9	25.6	28.9	19.7	22.4
14	0.164	22.2	19.4	20.5	22.2	18.5	20.4
15	0.494	30.3	20.0	25.5	27.4	19.0	22.5
16	0.547	29.9	22.3	24.8	27.9	22.7	24.0
17	0.520	29.3	20.0	23.2	26.3	19.3	21.8
18	0.577	26.4	20.3	22.5	26.3	20.0	22.4
19	0.096	20.8	15.4	18.4	20.9	15.1	18.2
20	0.499	21.9	17.1	18.0	21.9	16.5	18.4
21	0.337	22.6	19.4	20.0	23.9	18.0	20.2
22	0.413	20.8	19.0	19.5	22.2	17.5	19.1
23	0.413	29.4	20.7	25.7	28.5	19.0	23.5
24	0.550	29.8	23.4	26.5	27.5	21.6	24.9
25	0.397	30.3	19.6	23.8	28.1	18.3	21.8
26	0.467	32.0	20.7	23.9	30.1	20.6	22.8
27	0.191	21.3	17.8	19.3	20.6	17.7	18.9
28	0.476	19.2	18.5	18.8	19.7	18.5	18.7
29	0.476	25.8	21.2	23.2	24.9	20.7	22.7
30	0.042	16.8	13.6	16.0	16.9	12.7	15.8
31	0.157	19.4	14.3	17.2	18.6	14.7	16.8
32	0.157	16.1	13.4	14.4	15.4	13.0	14.1
33	0.220	19.6	10.1	14.4	19.3	10.3	13.4
34	0.392	20.4	15.1	18.4	18.4	14.9	17.0

Appendix B – Discharge, EMT and Heat Load Data

Table B-1. Aquatics Center Cell Flow Data

Storm Number	Total Cell Inflow (L)	Total Cell Outflow (L)	EMT Inlet (°C)	EMT Outlet (°C)	Heat Load In (MJ)	Heat Load Out (MJ)
1	19102.4	11827.9	22.5	20.3	1800	1005
2	0.0	0.0	0.0	0.0	0.0	0.0
3	0.0	0.0	0.0	0.0	0.0	0.0
4	0.0	0.0	0.0	0.0	0.0	0.0
5	0.0	0.0	0.0	0.0	0.0	0.0
6	0.0	0.0	0.0	0.0	0.0	0.0
7	0.0	0.0	0.0	0.0	0.0	0.0
8	16568.9	3458.9	27.5	22.3	1906	322.9
9	0.0	0.0	0.0	0.0	0.0	0.0
10	0.0	0.0	0.0	0.0	0.0	0.0
11	45790.8	16765.4	24.7	23.3	4732	1632
12	3781.7	2602.0	25.3	22.6	400.5	246.0
13	0.0	0.0	0.0	0.0	0.0	0.0
14	13552.0	2682.2	24.0	23.0	1364	257.7
15	77788.8	3060.8	25.9	22.9	8431	293.6
16	0.0	0.0	0.0	0.0	0.0	0.0
17	16382.7	2223.4	25.7	22.8	1766	212.4
18	1188.4	0.0	25.7	0.0	127.8	0.0
19	22395.2	7513.2	22.0	22.3	2059	700.9
20	0.0	0.0	0.0	0.0	0.0	0.0
21	0.0	0.0	0.0	0.0	0.0	0.0
22	0.0	0.0	0.0	0.0	0.0	0.0
23	0.0	0.0	0.0	0.0	0.0	0.0
24	0.0	0.0	0.0	0.0	0.0	0.0
25	0.0	0.0	0.0	0.0	0.0	0.0
26	0.0	0.0	0.0	0.0	0.0	0.0
27	97680.5	3050.1	22.3	21.3	9119	271.9
28	572.6	0.0	21.0	0.0	50.3	0.0
29	0.0	0.0	0.0	0.0	0.0	0.0
30	1680.2	0.0	19.8	0.0	139.2	0.0
31	0.0	0.0	0.0	0.0	0.0	0.0
32	9400.8	555.8	17.1	17.5	672.0	40.6
33	6480.2	1142.1	17.3	18.7	469.0	89.4
34	0.0	0.0	0.0	0.0	0.0	0.0

Table B-2. Campus Cell Discharge Data

Storm Number	Total Cell Inflow (L)	Total Cell Outflow (L)	EMT Inlet (°C)	EMT Outlet (°C)	Heat Load in (MJ)	Heat Load Out (MJ)
1	48220.6	44.8	21.6	19.6	1983	3.7
2	1544.3	19.5	23.7	20.4	292.6	1.7
3	111.7	0.1	28.0	20.9	24.0	0.0
4	42.2	0.2	27.2	21.2	17.8	0.0
5	121.8	5.5	24.2	20.9	16.9	0.5
6	2304.0	10.8	24.2	20.9	252.7	0.9
7	5939.5	12.1	24.1	20.7	1243	1.1
8	14664.0	62.4	25.8	21.1	1837	5.5
9	4584.6	8.9	26.2	21.2	1160	0.8
10	1224.0	0.8	25.2	21.3	47.9	0.1
11	145833.0	25368.5	25.6	22.6	8163	2400
12	13732.1	9.2	23.7	21.5	661.3	0.8
13	496.7	0.0	26.2	0.0	94.0	0.0
14	95350.0	11386.0	23.5	22.3	4717	106
15	46500.0	1221.0	26.4	21.4	2984	109.5
16	374.9	1.0	24.7	21.9	107.1	0.1
17	145417.0	17500.0	25.2	22.3	8204	1636
18	150423.5	20538.2	26.8	23.07	7114	1983
19	123791.8	25584.2	22.1	22.9	6637	2453
20	0.0	0.0	0.0	0.0	0.0	0.0
21	677.5	0.0	21.8	0.0	221.5	0.0
22	1846.7	1.3	21.3	20.4	512.7	0.1
23	1066.8	0.7	24.7	21.2	233.9	0.0
24	851.9	0.0	24.8	0.0	288.9	0.0
25	354.9	0.2	23.4	19.9	34.8	0.0
26	3171.0	18.9	23.0	21.3	869.7	1.7
27	73304.4	24390.0	21.9	21.6	5746	2207
28	605.3	0.0	20.1	0.0	124.4	0.0
29	1482.8	0.0	22.8	0.0	251.4	0.0
30	7110.5	230.5	17.6	18.5	1286	17.8
31	48.6	0.0	16.4	0.0	3.3	0.0
32	25992.0	49.4	16.2	16.5	2173	3.4
33	28178.6	4877.5	16.9	18.1	2110	368.3
34	275.2	0.0	16.3	0.0	57.2	0.0

Appendix C – Soil Data

Table C-1. Campus Cell Maximum Daily Soil Temperatures

Day No.	Date	Max Campus Bottom Inlet (°C)	Max Campus Bottom Outlet (°C)	Max Campus Sun (°C)	Max Campus Shade (°C)
1	7/10/2020	21.0	20.7	44.8	35.3
2	7/11/2020	21.1	-	45.5	36.8
3	7/12/2020	21.1	-	41.3	36.8
4	7/13/2020	22.2	-	38.6	34.2
5	7/14/2020	21.3	-	41.6	39.4
6	7/15/2020	21.3	-	40.6	38.8
7	7/16/2020	21.4	-	41.2	32.6
8	7/17/2020	21.5	-	36.9	35.4
9	7/18/2020	21.7	-	41.7	41.8
10	7/19/2020	21.8	-	44.2	41.8
11	7/20/2020	21.9	-	45.6	42.4
12	7/21/2020	22.0	-	34.7	36.0
13	7/22/2020	22.0	-	44.3	33.1
14	7/23/2020	22.1	-	38.6	28.7
15	7/24/2020	22.1	-	42.3	36.4
16	7/25/2020	22.0	-	44.2	39.0
17	7/26/2020	22.0	-	43.3	38.4
18	7/27/2020	22.0	-	42.3	29.5
19	7/28/2020	22.1	-	35.2	30.3
20	7/29/2020	22.2	-	42.5	37.8
21	7/30/2020	26.2	-	29.7	28.7
22	7/31/2020	24.0	-	33.7	30.4
23	8/1/2020	23.7	-	35.6	27.9
24	8/2/2020	23.4	-	41.6	34.3
25	8/3/2020	23.7	-	26.7	23.9
26	8/4/2020	23.3	-	38.2	32.1
27	8/5/2020	23.5	-	36.7	29.7
28	8/6/2020	23.0	-	30.0	27.7
29	8/7/2020	22.9	-	33.6	31.0
30	8/8/2020	22.8	-	38.0	32.5
31	8/9/2020	22.7	-	38.6	33.5
32	8/10/2020	22.7	-	39.3	38.2
33	8/11/2020	22.7	22.1	39.3	37.0
34	8/12/2020	22.7	22.2	30.8	30.0
35	8/13/2020	24.3	22.2	30.3	27.8
36	8/14/2020	24.8	24.7	28.7	26.4

Day No.	Date	Max Campus Bottom Inlet (°C)	Max Campus Bottom Outlet (°C)	Max Campus Sun (°C)	Max Campus Shade (°C)
37	8/15/2020	24.0	23.2	24.2	22.4
38	8/16/2020	23.5	22.8	24.5	25.2
39	8/17/2020	22.8	22.2	32.6	34.0
40	8/18/2020	22.5	21.9	32.5	34.7
41	8/19/2020	22.3	21.8	31.5	33.8
42	8/20/2020	22.3	21.8	29.9	34.5
43	8/21/2020	22.1	21.7	25.5	25.1
44	8/22/2020	22.0	21.6	28.8	32.3
45	8/23/2020	22.0	21.6	28.0	30.7
46	8/24/2020	22.0	21.6	28.5	32.4
47	8/25/2020	22.0	21.7	32.0	35.6
48	8/26/2020	22.0	21.8	29.7	34.5
49	8/27/2020	22.1	21.8	30.6	32.8
50	8/28/2020	22.2	21.9	31.3	34.2
51	8/29/2020	22.3	22.0	28.8	31.0
52	8/30/2020	22.3	22.0	29.5	34.2
53	8/31/2020	22.4	22.1	22.9	22.1
54	9/1/2020	22.2	21.8	26.7	26.5
55	9/2/2020	21.9	21.5	29.5	31.8
56	9/3/2020	22.0	21.6	29.6	33.7
57	9/4/2020	22.1	21.7	28.5	31.9
58	9/5/2020	22.1	21.7	29.1	32.2
59	9/6/2020	22.0	21.7	28.8	31.5
60	9/7/2020	21.7	21.4	29.7	33.0
61	9/8/2020	21.3	21.1	29.2	34.0
62	9/9/2020	21.2	21.0	25.4	30.8
63	9/10/2020	21.2	20.9	26.7	28.9
64	9/11/2020	21.3	21.0	30.4	35.4
65	9/12/2020	21.4	21.1	23.1	23.3
66	9/13/2020	21.3	21.1	26.0	27.8
67	9/14/2020	21.3	21.0	26.8	28.4
68	9/15/2020	21.2	20.9	24.0	25.8
69	9/16/2020	21.1	20.8	23.9	25.8
70	9/17/2020	20.7	20.4	18.7	18.1
71	9/18/2020	20.3	20.1	23.8	25.4
72	9/19/2020	20.0	19.8	21.2	21.7
73	9/20/2020	19.8	19.7	23.1	25.1

Day No.	Date	Max Campus Bottom Inlet (°C)	Max Campus Bottom Outlet (°C)	Max Campus Sun (°C)	Max Campus Shade (°C)
74	9/21/2020	19.3	19.2	22.2	25.8
75	9/22/2020	18.8	18.7	22.4	25.6
76	9/23/2020	18.3	18.3	21.4	24.8
77	9/24/2020	18.1	18.1	18.7	19.2
78	9/25/2020	18.1	18.1	17.1	16.9
79	9/26/2020	17.9	18.1	19.9	20.8
80	9/27/2020	17.9	18.1	22.3	25.1
81	9/28/2020	18.1	18.2	24.0	29.9
82	9/29/2020	18.2	18.3	18.7	18.7
83	9/30/2020	18.0	18.3	21.2	24.8

Table C-2. Aquatic Center Cell Maximum Daily Soil Temperatures

Day No.	Date	Aquatic Center Max 1.8 m (°C)	Aquatic Center Max 0.9 m (°C)	Aquatic Center Sun Max (°C)	Aquatic Center Shade Max (°C)
1	7/10/2020	-	-	-	-
2	7/11/2020	-	-	-	-
3	7/12/2020	-	-	-	-
4	7/13/2020	22.7	24.1	26.6	28.1
5	7/14/2020	21.6	23.6	28.0	25.8
6	7/15/2020	21.0	23.2	28.4	26.4
7	7/16/2020	20.6	22.8	28.7	26.5
8	7/17/2020	20.4	22.7	28.8	27.1
9	7/18/2020	20.2	22.6	29.8	28.1
10	7/19/2020	20.2	22.5	30.0	27.3
11	7/20/2020	20.1	22.5	29.9	28.4
12	7/21/2020	20.1	22.6	29.2	28.0
13	7/22/2020	20.0	22.6	29.4	26.9
14	7/23/2020	20.0	22.6	28.6	25.4
15	7/24/2020	20.0	22.5	28.3	27.3
16	7/25/2020	20.0	22.5	28.9	28.0
17	7/26/2020	21.4	24.9	29.2	26.9
18	7/27/2020	22.2	25.2	29.5	25.7
19	7/28/2020	22.1	24.9	28.2	26.2
20	7/29/2020	21.9	24.6	29.2	28.4
21	7/30/2020	23.0	25.0	26.8	25.9
22	7/31/2020	23.8	24.9	26.6	26.5

Day No.	Date	Max Campus Bottom Inlet (°C)	Max Campus Bottom Outlet (°C)	Max Campus Sun (°C)	Max Campus Shade (°C)
23	8/1/2020	23.9	24.7	28.1	26.1
24	8/2/2020	23.4	24.5	27.4	25.3
25	8/3/2020	24.1	24.5	24.5	23.2
26	8/4/2020	23.7	24.2	25.8	24.1
27	8/5/2020	23.5	24.3	26.8	24.8
28	8/6/2020	23.3	24.5	26.8	24.9
29	8/7/2020	22.9	24.4	28.2	26.2
30	8/8/2020	22.7	24.2	29.3	26.9
31	8/9/2020	22.5	24.1	29.6	27.1
32	8/10/2020	22.3	24.0	29.7	27.1
33	8/11/2020	22.2	23.9	30.0	26.9
34	8/12/2020	22.1	23.8	26.9	26.0
35	8/13/2020	23.5	24.5	27.5	26.0
36	8/14/2020	24.1	24.7	27.1	25.1
37	8/15/2020	25.0	24.8	24.1	22.8
38	8/16/2020	23.4	22.8	25.2	23.5
39	8/17/2020	22.6	22.8	28.8	24.1
40	8/18/2020	22.3	22.6	28.8	24.7
41	8/19/2020	22.0	22.5	28.7	24.8
42	8/20/2020	21.9	22.5	27.9	25.5
43	8/21/2020	21.7	22.5	26.2	24.0
44	8/22/2020	21.7	22.4	29.4	26.1
45	8/23/2020	21.6	22.4	25.8	24.5
46	8/24/2020	21.5	22.4	26.7	26.8
47	8/25/2020	21.4	22.4	27.4	27.4
48	8/26/2020	21.4	22.5	27.1	27.8
49	8/27/2020	21.3	22.5	26.8	27.0
50	8/28/2020	21.3	22.5	27.6	27.8
51	8/29/2020	21.3	22.6	26.4	25.7
52	8/30/2020	21.3	22.6	26.7	27.8
53	8/31/2020	22.2	22.9	23.2	22.5
54	9/1/2020	22.0	22.3	24.2	24.3
55	9/2/2020	21.7	22.1	25.7	26.4
56	9/3/2020	21.5	22.1	25.5	26.1
57	9/4/2020	21.3	22.1	25.3	26.0
58	9/5/2020	21.2	22.2	24.7	26.9
59	9/6/2020	21.2	22.2	24.1	26.7
60	9/7/2020	21.2	22.1	24.8	27.6

Day No.	Date	Max Campus Bottom Inlet (°C)	Max Campus Bottom Outlet (°C)	Max Campus Sun (°C)	Max Campus Shade (°C)
61	9/8/2020	21.1	22.0	24.8	27.3
62	9/9/2020	21.1	21.9	23.9	24.4
63	9/10/2020	21.0	21.8	24.7	26.8
64	9/11/2020	21.0	21.8	26.0	29.6
65	9/12/2020	20.9	21.9	23.7	24.1
66	9/13/2020	20.9	21.9	24.8	27.5
67	9/14/2020	20.9	21.9	24.5	26.3
68	9/15/2020	20.8	21.9	22.2	22.2
69	9/16/2020	20.8	21.8	21.8	23.1
70	9/17/2020	20.8	21.7	19.3	18.4
71	9/18/2020	20.7	21.5	21.2	22.6
72	9/19/2020	20.7	21.2	19.8	21.5
73	9/20/2020	20.6	20.9	19.2	23.4
74	9/21/2020	20.5	20.6	19.1	23.1
75	9/22/2020	20.3	20.3	19.7	23.2
76	9/23/2020	20.2	20.0	19.7	21.2
77	9/24/2020	20.1	19.7	18.7	18.6
78	9/25/2020	20.0	19.6	17.5	16.8
79	9/26/2020	18.2	18.6	19.5	19.5
80	9/27/2020	18.4	18.3	20.8	21.8
81	9/28/2020	18.5	18.4	21.6	23.1
82	9/29/2020	18.5	18.4	19.2	19.3
83	9/30/2020	18.2	17.9	17.8	19.1